technische universität
dortmund

TU Dortmund University

Optical Action Potential

On the Physical Phenomenology of Nerve Pulse Propagation

Dissertation

zur Erlangung des akademischen Grades Dr. rer. nat.

vorgelegt von

Simon Fabiunke

Medizinische und Biologische Physik

Fakultät Physik

Technische Universität Dortmund

Dezember 2021

1. Gutachter:

Prof. Dr. Matthias F. Schneider

2. Gutachter:

Prof. Dr. Luis Bagatolli

Vorsitzender der Prüfungskommission:

Prof. Dr. Marc Aßmann

Vertreter der wissenschaftlichen Mitarbeiter:

Dr. Michael Paulus

Datum des Einreichens der Arbeit: 21. Dezember 2021
Datum der Disputation: 05. April 2022

"There is nothing like looking, if you want to find something...
You certainly usually find something, if you look,
but it is not always quite the something
you were after."

The Hobbit
J.R.R. Tolkien

Abstract

Voltage sensitive dyes have been used as an alternative route to detect membrane potentials. This replaces electrophysiological equipment and allows to study action potentials with optical tools. Changes in fluorescence emission are most commonly translated into changes in transmembrane potentials. In this thesis, it is demonstrated that the emission energy of the fluorescent dye Di-4-ANEPPDHQ is a state variable. Incorporation of the dye in artificIal lipid membranes, where ion transport is obsolete, changes of the emission spectrum as a function of lateral pressure and temperature were detected, as well as in the presence of lateral propagating pulses. It is found that despite the complete absence of transmembrane ion movement, the spectrum shifted about 20 nm at the main transition, which falsifies the Nernst-potential as the origin of the changes in emission.
To underline the relevance for action potentials in living systems, the same dye is incorporated into an excitable plant cell to investigate action potentials. There, a very similar blue shift of the emission spectrum is found as in the monolayer pulse experiments. In summary, these experiments show that Di-4-ANEPPDHQ (presumably all dyes), should be seen as a phase state reporter. This is entirely consistent with the interpretation of the nervous impulse as a propagating state change as has been proposed by others. This interpretation allows to map the state and state changes optically not only of nerves, but even of the entire brain.

Kurzfassung

Spannungssensitive Fluoreszenzfarbstoffe werden in der Zellforschung als Alternative zur Vermessung von Membranpotentialen verwendet. Dadurch werden elektrophysiologische Geräte ersetzt und Nervenpulse werden durch optische Techniken vermessen. Die Änderung des Emissionsspektrums werden üblicherweise in Änderungen des Membranpotentials übersetzt. In den Experimenten dieser Arbeit wird gezeigt, dass die Emissionseigenschaften des Farbstoffes Di-4-ANEPPDQH eine Variable des thermodynamischen Zustandes ist. Einbettung in künstliche Lipid-Systeme (Monolayer, Vesikel), in denen kein Ionentransport stattfindet, zeigen Änderungen der Emission sowohl als Funktion des lateralen Drucks, der Temperatur als auch in Anwesenheit von akustischen Pulsen. Es kommt zu einer Verschiebung des Emissionsspektrums um ca. 20 nm während der Hauptphasenumwandlung der untersuchten künstlichen Systeme. Um die Relevanz für biologische Prozesse zu unterstreichen, wurden gleiche Untersuchungen in einer erregbaren Pflanzenzelle vorgenommen. Es konnte eine signifikante Ähnlichkeit der Aktionspotentiale zu den akustischen Pulsen in Lipidmonolagen im optischen Signal gezeigt werden. Zusammenfassend zeigen die Experimente der Arbeit, dass Di-4-ANEPPDHQ (vermutlich alle Farbstoffe) als Zustandsreporter gesehen werden können. Dies ist konsistent zu der Annahme, dass es sich bei Nervenpulsen um eine propagierende Phasenumwandlung handelt. Diese Interpretation der Fluoreszenz lässt nicht nur die Vermessung des Zustandes von Nerven zu, sondern auch des gesamten Gehirns.

Contents

List of Figures

Summary

Information transfers in a biological system are typically described by biochemical reactions of various molecules. These pathways are already complex for one single cell and do not provide a macroscopic description of cell activity. Among others, the action potential, a transient change of the transmembrane potential, is described as a consequence of the activity of specific proteins. Other thermodynamic parameters, which are also changing during the propagation of nerve pulses, are not even implemented in the textbook theory. However, it is well known that also thermal, mechanical, chemical, optical etc. changes occur during action potentials. For these reasons a cooperative description has been suggested by K. Kaufmann. In his theory the action potentials are proposed to be nonlinear acoustic pulses controlled by the thermodynamic state of the propagation medium (e. g. lipid membrane). The influence of the thermodynamic state of biological material is of particular interest. Starting with a thermodynamic system which follows the second law of thermodynamics leads to clearly falsifiable predictions.

But in general, the state of a living system is not easily accessible. However, it is known that fluorescent dye molecules which are embedded into a membrane, change their emission properties when environmental properties such as ordering, electrical potential etc. are altering. Minimal concentrations of dye molecules are sufficient to get a signal and therefore the influence on the biological system can be neglected. Fluorescence seems to be one opportunity to get access to thermodynamic state diagrams in living matter.

In this thesis the correlation of the emission properties of the fluorescent dye molecule Di-4-ANEPPDQH to the thermodynamic state of a lipid membrane is investigated. Experimentally, the dye shows in static and dynamic measurements that the emission energy change step-like (nonlinear) during the main phase transition of an artificial lipid system (disordered-ordered transition). A variation in emission wavelengths on the order of 10 nm/°C are observed at the transition regime. The width of the emission spectrum is also maximal at the phase transition. These results are conserved in a lipid free system (dye solved in DMSO). It indicates that the emission properties are strongly correlated to thermodynamic properties of the micro chemical environment (solvation shell) and do not correspond to specific parameters of the system. Similar dye signatures are observed when an artificial membrane dynamically changes its phase state during nonlinear acoustic pulses.

In the second part of this thesis, the same fluorescent dye is incorporated into the membrane of a living plant cell (*Chara Australis*) to measure the optical state diagram of this organism. Thereby, the same mechanism as in artificial systems is observed.

By cooling or acidification of the cell environment, the emission spectrum of the incorporated dye molecules shifts to smaller wavelengths. This result indicates that the cell membrane undergoes a disordered-ordered transition in the vicinity of the living conditions. Accordingly, action potentials in *Chara Australis* cells are also represented by an analogous dye signature. This similarity allows the conclusion that a phase transition occurs during the propagation of the action potential. This should also have a direct influence on all variables of the chemical environment such as thermal, mechanical, optical, chemical etc. Consequently, these results support the assumption that an action potential can be described as a propagation phase transition which is analogous to a nonlinear acoustic wave in a 2-dimensional interface.

In summary, fluorescent dye molecules are indeed practicable to investigate the phase state of a living system. By incorporating a small concentration of the molecules to the system of interest, changes in the emission properties are clearly correlated to the thermodynamic phase state. The observation of a phase transition during an action potential opens up a new phenomenology of nerve pulse propagation corresponding to the theories by Kaufmann, Heimburg, Wilke etc. The access to the state diagram of cells leads to clear assumption of excitability of cells and enzyme activity even in human neurons and it also gives a more fundamental understanding of life.

1 Introduction

Electrical phenomena in nerve cells were probably among the first physical investigations in biology. Already in the 18th century Galvani (Galvani (1791)) demonstrated that the muscles of frog legs twitch by electrical excitation. While Galvani called the phenomenon "animal electricity", Volta stated that nerve pulses are electrical conduction phenomena (Volta and Banks (1800)). The access to electrical properties of the cell has coined this imagination of the role of electricity in life until today. Also in science fiction, Frankenstein's creature was awakened to life by electricity inspired by the scientific investigations.

In the 19th century the conceptual foundation of the cell theory was built although the existence of a plasma membrane as a boundary of cells was not accepted until the 20th century. The description of cells bounded by a membrane was based on experiments of permeability and electrical membrane potentials (Bernstein (1902), Donnan (1924), Ostwald (1890)). The fluxes of ions through a semipermeable membrane were related to the nerve pulse propagation (action potentials) and the changes of the membrane potential.

In the 1950s Hodgkin and Huxley (HH) developed a mathematical model of action potentials (Hodgkin and Huxley (1952a)). In their description, the membrane is built as an electrical circuit with resistors and capacitance representing the proteins and the lipids. They and Sir J. C. Eccles were awarded with the Nobel Prize in Physiology or Medicine in 1963. A main criticism of the theory is the restriction to the purely electrical aspects of the nerve pulse. Meanwhile there is strong experimental evidence that an action potential is accompanied by changes of mechanical, chemical, magnetic and optical variables (Tasaki (1999), Tasaki (2008), Tasaki et al. (1968), Wikswo et al. (1980)). One striking observation was also that there is an increase of the temperature followed by an active cooling of the system (Ritchie and Keynes (1985)). In the HH model, a nerve pulse should only generate heat (current through resistors). Even HH were aware of the fact that their model is a mathematical description of the phenomenon and not a fundamental physical theory:

> *The agreement must not be taken as evidence that our equations are anything more than an empirical description of the time-course of the changes in permeability to sodium and potassium. An equally satisfactory description of the voltage clamp data could no doubt have been achieved with equations of very different form, which would probably have been equally successful in predicting the electrical behavior of the membrane.* (Hodgkin and Huxley (1952a))

Nowadays it is considered that the ion-conducting objects are specific ion-channel proteins which are embedded into the cell membrane (Mosaic-Model (Singer and Nicolson (1972))). The activity of these proteins were characterized by the patch clamp technique developed by Neher and Sakmann (Neher and Sakmann (1976)). Nevertheless, the description of nerve pulses does not contain any other thermodynamical aspects. The common belief is that proteins mainly give biological function and the lipids function as a "framework". Consequently, all substitutes of the cell such as water or ions are understood to be in a solution, separated by a thin membrane. A cooperative behavior of this cell system is mostly neglected. But, as one single molecule of H_2O does **not** give the characteristics of water as a fluid, it is not convincing that processes in biology can be described by single molecules.
Based on thermodynamics, changes in all observables have been suggested to be the manifestation of the same physical origin. According to a theory by K. Kaufmann (Kaufmann (1989a), Kaufmann (1989b)), the action potential can be considered as an adiabatic pulse similar to sound. Heimburg and Jackson (Andersen et al. (2009), Heimburg and Jackson (2007)) extended Kaufmanns theory stressing in particular the importance of nonlinear state changes during propagation within the membrane.
Experiments have shown that nonlinear pulses can propagate through a protein-free lipid monolayer when the system, close to a transition, is stimulated above a specific threshold (Shrivastava et al. (2018a), Shrivastava and Schneider (2013)). The similarity of propagation of these nonlinear pulses in model systems as well as in various complex organisms, underlines that the specific composition of molecules should not play an important role. Therefore, the question arises, which properties an interface must have in order to form such pulses and which physical principles can capture all of these. In theory and with experimental evidence these pulses occur when a phase transition of the interface is crossed (Mussel and Schneider (2019), Shrivastava and Schneider (2014), Shrivastava and Schneider (2013)). But there is no clear experimental evidence that action potentials in living systems are accompanied by a change of state of cell interfaces and therefore behave such as a nonlinear acoustic phenomenon.
In this thesis, the role of the thermodynamic state of lipid-based membranes in biological material during the propagation of an action potential is investigated. Thus, not only the state can regulate chemical reactions but also vice versa. Any possible perturbation of the system such as fluctuations in temperature, pH or electrical potential could be a trigger for solitary pulses, when the excitation threshold is exceeded. This results in varieties of possibilities whereby the system regulates itself or reacts to external influences.
From a thermodynamic perspective, the phase state of a biological system is an important information which leads to falsifiable predictions. State diagrams describe the empirical behavior of an observed system, which is not created by the structure of single molecules. Experimentally, there are some indicators that cells undergo phase

transitions in the vicinity of their resting state (Heimburg and Jackson (2005), Hazel et al. (1998)).
In biology, the thermodynamic phase state of the observed system is not easily accessible. However, fluorescence dye molecules offer an opportunity to get access to the phase state of the chemical environment of the dye. Many dyes are thought to be sensitive to changes in voltage. These different fluorescent molecules have been incorporated into cells to optically measure action potentials (Cohen et al. (1978); Foley and Muschol (2008); Loew et al. (1992)) or to characterize the fluidity (phase) of the system (Georgescauld and Duclohier (1978); Tasaki et al. (1972). This indicates that it is likely that optical changes can arise from different mechanisms and that state changes of the membrane material take place. Implementing transition behavior to the system leads to nonlinearities which are directly followed by biological functions (Fichtl et al. (2016), Fichtl et al. (2018)). Here, the thermodynamic state of lipid membranes is observed by fluorescence spectroscopy in quasi-static and dynamic measurements in artificial membranes as well as in an excitable plant cell. By characterization of the emission properties at the main transition regime in artificial membranes, experimental evidence is gathered that a phase transition takes place during the propagation of an action potential.

Theoretical Background

2 Theoretical Background

2.1 Structure of Biological Membranes

First, the biological background of membranes will be discussed. The structure of cells and molecules was and still is an important part of biology. But nevertheless, the restriction to single molecules led to a high complexity of chemical pathways. This puzzle of reactions and processes seems to be unsolvable.

Already in the 17th century the scientist Robert Hooke discovered similarities between the microscopic structure of cork and honeycomb under a microscope. He gave these structures the name cellula, which he later extended to describe the structure of living matter. In the 1830s, Schleiden and Schwann presented the theory, still valid today, that cells are the basic unit of all living systems. In the 19th century the existence of a membrane around the cell was not proven. The membrane was often described as a secondary and unnecessary structure. Observation of a jelly-like substance inside the cell led to the protoplasm theory, where the activity of the protoplasm (living jelly) determined the properties of the cell.
The separation of the cells by a semi-permeable membrane were coined in 1899 by Charles E. Overton. He investigated the permeability of several chemical components in cells. He noticed that polar groups could lower the permeability, whereas elongation or etherification could increase the permeability. This correlation with the lipophilic character of the compounds and their permeability led to the hypothesis that cells are surrounded by a thin membrane which has properties such as oil. With the agreement of earlier descriptions of semi-permeable membranes on the surface of cells (1877 Pfeffer), the assumption arose, that membranes are mainly composed of lipids.
Today it is known that cell membranes are composed of approximately equal parts of lipids and proteins by mass. **Figure 2.1** shows the chemical structure of types of membrane forming lipids. Although there exist a variety of different membrane lipids, in this work only phospholipids will be studied as there are one of the main representatives within biological lipid membranes. Phospholipids are phospho-esters of glycerol with two carbon chains. The fatty acids are attached via glycerol to a phosphate head group that can carry various other polar substitutes. Lipids have the property that the polar head group orientates to the water and the non-polar carbon chains orientate towards each other. Thus, lipids independently form various

structures in aqueous solutions. In biophysics this ability is called polymorphism and describes the variety of different structures which can be formed. Spheres of lipid molecules (micelles), pairs of layers (in biological systems bilayer) as well as tubular (hexagonal phases) and various cubic arrangements occur. The idea that

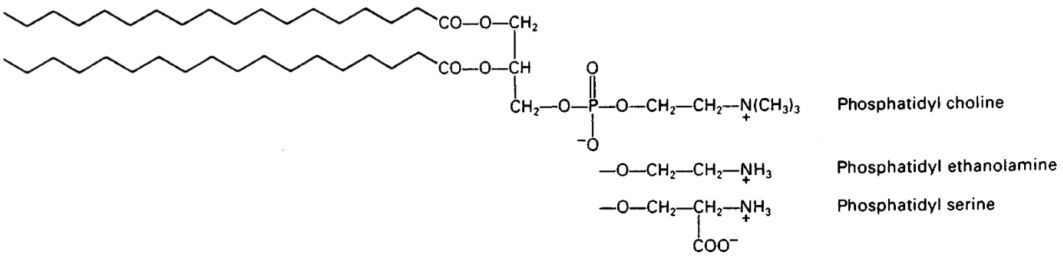

Figure 2.1: Chemical structure of phospholipids with different head groups (figure taken from Aidley (1998)).

cell membranes are basically formed by a lipid bilayer was made popular by the experiments of Grendel and Gorter (Gorter and Grendel (1925)). They spread extracted lipids from erythrocyte cells on water, compared the surface to the total surface of cells and found a 2:1 ratio. Despite known theoretical and experimental mistakes, this study has often been cited as the foundation of the lipid bilayer nature of cells. As mentioned before, the membrane of cell is not purely composed of phospholipids, but includes carbohydrates, cholesterol or proteins. Investigations of protein structures with X-ray crystallography and the development of electron microscopy led to the famous fluid mosaic model by Singer und Nicolson (**Figure 2.2**, Singer and Nicolson (1972)). The model describes that the hydrophobic parts of the proteins are embedded into the non-polar environment, whereas the hydrophilic parts reach into the polar environment of the aqueous medium. Molecules can penetrate the membrane or be loosely attached to the surface. The function of proteins is still part of the discussion.

The general structure of cells and the function of proteins embedded into a thin membrane makes it clear that there is a particular interest in interfaces of cells. But the complexity of life where the function of the system is given by several single molecules does not give a macroscopic understanding of biological processes. Also, a single cell consists of a variety of different molecules, which are responsible for several interactions inside the organism. These include small molecules such as ions, sugar, fatty acids or water as well as large biomolecules such as proteins or phospholipids. From the view of a physicist, the goal must be to find a cooperative macroscopic description where physical principles such as conservation laws are included.

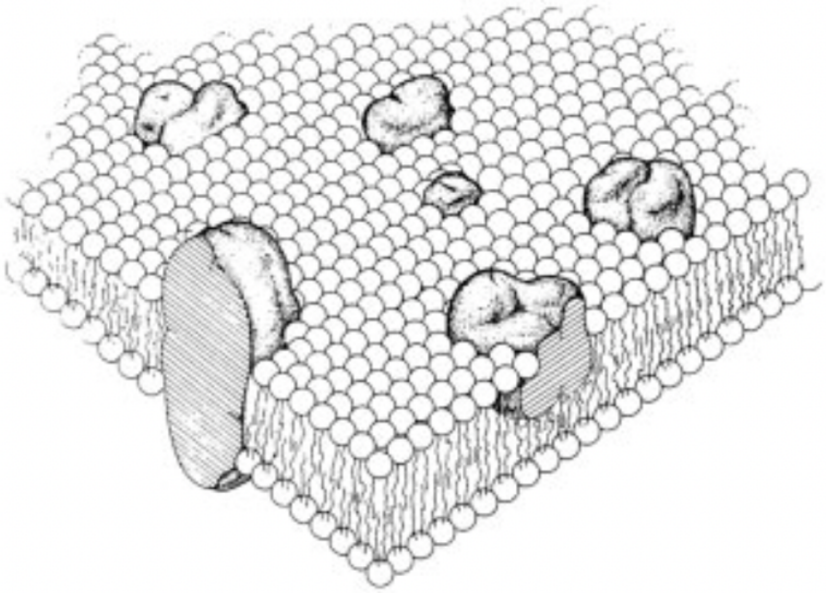

Figure 2.2: Fluid mosaic model by Singer and Nicolson (1972). The figure shows a schematic 3D cross section of a lipid membrane. The proteins (solid bodies) are not homogeneously distributed in the lipid bilayer. Some proteins penetrate the membrane (integral proteins), and some proteins are loosely attached (peripheral proteins).(Figure taken from Singer and Nicolson (1972))

2.2 Thermodynamics of Interfaces

The thermodynamics is a universal tool to describe physical systems. With this an integrated representation of different disciplines in physics e. g. mechanics, electromagnetism, quantum mechanics, etc. is possible. A central role of a thermodynamic description is the state of the system, where **each** variable of the system has a certain value. The system is fully described at all times by the values of all independent variables. As a result, all interactions of a system cannot independently be defined but are connected to each other.
Especially the investigation of soft matter, which in general includes cells (living systems), essentially needs such an integrated description of all aspects of the system, as all these separated disciplines are inseparably linked to each other. This means, that an independent description of every single process in cells, such as action potentials or the regulation of chemical reactions, cannot contribute to a deeper understanding of the complex cell communication. When faced with countless chemical processes, which are connected to various secondary reactions, a molecular model seems to be hopeless for a complete description of life. In thermodynamics, a molecular model is normally used to calculate the probabilities of the state and then to calculate the entropy of the system from these probabilities.
The question arises whether thermodynamics can be applied to a living system without starting at the molecular level. Following Einsteins inversion, the determination of empirical thermodynamic quantity such as heat capacity, compressibility, electrical capacity, radiation spectra etc., connected with the principle of Boltzmann, can be used in order to define the entropy of the specific states of the system (Einstein (1910), Einstein (1903)). Thereby, the empirical values (i. e. susceptibilities) are directly linked to the fluctuations of the system and at least to the entropy potential. Consequently, the measurable value of a system offers access to the thermodynamic state and leads to testable predictions.
In biology, the application of this procedure seems not to be trivial, as the system which it is to apply is ambiguous. A closer look to living systems shows that cells are a framework of several interfaces. The hydration shells around the molecules and ions build an interfacial system for most of the water inside of the cells. Not only for this reason the interface seems to play an important role for the understanding of a living system. It was Konrad Kaufmann in the 1980s (Kaufmann (1989b)) who applied Einsteins approach to the living system. As Einstein recognized (Einstein (1910)) that the surface of a droplet of water has its own entropy, K. Kaufmann also recognized that the interfaces of cells have their own entropy. Thus, the entropy of interfaces is an independent decoupled quantity. Furthermore, the macroscopic properties of the interface built of different components are derived from the entropy. The entropy $S(n_i)$ is mathematical completely described by the thermodynamic variables n_i of

the system and it can be approximated by a Taylor series near the thermodynamic equilibrium regime n_0

$$S(n_i) \approx S_0 + \frac{\partial S}{\partial n_i}\bigg|_{n_i=n_0} \delta n_i + \frac{1}{2}\frac{\partial^2 S}{\partial n_i^2}\bigg|_{n_i=n_0} (\delta n_i)^2 + (\sigma)^3 \tag{2.1}$$

At the thermodynamic equilibrium the entropy is in maximum and the thermodynamic forces, which push the system back towards the equilibrium state, disappear $\left(\frac{\partial S}{\partial n_i}\right) = 0$. Insert into the Boltzmann-principle ($S = k_\mathrm{B} \ln(P)$, k_B Boltzmann-constant; P: Probabilities) it yields to:

$$P(n_i) = \exp\left(-\frac{S(n_i)}{k_\mathrm{B}}\right) \tag{2.2}$$

$$P(n_i) \approx \exp\left(-\frac{S_0}{k_\mathrm{B}}\right) \cdot \exp\left(-\frac{1}{2k_\mathrm{B}}\frac{\partial^2 S}{\partial n_i^2}\bigg|_{n_i=n_0} (\delta n_i)^2\right) \tag{2.3}$$

The probabilities P of the specific microstate of an observable n_i correspond to a gaussian distribution. When the system is in the most probable state (equilibrium), the entropy is maximal. The state of the system fluctuates around the maximum. At an improbable state the system will be driven into a more probable state. This is equivalent to an increase of entropy over time. The second derivatives $\left(\frac{\partial^2 S}{\partial n_i^2}\right)$ describe the fluctuations $\langle(\partial^2 n_i)\rangle$ of the system. Large fluctuations $\langle(\partial^2 n_i)\rangle$ of the distribution lead to a wide gaussian distribution and a high curvature of the entropy potential. Small fluctuations imply a narrow distribution and a small curvature of the entropy potential (s. **Figure 2.3**). The second derivatives of a potential are also called the thermodynamic susceptibilities and are connected to measurable values and macroscopic properties of the observed system:

$$\langle(\delta n_i)^2\rangle = -k_\mathrm{B}\left(\frac{\partial^2 S}{\partial n_i^2}\right)^{-1} \tag{2.4}$$

For example, the fluctuations of the area A are proportional to the isotherm compressibility κ_T. The **equation** (2.5) shows that high fluctuations of the area lead to a high compressibility. Therefore, the distribution of the area equals a wide gaussian distribution.

$$\langle(\delta A)^2\rangle = -k_\mathrm{B}\left(\frac{\partial^2 S}{\partial A^2}\right)^{-1} = k_\mathrm{B} A T \kappa_T \tag{2.5}$$

The measurement of such susceptibilities directly leads to predictions about the entropy potential and thus about the entire system. From Einsteins point of view, the thermodynamic forces and fluctuations can be directly derived from the entropy

potential without a microscopic model. The macroscopic properties of a thermody-

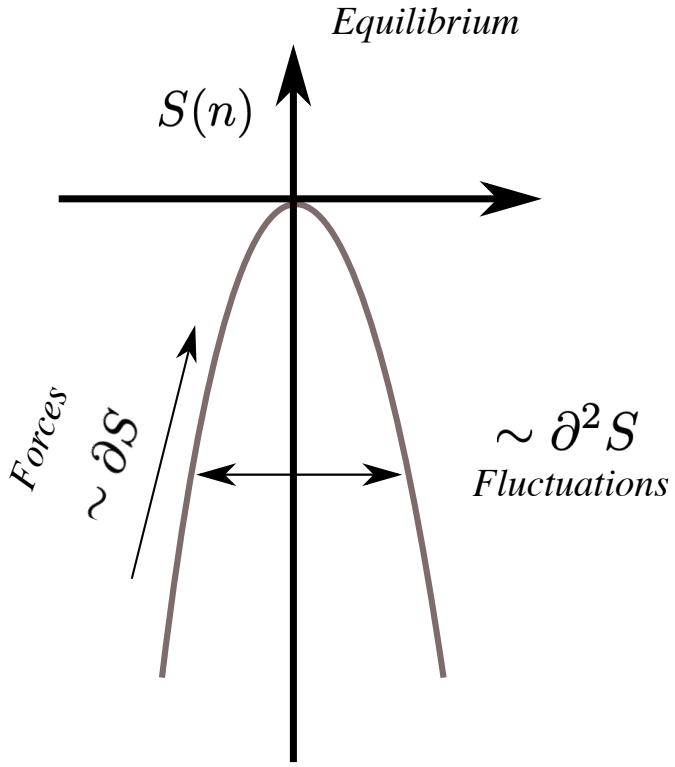

Figure 2.3: :Entropy potential as a function of a thermodynamic observable n. A wide-potential leads to high fluctuations and weak thermodynamic forces, which push the system back to the equilibrium. A narrow-potential leads to small fluctuation and strong thermodynamic forces.

namic system such as proteins or membranes is not always easily accessible. From the phenomenology of phase transitions, it can be shown that all susceptibilities such as compressibility κ_T, heat capacity c_p, electric capacitance C_{el} etc. of the thermodynamic system are proportional (Steppich et al. (2010)).

$$\kappa_T \propto c_p \propto C_{\text{el}} \tag{2.6}$$

The correlation of **all** susceptibilities can be used to estimate difficult accessible observables. The next section will discuss the thermodynamics of a lipid monolayer film at a water-air-interface where a state-phase diagram can be connected to the entropy potential of the interface.

2.2.1 Phase States

The properties of a macroscopic system are completely characterized by its thermodynamic phase diagrams. These diagrams describe the systems interaction with all physical variables (T, p, V, A etc.) and their measurable macroscopic properties. In such a phase diagram every point belongs to a certain state of the system, whereby different states can belong to a specific phase state.
The most common phases surely are the main aggregate states of water. At normal conditions water freezes at 0 °C, i. e. becomes solid, and boils at 100 °C, i. e. changes into the gas phase. These specific temperatures are not fixed but depend on other physical variables of the system such as pressure or the chemical potential as well. All changes of boundary conditions alter the state lines in the phase diagram of the thermodynamic system.
Different phases do not only exist in pure water, but are also present in soft matter, analogously. For example, bilayer made of phospholipids can exist in different phase states and undergo phase transitions. Calorimetric experiments have shown that even in cell membranes (native E. coli membranes) such state changes take place near to the growth temperature (Heimburg and Jackson (2005)).
To simplify, the phase states of a lipid monolayer at an air-water interface are described. With a Langmuir film balance, it is technically possible to create a monolayer based on lipids at an air-water interface and to control the state by area/pressure with a moving barrier (Moehwald (1995)). The general conclusions can also be applied to any other system. **Figure 2.4** shows a typical lateral pressure-area ($\pi - A$) isotherm of a lipid monolayer at an air-water-interface. As mentioned above, the lateral pressure π is also a function of all other variables of the system $\pi(A, pH, T, c[\text{Ions}]^+)$. But the pressure $\pi(A)$ is usually recorded as a function of area at constant temperature, pH etc.
With a large area the lipids are in a gas-like phase, where the carbon chains are in a disordered state and the lipids are decoupled. By compressing, a coherent layer of lipids is formed (**Figure 2.4**(a)). The layer behaves such as a liquid (liquid-expanded-phase or disordered-phase). Further compression leads to a plateau regime, where the area still changes, and the pressure does not. This regime corresponds to the phase transition of the system (**Figure 2.4** (b)). The compression causes a rearrangement of the carbon chains and therefore do not increase the lateral pressure. At the coexistence regime of the monolayer the second derivatives of the entropy potential (susceptibilities) are maximal. **Figure 2.4** also shows the maximum of the compressibility κ_T of the monolayer as a function of the area per molecule A

$$\langle(\delta A)^2\rangle = -k_\mathrm{B}\left(\frac{\partial^2 S}{\partial A^2}\right)^{-1} = k_\mathrm{B} A T \kappa_T. \tag{2.7}$$

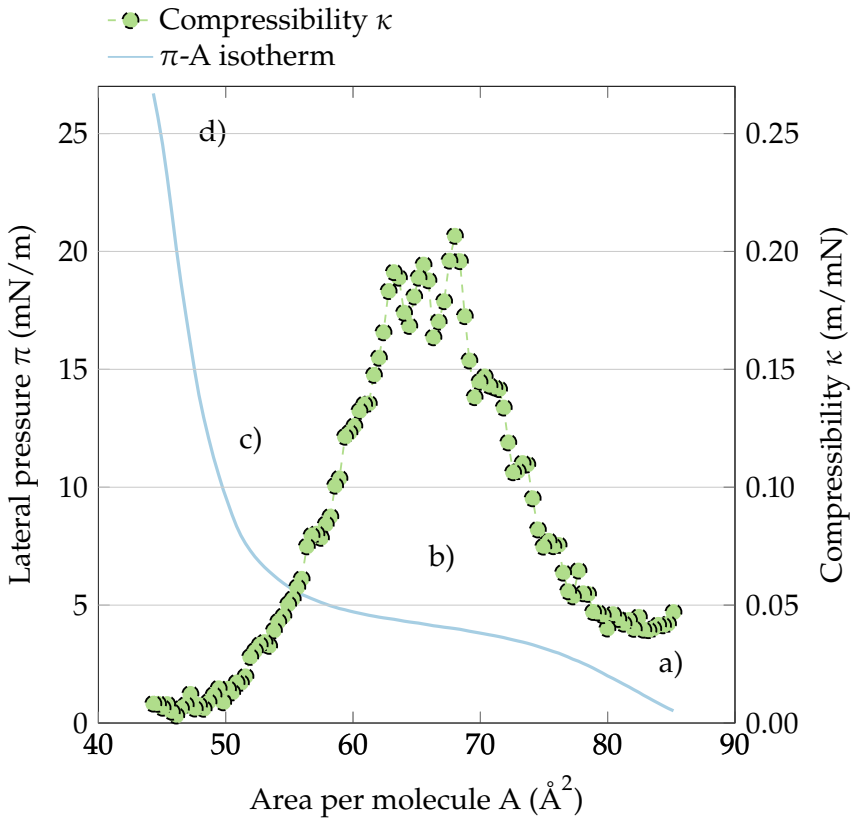

Figure 2.4: Pressure-area isotherm and compressibility κ_T of a DPPC monolayer at the water-air-interface The lateral pressure is plotted as a function of the area per molecule. At the point a) the lipids form a coherent layer and are in the disordered phase. The carbon chains are totally disordered. With increasing pressure, the lipids undergo a transition b). In the transition regime the lateral pressure do not change and a plateau regime is bulit. In the ordered phase (solid) the chains oriented at a small angle to the surface c). Further compression of the density leads to the crystalline phase where the carbon chains are vertical to the surface e). The circles represent the compressibility κ_T as a function of the area per molecule. It shows a significant maximum at the transition regime. The compressibility of the monolayer is also higher at the disordered phase than at the ordered phase.

This means, that during a phase transition of lipids the fluctuations of the area are at a maximum and the entropy potential is wide. Furthermore, the transition yields in a strong nonlinearity of the system, what will be the basis of biological function and nerve pulse propagation described later. When the transition is completed (**Figure 2.4**(c)) the layer is in an ordered phase (liquid-condensed) and the pressure increases linear with decreasing area again. In some case a second phase transition takes place at higher pressures, which is indicated by a change of the slope.
Changes of the state do not only effect mechanical properties of a membrane, but also change the heat capacity or the electrical surface potential. The surface potential is

described by the dipole moments of the lipids, which is determined by the fatty acids and the head groups of the certain lipids. It is indeed observed that the fluctuation of charges and therefore the electrical capacity of the interface is in maximum during transition (Fichtl (2015), Steppich et al. (2010)).
Apart from the lipid monolayer, it is not always possible to measure the pressure/-compressibility or heat capacity of a system to identify a transition regime in a system. One possibility to examine the thermodynamic state is given by optical methods with fluorescent dyes. It has been shown that fluorescent dyes which were embedded into a system change their emission properties at the transition point (Brewer et al. (2010); Parasassi et al. (1998); Shrivastava and Schneider (2013)). Equal to the electrical potential, magnetism or other thermodynamic observables, there is a maximum in an optical susceptibility at the transition. In fact, when a fluorescent molecule is incorporated into a membrane it becomes part of the membrane and cannot be described independently.
In the past many different fluorescent dyes were developed to capture the thermodynamic state/lipid packing of lipid membranes, especially the main disordered-ordered transition. In the literature, several environmental sensitive (solvatochromic) dyes have been reported such as Prodan, Laurdan or di-4-ANEPPDHQ (Dinic et al. (2011); Parasassi et al. (1998)). These dyes are known to change their emission properties such as a blueshift of the emission/absorption spectrum when the membrane becomes stiffer or when hydrational water gets ordered (Parasassi et al. (1991)). The coupling of the fluorescent dye and the lipid membrane will be discussed in more detail in **chapter 2.4.1** .

2.2.2 Two-Dimensional Acoustic Pulses

The formation of different phase states of a lipid membrane are not only consequences of quasi-static changes of the environment. Changes induced by perturbations can affect the state as well if they are strong enough. Such perturbation of the system will propagate through the membrane as a consequence of the conservation of mass and momentum. The propagation of such perturbation, which for example can be triggered with evaporation deposition of solvent molecules at a lipid monolayer, have already been investigated (Fichtl et al. (2016); Griesbauer et al. (2010); Heimburg and Jackson (2005); Shrivastava et al. (2015); Steppich et al. (2010). The velocities of these pulses are between 0.5 m/s and 2.6 m/s (Griesbauer et al. (2010)). Interestingly, the propagation of longitudinal waves within a lipid monolayer fulfils the properties of acoustic sound waves. For example, the velocity depends on the elastic properties of the membrane and follows equivalent to sound the square root of the inverse compressibility $v \propto \sqrt{1/\kappa}$. Consequently, the dynamic change such as the alteration

of the pressure is described by the continuity equation (2.8) and the Euler-equation (2.9):

$$\frac{\partial \rho}{\partial t} + \operatorname{div}(\rho \vec{v}) = 0 \tag{2.8}$$

$$\frac{\partial \vec{v}}{\partial t} + (\vec{v}\,\nabla)\vec{v} = -\frac{1}{\rho}\nabla\pi \tag{2.9}$$

with the velocity v of the single particles, the density ρ and the lateral pressure of the monolayer. To describe the sound waves within a monolayer, we will only deal with longitudinal waves in x-direction. Therefore, in the following $\pi(x,t)$ and $\vec{v_x}((x,t),0)$ applies. Furthermore, only changes in the density ρ' and pressure π' were considered, which are small against the equilibrium values ($\rho' \ll \|\rho_0\|$ and $\pi' \ll \|\pi_0\|$)

$$\rho = \rho_0 + \rho' \tag{2.10}$$

$$\pi = \pi_0 + \pi' \tag{2.11}$$

Additionally, when equilibrium values are independent in time t and location x, a relation for adiabatic processes between density ρ and pressure π can be determined by a Taylor series of π, $\rho' = \left(\frac{\partial \pi_0}{\partial \rho_0}\right)_S^{-1}$. If we also assume this is independent of frequency and amplitude, it can be followed:

$$\left(\frac{\partial \pi_0}{\partial \rho_0}\right)_S^{-1} = m\left(\frac{\partial \frac{1}{A_0}}{\partial \pi_0}\right)_S = -\frac{m}{A_0^2}\left(\frac{\partial A_0}{\partial \pi_0}\right)_S = -\rho_0 \kappa_S \tag{2.12}$$

where $\kappa_S = -\frac{1}{A_0}\left(\frac{\partial A_0}{\partial \pi_0}\right)_S$ denotes the adiabatic compressibility and the density is written as $\rho_0 = \frac{m}{A_0}$ with the area A_0 of the monolayer and the mass of the lipids m. Neglecting terms of second order, this leads to a simplification of **equation** (2.8):

$$\frac{\partial \pi'}{\partial t} = -\frac{1}{\kappa_S}\frac{\partial v_x}{\partial x} \tag{2.13}$$

An additional derivation in time t and insertion in the Euler-equation yields to the general wave equation of the lipid monolayer.

$$\frac{\partial^2 v_x}{\partial t^2} - c^2 \frac{\partial^2 v_x}{\partial x^2} = 0 \tag{2.14}$$

where c denotes the velocity of the sound wave $c = \sqrt{\left(\frac{\partial \pi}{\partial \rho}\right)} = \sqrt{\frac{1}{\rho_0 \kappa_S}}$. With a decoupled system in a biological system such sound-like phenomena should exist. Any

perturbation of the system (here membrane, 2D) can consequently trigger an acoustic wave. Experimentally, it has been shown that the excitation in vicinity to a transition point of the lipids can lead to non-linear acoustic waves (solitary waves) when a specific threshold is crossed.

2.3 Basics of the Nervous Conduction

Since a biological system mainly consists of interfaces, it is high probable that acoustic pulses also exist inside cells. Which role these pulses play regarding to biological function is not clarified yet. However, these pulses have a great similarity to action potentials. In this section the electrophysiological basis of action potentials and the parallelism to a propagating local state change will be discussed in detail.

2.3.1 Resting Membrane Potential

One main property shared by almost all cell types is the difference in ion concentration between inside and outside of the cell. This results in an electro-chemical potential $E([c]_{(i,o)})$ across the interface of the cells, which is described by the Nernst equation

$$E = \frac{RT}{F} \ln\left(\frac{[c]_o}{[c]_i}\right) \tag{2.15}$$

where R denotes the universal gas constant, F the Faraday constant, T the temperature and c the respective concentration inside i and outside o of the cell. The resting potential (equilibrium) typically lies between $-10\,\mathrm{mV}$ and $-200\,\mathrm{mV}$ depending on the cell typ. In table 2.1 the ion concentration of a frog muscle and a squid axon are given. The distributions between cytoplasm and the external medium are mainly similar for potassium, sodium and chloride, whereas for calcium and magnesium the reverse is true. From these concentrations the Nernst potential can be calculated. It should be mentioned here that the description by the Nernst equation is not

Table 2.1: Ionic concentrations in frog muscels and squid axon Aidley (1998).

	Frog muscle		**Squid axon**	
	External	Internal	External	Internal
K^+	2.25	124	20	400
Na^+	109	10.4	440	50
Cl^-	77.5	1.5	560	40
Ca^{2+}	2.1	4.9	10	0.4
Mg^{2+}	1.25	14.0	54	10

applicable, when the concentration of the inner/outer concentration equals zero. Furthermore, the magnitude of the potential is determined by the pre-factor of the equation $RT/F \sim -26\,\mathrm{mV}$ rather than by the natural logarithm.
In general, it is assumed that the potential is mainly defined by the concentration gradients of potassium, sodium and chloride. Therefore, the equilibrium potential is

suggested by considering the gradients and conductivity of the membrane for these specific ions (Goldman equation (2.16)).

$$E_m = \frac{RT}{F} \ln \left(\frac{P_{Na}[Na^+]_{out} + P_K[K^+]_{out} + P_{Cl}[Cl^-]_{in}}{P_{Na}[Na^+]_{in} + P_K[K^+]_{in} + P_{Cl}[Cl^-]_{out}} \right) \tag{2.16}$$

where P_{ion} describe the selectivity of the specific ions, $[ion]_{out/in}$ is the extracellular and intracellular concentration of the ions, R is the universal gas constant, F is the faraday constant and T is the temperature. Other ions such as calcium are not included, although calcium for example is relevant by the motion of muscles etc. Furthermore, experiments by Tasaki showed that nerve cells become inexcitable in absence of external divalent cations (Tasaki et al. (1965)).

The observation that ions can pass through the semi-permeable lipid membrane led to the introduction of the so-called ion-channels. These proteins are incorporated into an excitable cell membrane and are assumed to be responsible for the ion transfer through the membrane, where the ions can pass according to their electrochemical gradient.

This hypothesis is based on the assumption, that ions cannot cross through a pure lipid membrane. By the fact, that only ions of a certain size and charge should pass through the channels, many different ion-channels for Na^+,Cl^-,K^+,Ca^{2+} etc. were postulated. Furthermore, to explain a stable resting potential, ion-pumps had to be introduced, which actively transfer the ions against their electrochemical potential by using metabolic energy derived from the hydrolysis of ATP (*adenosine triphospate*). Without any active transport the membrane potential ΔV collapses. After the hypothesis of channels and pumps was born, the number of different proteins exploded. Today, the number of different channels is well over 100. Also channels for the transport of water molecules through the membrane were established (Dempster et al. (1992)).

The discovery of the patch clamp method in the late 1970s allowed to measure the current across a small spot of the cell membrane. In these experiments a tip of a micropipette is connected to the surface of a cell. After a patch of the membrane is plucked into the pipette orifice, a bias voltage is applied, and the current is measured. There are single steps in current, which were connected to the opening and closing of protein channels. In 1991 Erwin Neher and Bert Sakmann were awarded with the Nobel Prize for the development of the method (Neher and Sakmann (1976); Neher et al. (1978)). The quantization of the current seems to leave no doubt about the channel-hypothesis. However, it has been shown that similar current steps can be measured in pure lipid membranes. In these so-called black-lipid membrane experiments, two compartments of water were connected by a small hole ($\sim \mu m^2$) which is covered by a single lipid bilayer. This bilayer separates the two compartments, and two electrodes were used to record the current flow through the bilayer. Experimentally, single steps in the current across the membrane occur when a bias voltage is applied (Antonov et al.

(2003)). It should be mentioned that these steps only appear at a specific temperature. It has been shown that the conductance of these membranes is controlled by the thermodynamic properties of the lipids (**Figure 2.5**, right, (Wunderlich et al. (2009)). These fluctuations in current are very similar to the open and close-events in patch-

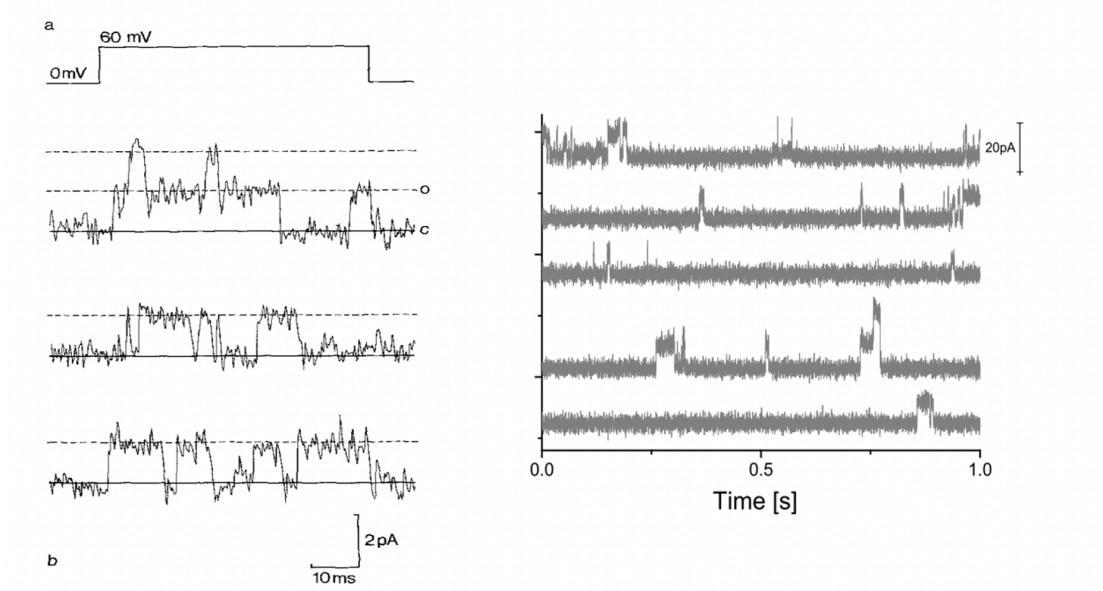

Figure 2.5: (Left) Channel current recordings from cell-attached patches (figure taken from (Edwards et al. (1989)). (right) Typical current trace in black lipid membrane experiment at the phase transition regime of the lipids (figure taken from (Wunderlich et al. (2009)).

clamp experiments of cells (**Figure 2.5**, left (Edwards et al. (1989)). Consequently, protein channels are not necessarily the origin of these fluctuations (steps) in current. But not only lipid membranes show this step-like behavior. Furthermore, the laboratory of Fred Sachs (Sachs and Qin (1993)) replaced the cell membrane with a silicon rubber and the channel events do not disappear. This demonstrates that the foundation of these phenomena cannot be related to the nature of single molecules (proteins, lipids etc.), but rather to a deeper physical principle of interfaces. Nevertheless, also with the knowledge of these experiments the hypothesis of the channels and pumps is still the main accepted theory and is also used to describe nerve pulse propagation.

2.3.2 Electrophysiological Action Potential

Alterations of the membrane potential occur among other phenomena during the propagation of nervous pulses, also known as action potentials. These are one of the main mechanisms of cellular communication. The action potentials are present in

neurons, but also in several other kind of cells such as muscle cells or plant cells. The signals propagate between cells or to synapses and control activities of cell reactions and build the basis of communication in an organism. An action potential is a nonlinear pulse with threshold and amplitude saturation (all-or-none characteristic). In other words, the amplitude of the action potential is independent of the excitation strength when a pulse is triggered.

In standard textbooks this phenomenon is described as a transient electrical change of the membrane potential of the cells. In the 1950s Hodgkin and Huxley mathematically described these cell activities as an electrical circuit with capacities and resistors (Hodgkin and Huxley (1952a)). **Figure 2.6** (left) shows the conceptual circuit of this model. The channel proteins are represented by resistors and the membrane by a capacitance. It is assumed, that the concentration gradients worked as a battery and the electromotive force is given by the Nernst-equation. Sodium and potassium in particular are supposed to be crucial. Other ions, which should mainly be chloride, are described by E_{leak}. The batteries are in serial connected to the resistors. The resistors are variable and are determined by the permeability of the ions. To develop this model Hodgkin and Huxley studied the membrane potential of a giant squid axon. They inserted electrodes into a squid axon to measure the ion current which flows through the membrane when the membrane potential suddenly changed from the resting state and held at the new level constant (voltage clamp; Hodgkin and Huxley (1952b)). From these experiments, they concluded that the action potential is based on discrete currents of specific voltage gated ion channels. The conductance of these channels are switched off and on by changes in the membrane potential.

The right-hand side of **Figure 2.6** displays a typical electrical response of the

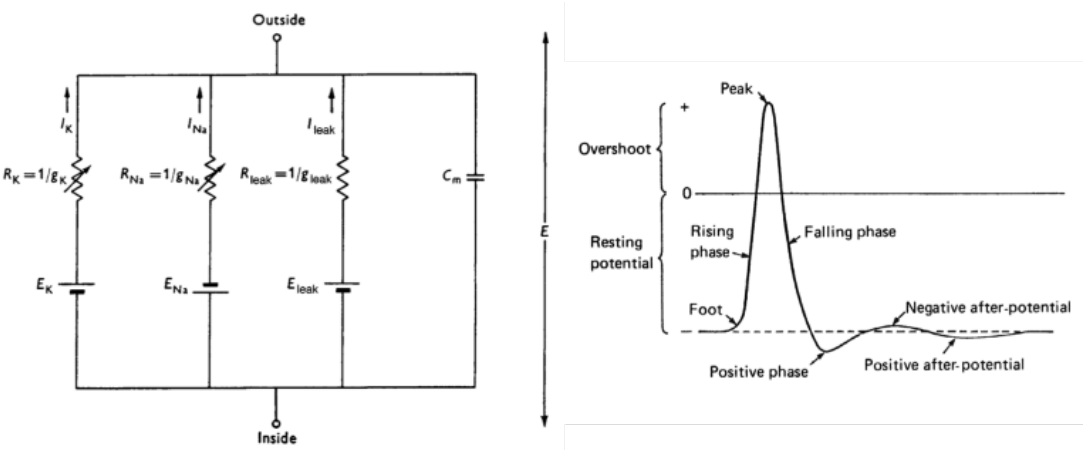

Figure 2.6: Conceptual model of the action potential. (left) The electrical circuit of a cell membrane. The ion channels are represented as resistors R_{Na}, R_{K}, R_{leak}. and the membrane as the capacitance C_m. The variable resistors are proportional to the open voltage gated channels. (Right) The Diagram shows the nomenclature applied to an action potential (figure taken from (Aidley (1998)).

cell membrane potential to an action potential. An excitation is followed by the rising phase of the membrane potential (depolarization), which is described by a short opening of sodium channels and therefore changing the flow of sodium through the membrane. Afterwards, the permeability of potassium increases, and the membrane potential repolarizes (falling phase). In some cells, the membrane potential undershoots (hyperpolarization) the resting potential after the pulse. It persists until the permeability returns to the equilibrium state. This is explained by the assumption that the K^+-channel proteins do not close directly when the resting potential is reached. These changes during an action potential are in neurons about 100 mV in 1-100 ms.
Based on experiments by Cole and Curtis (Cole and Curtis (1938)) the capacitance was defined to be independent of changes in voltage. Therefore, it has to be assumed that the capacitance of the membrane does not change during the propagation of the action potential. However, it has been shown that a swelling of the cell surface appears during nerve pulses (Fillafer et al. (2018); Tasaki (2008); Tasaki (1999)). This means, that the capacitance has to differ ($C = \epsilon A/d$; dielectric constant ϵ, area A, separation of the plates d), which the model does not contain. Furthermore, while Cole and Curtis observed that the capacitance remained unchanged at mainly 20 kHz, in 1979 Takashima measured a change of the capacitance at lower frequencies (Takashima (1979)).
Additionally, based on the Goldman equation only potassium and sodium play a central role for nerve pulse propagation. But in the past, experiments have shown that the propagation of an action potential is also in absence of potassium or sodium possible (Tasaki (1999)). The restriction of the mechanism to these two specific ions seems therefore to be misleading. Also, other aspects that additionally occur to the changes of the transmembrane potential during nerve pulse propagation are not even included to the model.
The propagation of the action potential through the membrane is mathematically described by the cable theory. A central point are different variations of the cable equation, a partial differential equation of the membrane potential $V(x,t)$

$$\frac{1}{r_\mathrm{l}}\frac{\partial^2 V_\mathrm{m}(x,t)}{\partial x^2} = c_\mathrm{m}\frac{\partial V(x,t)}{\partial t} + \frac{V_\mathrm{m}(x,t)}{r_\mathrm{m}} \tag{2.17}$$

where c_m represents the capacitance of the membrane, r_m is the transversal resistance of the current through the membrane and r_l describes the longitudinal resistance. The linear cable equation (2.17) only holds if the membrane properties are constant.

2.3.3 Local Propagating Phase Transition

Many different works, but especially Tasaki showed that the action potential is also accompanied by mechanical, thermal, optical, magnetic alterations (Tasaki (1999); Ritchie and Keynes (1985); Tasaki et al. (1968); Wikswo et al. (1980)). A mechanical deformation, changes in birefringence and turbidity as well as an increasing temperature followed by a decreasing temperature propagate along the cells. The question arises which properties of a system are important for action potentials and what are possible triggers of such pulses? A complete physical description should include all aspects and manifestation of the phenomenon what is not fulfilled in the Hodgkin and Huxley-Model. The reversible heat release and the overall conservation of entropy is indeed a typical property of sound.
According to a theory suggested by Konrad Kaufmann the nerve pulse propagation is based on nonlinear acoustic pulses propagating through the interfaces of cells. Any perturbation can cause a local phase transition which propagates along a lipid bilayer, based on the conservation of momentum and mass. The authors T. Heimburg and A. Jackson extended this theory and stressed the importance of nonlinear state changes during the propagation (Heimburg and Jackson (2005)). In this description only a nonlinearity in vicinity of the equilibrium state is needed to excite such pulses.
In the past, acoustic pulses have been excited in lipid-based interfaces in the vicinity of a disordered ordered transition. These acoustic pulses are in the simplest case defined by the phase state of the system such as velocity ($v \propto \sqrt{(\rho/\kappa)}$) or threshold behavior as described above. According to the theory, these density pulses at the interface share some main properties of action potentials in cells.

1. Nonlinear acoustic pulses in a lipid monolayer near a phase transition show such as action potentials in living systems a saturation of the amplitude and a threshold behavior. This means that a pulse can only be triggered above a specific excitation strength. When this threshold is reached a pulse with the full amplitude propagates through the medium even when the excitation strength is increased (all-or-none principle) (Shrivastava and Schneider (2014)).
2. In living systems action potentials interact upon collision (Follmann et al. (2015); Fillafer et al. (2017); Tasaki (1949)). Depending on the state of the lipid monolayer it has been experimentally demonstrated that acoustic waves at a monolayer can also interact linearly, nonlinearly or annihilate upon collision (Shrivastava et al. (2018b)).
3. The velocity of action potentials varies by order of magnitudes between different organisms (Beilby (2007); Leys (2015)). Lipid systems have shown velocities in similar orders of magnitudes (Shrivastava and Schneider (2014); Shrivastava et al. (2015); Griesbauer et al. (2012)).

4. As mentioned above action potentials are not a purely electrical wave, but rather a manifestation of all variables (electrical, chemical, optical, thermal, mechanical etc.). Nonlinear acoustic pulses influence not only temperature and pressure such as common acoustic waves (e. g. speaking, music), but they are strongly coupled to chemical reactions at the interface. The coupling of the physical observables is described by Maxwell relations.
   Experimental, it has been shown that acoustic pulses in lipid-based systems were identified in multiple variables such as pH, pressure, surface potential etc. (Fichtl et al. (2018); Fichtl et al. (2016)) such as an action potential.

The propagating phase transition could not only influence enzyme activity and transport processes through the membrane, but also control cell processes. Thereby the communications between cells or organs are not determined by the complexity of all molecules but only by the state of the system. Which does not mean that the composition of the system/interface does **not** matter in any sense but rather it offers the opportunity to regulate the state of the interface and therefore control the biological function.

2.4 Fluorescence as an Observable of the Thermodynamic State

Several studies have used fluorescent dyes to characterize the macroscopic properties such as membrane packing (Jin et al. (2006)), electrical potential (Gross et al. (1994)) or chemical reactions etc. in biological systems. With a typical timescale of nanoseconds, the fluorescence provides the opportunity to study rapid processes at the interface of the cell such as nerve pulse propagation ($t \sim$ ms). Furthermore, these experiments offer the possibility to correlate several parameters such as rotation and diffusion of molecules, as well as local pH, polarity, hydration or ion concentrations. For this purpose, various dyes have been developed. Among others, some dye molecules specifically change their emission properties with the solvation shells such as Laurdan, Prodan, Di-4-ANEPPDHQ (Dinic et al. (2011); Parasassi et al. (1998)) or with the electric fields of the environment such as the ANEPP-family (Obaid et al. (2004)). Different solvents lead to an alteration of the emission spectrum of such fluorescent dyes. In this work the initially potentiometric designed dye Di-4-ANEPPDHQ (Obaid et al. (2004)) is used, which has also been applied to detect lipid packing (Amaro et al. (2017); Sezgin et al. (2014)).

2.4.1 Fluorescence

A fluorophore is a molecule which absorbs a photon with a specific wavelength and reemits a photon with a different specific wavelength. The absorption energies and energy of the re-emitted photons depend on the fluorophore and the surrounding chemical environment. The absorption of photons by molecules is described by the Lambert-Beer law. The decrease of the intensity dI depends on the thickness of the passed medium dx and the absorption constant α

$$-dI = \alpha \cdot I \cdot dx \tag{2.18}$$

When approximating the cross section of a molecule and considering the speed of light, the time constant of this absorption typically is about 10^{-15} s. Additionally, the absorption of light is connected to the energetic excitation of a molecule from the state E_m to a state E_n. The distribution of the energy states E_i is given by the Boltzmann-distribution

$$N_i \propto N \exp\left(-\frac{E_i}{k_\mathrm{B}T}\right) \tag{2.19}$$

Let E_n be the energy of an electronic state of a molecule and E_m the energy of the next higher subshell that does not contain electrons (Pauli exclusion principle). When the energy of an incoming photon carries the energy difference ΔE corresponding to the different energy levels

$$\Delta E = E_n - E_m = E_\mathrm{Photon} = h\nu \tag{2.20}$$

where h is the Planck constant and ν the frequency of the electromagnetic radiation, a photon can be absorbed. Additionally, a molecule has rotational, vibrational levels which can be excited by an incident electromagnetic wave. In general, the transition between the states of a molecule has different probabilities and therefore some absorption/emission lines will be more probable than others. In general, fluorescence only occurs with electronic excitation, whereby an electron will jump to a vacant higher energy level with the energy $E_n + E_\mathrm{Photon} = E_m$.
The energy which is necessary to excite the molecule/atom is comparable to the separation of the orbitals of atoms and is about 1 eV to 10 eV. This corresponds approximately to a wavelength of 1250 nm to 125 nm. In first order approximation the electronic excitation mainly occurs at the visible and the ultraviolet range of light.
Fluorescence occurs when a singlet state of the molecule is excited. In this case all electrons are paired in up and down spin pairs. After excitation, different processes can lead to a return to the ground state. The electron can immediately drop back to the ground state (elastic scattering) and a photon with the same wavelength as the

incoming photon is emitted. Furthermore, some part of the energy can be lost by vibrational relaxation processes and the electron drops down to lower vibrational modes of the excited state. After this relaxation process (10^{-12} s - 10^{-10} s) the electron can fall to the ground state under the emission of a photon with lower energy as the incoming photon. Thereby, the emission spectrum is shifted compared to the absorption to lower energies. This radiationless loss of the energy level is called Stoke-Shift. In general, the interaction processes follow the Franck-Condon-Principle.

In general, molecules relaxate at different vibrational ground state from a unit electronic excited state. The shape of the emission spectrum only depends on the location of the vibrational level of the ground state. The lifetime of this process normally is in the range of nanoseconds. Organic fluorescent dyes are mostly built out of many atoms with a variety of complex vibration spectra. Therefore, many ways exist how the dye falls into the lowest vibrational level.

2.4.2 Fluorescence and Phase State

This work is motivated by the role of thermodynamic states of the interfacial environment of molecules inspired by K. Kaufmann and his studies about the action potential and catalysis (Kaufmann (1989b)). The theory follows Einsteins approach of thermodynamics. In this section, the phenomenon of fluorescent emission will be discussed and placed into the picture of thermodynamics.
Firstly, all observables of a system have to obey the second law of thermodynamics and therefore have to fluctuate. These fluctuations can be extracted from the thermodynamic state diagrams (area-pressure, calorimetric, etc.). According to these predictions, also a fluorescent dye molecule has to follow these fluctuations. In general, the emission frequency of a fluorescent dye is determined by the energy difference between the ground and the excited state of the single molecule. A specific state provides a specific frequency. Without any fluctuation (e. g. at 0 K) the dye molecule should only have a single emission state and therefore emission lines occur rather than an emission spectrum. But since there are fluctuations of the quantum mechanical state (vibrational, rotational etc.), these fluctuations lead to spectral emission. Furthermore, the width of the emission spectrum is a function of the temperature T and therefore has to be an observable of the thermodynamic state. In vacuum, these fluctuations are related to the distribution of the energy levels of the single molecules. From Planck's

law A. Einstein derives the relative energy fluctuations $\langle \left(\frac{\epsilon}{E}\right)^2 \rangle$ (Klein et al. (1993))

$$\rho(\nu) = \frac{8\pi h\nu^3}{c^3} \frac{1}{e^{h\nu/k_B T} - 1} \quad \text{(Planck's law)} \tag{2.21}$$

$$\langle \left(\frac{\epsilon}{E}\right)^2 \rangle = \frac{h\nu}{E} + \langle E \rangle \frac{c^3}{8\pi\nu^2 V d\nu} \quad \text{(fluctuations)} \tag{2.22}$$

with the frequencies ν, the Volume V, Planck constant h and the speed of light c. The distribution of the quantum mechanical states of the excited molecules lead to an energy distribution of the emitted photons. It can be concluded, that the width of the spectral emission reflects the probability distribution of the radiation energy.

This situation significantly changes when we look at a solvent-dye complex. Now, the emission energies are also affected by the interaction energy between solvent and dye molecules (s. **Figure 2.7**). In vacuum there are two states, the ground state and the excited state of the fluorescent molecule, which are only determined by the energy levels of the dye molecule (**Figure 2.7** left-hand side). When a solvent can interact with the dye, these energy levels are changed (**Figure 2.7** right-hand side). Therefore, an additional interaction energy term $\Delta E_{\text{Solvent}}$ must be added to the vacuum emission energy ΔE_{vac}

$$\Delta E_{\text{em}} = \Delta E_{\text{vac}} - (\Delta E^*_{\text{sol}} + \Delta E^0_{\text{sol}}) = \Delta E_{\text{vac}} - \Delta E_{\text{Solvent}} \tag{2.23}$$

This additional term $(\Delta E^*_{\text{sol}} + \Delta E^0_{\text{sol}})$ is usually described as solvatochromic properties of the dye molecule. In this case, the emission energy is also related to the local chemical environment.

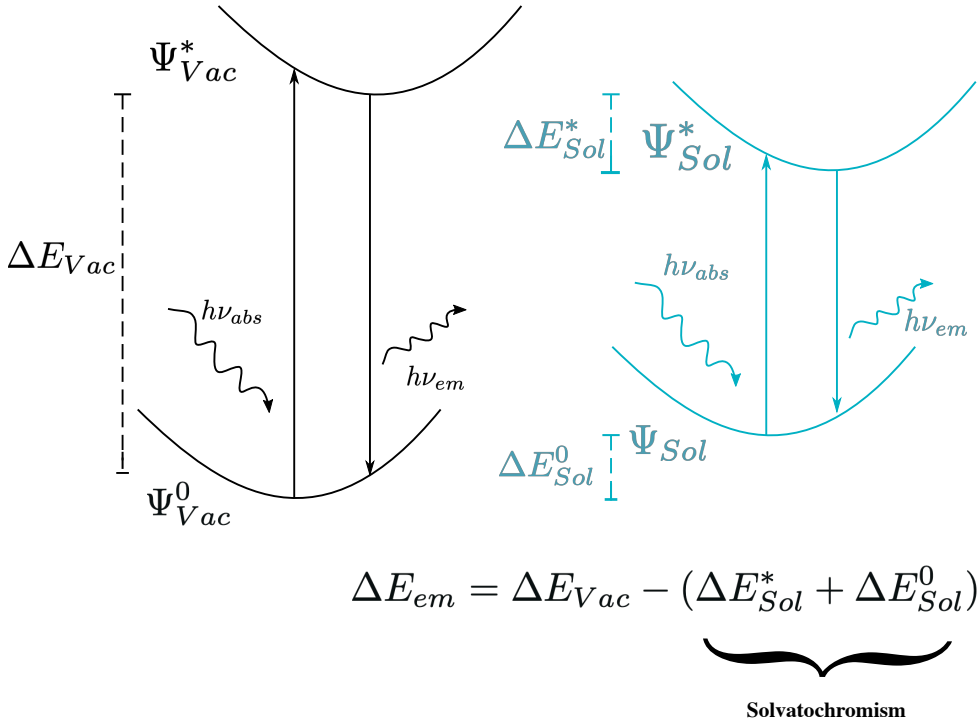

Figure 2.7: Schematics of the fluorescence emission energy. A schematic representation of an excitation process and the variation in energy of the excited state of the fluorophore in a solution. The absorption of a photon creates an excited electron state of the fluorophore. In vacuum there are the two energy levels Ψ^*_{vac} and Ψ^0_{vac}. The difference between these levels ΔE_{vac} corresponds to the emission energy (wavelengths). When a solvent molecule interacts (solvent shell) with the dye molecule the different energy levels Ψ^*_{sol} and Ψ^0_{sol} occur. Due to the interaction, the emission energy is typically lowered.

Solvatochromism describes the process of changing energy levels of fluorescent dyes as a function of the polarity of the surrounding solutes. A description of the spectral shift with dipole moments of the dye molecule and properties of the solvent is given by the Lippert-Mataga-equation:

$$\Delta\nu = \nu_{\text{abs}} - \nu_{\text{em}} = \frac{2(\mu_e - \mu_g)^2}{chc^3}\left[\frac{(\epsilon_S - 1)}{(2\epsilon_S + 1)} - \frac{(n^2 - 1)}{(2n^2 + 1)}\right] \tag{2.24}$$

The shift is described by the dipole moments of the fluorophore of the excited μ_e and the ground state μ_g, the properties of the solvent (refraction index n and dielectric constant ϵ_s), the speed of light c, the Planck-constant h, and the Onsager radius a. One criticism is that the description assumes a spherical chromophore which is not a good approximation for big fluorescent molecules. Furthermore, the interaction between the solvent molecules is not included. This means that when the dye molecule is part of a system a simple combination of the single solvent and the single dye properties will not give a physical description. Such as the compressibility at the melting point of water is not a superimposition of the compressibility of ice and water, the dye-solvent complex has to be treated as a new thermodynamic state with new properties. Therefore, the dielectric constant and the refraction index are unknown variables of the state of the solvent shell.
However, the fluctuations of the electrostatic interaction energy δE should be related to the fluctuations of the frequencies ν_{em} of the emitted photons

$$\langle \delta E_{\text{Sol}}^2 \rangle \propto h \langle \delta \nu_{\text{em}}^2 \rangle \tag{2.25}$$

If a coupling exists between the dye and the surrounding solution, the emission spectrum of the dye has to change with different solvation shells (states). In the case of the used fluorescent dye Di-4-ANEPPDHQ, it can be shown that the emission properties indeed alter with different solvent molecules (s. **Figure 2.8**). Here, 1 mM of Di-4-ANEPPDHQ was disolved in the different solvents, respectively. The emission spectrum was recorded by a spectrum analyzer (Wasatch Photonics). In general, the interaction between solvent and fluorescent dye molecule leads to lower frequencies in emission. In **Figure 2.8** it can be seen that higher polarity led to a lower emission frequencies (higher wavelengths). This means, that the interaction energy between dye and solvent increases when the polarity increases.
It has to be expected, that fluctuations in one observable effect another. For instance, fluctuations of the area of a lipid layer are directly coupled to fluctuations of the surface charge or dipole density including surfacial proton or ion concentrations and this will also change the surface potential. Here the interaction with the dipole moments of the solvation shell seems to be the origin of the changes in the emission spectrum.

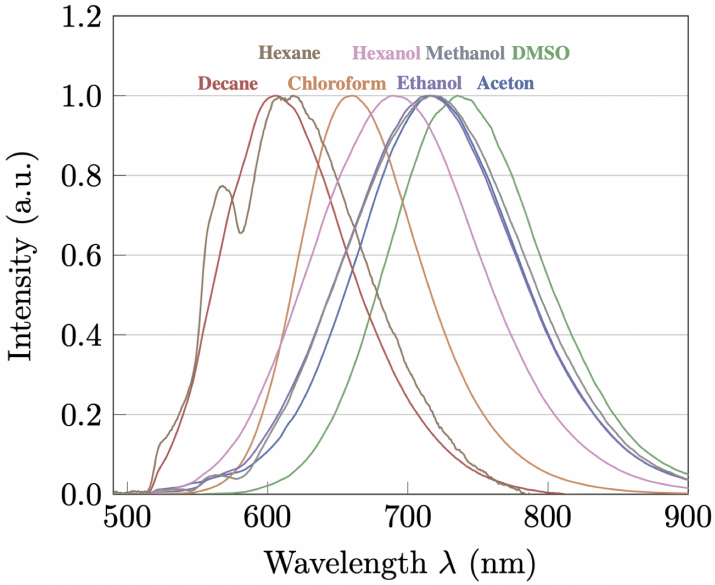

Figure 2.8: Emission spectrum of the dye molecule Di-4-ANEPPDQH in different solvents. The emission spectrum of the fluorescent dye shifted with different solvent molecules to different emission maxima. From left to right: Decan, hexane, chloroform, hexanol, ethanol, methanol, aceton, DMSO.

When the dye is embedded into a lipid system, the lipid molecules become the solvent. The fluctuations of this complex are just maximal in the phase transition of the lipids as described in section 2.2.1. From this it can be concluded that the width of the emission spectrum is also maximal and directly correlated to the thermodynamic susceptibilities of the complex such as the heat capacity c_p etc.

$$\langle \delta H^2 \rangle \propto \langle \delta \lambda^2 \rangle \propto c_p \tag{2.26}$$

Structural changes of the lipid matrix and therefore changes of the dipole density are potential triggers for changes of the emission of the fluorophore. However, it is important to say that this correlation between emission spectrum and enthalpy/dipole density is not of an electrical origin. The parameter which are accessible in experiments are all related to the state of the interface.

Based on the theory of Konrad Kaufmann we have to look at the entropy of the interface. The following is inspired by the works of B. Fichtl about catalysis (Fichtl (2015)) and S. Shrivastava about fluorescence (Shrivastava et al. (2018a)).

The dye molecule interacts with the lipid interface so that we get two subsystems which are not independent of each other. Let us assume that E_F is the energy of the fluorophore and E_I is the energy of the rest of the interface (mainly water and lipids). Thus, the entropy potential is determined by the energy of the entire interface (subsystem 1 + subsystem 2). Taylor expanding the entropy potential for the two

energies (E_I, E_F) at the equilibrium yields:

$$\begin{aligned} S(E_I, E_F) = &\frac{\partial S}{\partial E_I}\delta E_I + \frac{\partial S}{\partial E_F}\delta E_F + \frac{1}{2}\frac{\partial^2 S}{\partial E_I^2}\delta E_I^2 + \frac{1}{2}\frac{\partial^2 S}{\partial E_F^2}\delta E_F^2 \\ &+ \frac{\partial^2 S}{\partial E_I \partial E_F}\delta E_I \delta E_F \end{aligned} \tag{2.27}$$

With an entropy maximum at the equilibrium energies (E_I^0, E_F^0), we get $\frac{\partial S}{\partial E_I} = \frac{\partial S}{\partial E_F} = 0$ and equation (2.27) can be reduced to:

$$S(E_I, E_F) = \frac{1}{2}\frac{\partial^2 S}{\partial E_I^2}\delta E_I^2 + \frac{1}{2}\frac{\partial^2 S}{\partial E_F^2}\delta E_F^2 + \frac{\partial^2 S}{\partial E_I \partial E_F}\delta E_I \delta E_F \tag{2.28}$$

Using some thermodynamic relations, the first term of the equation can be simplified to

$$\frac{1}{2}\frac{\partial^2 S}{\partial E_I^2}\delta E_I^2 = \frac{1}{2}\frac{1}{T^2 c_I}\delta E_I^2 \tag{2.29}$$

where c_I is the heat capacity of the interface. Analogously, the second term can be written as:

$$\frac{1}{2}\frac{\partial^2 S}{\partial E_F^2}\delta E_F^2 = \frac{1}{2}\frac{1}{T^2 c_F}\delta E_F^2 \tag{2.30}$$

with the heat capacity c_F of the fluorophore subsystem. These two terms are independent and describe the two subsystems, the interface (lipids and water) and the dye molecules. The changes of the energy of the emission are assumed to be correlated to the change of the interaction energy between the dye molecules and the rest of the interface $\delta E_F = \delta(E_{\text{vac}} + \delta E_{\text{sol}}) \propto \delta E_{\text{sol}}$.
Thus, the third term of equation (2.28) (coupling of the subsystems) yields:

$$\frac{\partial^2 S}{\partial E_I \partial E_F}\delta E_I \delta E_{\text{sol}} = \frac{1}{T}\frac{\partial}{\partial E_{\text{sol}}}\frac{1}{T}\delta E_{\text{sol}}\delta E_I = -\frac{1}{T^2}\frac{\partial T}{\partial E_{\text{sol}}}\delta E_{\text{sol}}\delta E_I \tag{2.31}$$

Using all terms and that the changes of the emission energy is proportional to the changes of the emission frequency $\delta E_{\text{sol}} \propto \delta \nu_{\text{em}}$ we get the entire entropy potential:

$$S(E_I, E_{\text{sol}}) = -\frac{1}{2T^2}\left(\frac{1}{c_I}\delta E_I^2 + \frac{1}{c_F}\delta E_F^2 + 2\frac{\partial T}{\partial \nu_{\text{em}}}\delta \nu_{\text{em}}\delta E_I\right) \tag{2.32}$$

The third term describes the coupling between the fluctuations of both subsystems. The coupling parameter $\left(\frac{\partial \nu_{\text{em}}}{\partial T}\right)^{-1}$ can directly be measured, independently. Phenomenological, it has been shown that there is a discontinuity of the emission frequency $\nu_{\max}$

of solvatochromic dye molecules at a disordered-ordered transition of a lipid-dye system (Parasassi et al. (1998)). This is equivalent to a jump in the interaction energy of the lipid-dye complex. In this view, the wavelengths (frequencies) of the emission maximum represent the interaction energy. This means on the one hand, that high fluctuations of the lipids are represented by higher susceptibilities during the transition (high heat capacity). On the other hand, a jump of the emission energies indicates that also the coupling of the subsystems is in a maximum. Therefore, it can be concluded that the fluctuations of the emission also have to be maximal which is equivalent to a wide emission spectrum at a transition point.
Experimentally, it should be possible to determine the phase state of the chemical environment of a biological system by the change of the fluorescent emission. It is of course still crucial which system is observed or where the dye molecules are embedded, respectively. Furthermore, only relative changes of the emission wavelengths indicate a phase transition because each system (neurons, plant cells, vesicles etc.) will in turn have a different microscopic state. Therefore, the position of the emission peak does not allow any statement about the phase, whereas the width of the emission spectrum is indeed a direct indicator of a transition. The fluctuations of the environment are clearly connected to the fluctuation of the dye molecule. The dye-solvent complex has to be treated as a phenomenological thermodynamic observable.
By measuring the emission property of the fluorescent dye (width, wavelength, lifetime etc.) consequences for the entropy potential of the observed system can be concluded. In the literature there is clear evidence that the emission spectrum of a solvatochromic dye molecule shifts with the ordering of a lipid membrane (Jin et al. (2006); Jin et al. (2005); Parasassi et al. (1998)). Therefore, these dyes are used to observe phase transitions in artificial systems. How the emission spectrum actually depends on the surrounding and lipids whether there is a coupling, will be discussed in experiments with artificial and biological systems in the next chapters.

Phase State of Soft Matter

3 Phase State of Soft Matter

3.1 Introduction

Lipid membranes do not only separate interior and exterior compartments of cells but also several processes including protein-interaction take place at the biological interfaces. Furthermore, artificial membrane systems such as vesicles or monolayers at the air-water interface show that lipids can undergo phase transitions. These transitions are assumed to play an important role in biological processes such as nerve pulse propagation (Heimburg and Jackson (2005); Kaufmann (1989a)). The experimental evidence of a phase transition in an intact membrane of living cells are scarce and is still challenging.
Changes in emission properties of fluorescent dyes have been often used to study biological functions and structures in physics and biology. In particular, dyes indicate changes in ion concentrations or electrical potential when embedded into cell structures (interfaces). Accepting the HH-theory of APs, fluorescent dyes are usually described as sensitive to the membrane potential (electrochromic dyes). But these dyes are often specific to different variables, depending on the experiment. It is believed that a response mechanism could be suppressed in one experiment and offers new interpretation at different experimental conditions:

> *"Unfortunately, it is always possible that a response mechanism which is suppressed in one experiment, say a model membrane, may emerge in a different application of the same probe. This is the main reason, we believe, that our hopes for a universal electrochromic probe have proven unrealistic"*(Loew et al. (1992)).

Thereby new applications of the same dye were constructed. Theoretically, the emission properties such as wavelength or energy distribution of the fluorescent dye molecules are strongly correlated to the thermodynamic state of the observed system. Such as the linear relationship between compressibility, heat capacity thermal expansion coefficient and electric capacity, solvatochromic dye molecules show this proportionality to the state.

Here, the fluorescent dyes LAURDAN or Di-4-ANEPPDHQ (s. **Figure 3.1**) incorporated into artificial lipid membranes are experimentally characterized in static

state diagrams and dynamic pulse experiments in order to establish the thermodynamic phenomenology to fluorescent dyes in biological systems. Furthermore, it is demonstrated that the relationship between enthalpy and area or enthalpy and charge consequently leads to a linear relationship between the emission wavelengths and enthalpy of the system.

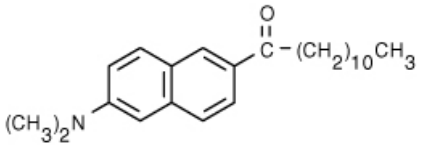

LAURDAN (6-Dodecanoyl-2-Dimethylaminonaphthalene)

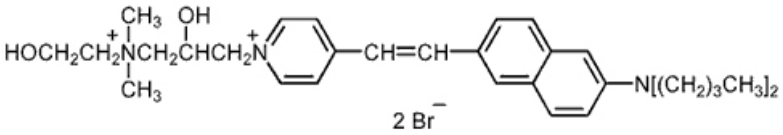

Di-4-ANEPPDHQ

Figure 3.1: Chemical structure of solvatochromic fluorescent dyes LAURDAN and Di-4-ANEPPDHQ.

3.2 Material and Methods

3.2.1 Chemicals

Di-4-ANEPPDHQ was purchased from Thermo Fisher Scientific and dissolved in chloroform (1 mg/mL). The three types of phospholipids, 1,2 dimyristoyl-sn-glycero-3-phospho-L-serine (DMPS), 1,2-dilauroyl-sn-glycero-3-phospho-L-serine (DLPS) dissolved in chloroform:methanol:water (65 : 35 : 8) and 1,2-dimyristoyl-sn-glycero-3-phosphocholine (DPPC) dissolved in chloroform were obtained from Avanti Polar Lipids. LAURDAN and all other reagents were purchased from Sigma Aldrich.

3.2.2 Phospholipids

For vesicle preparation, 10 µL Di-4-ANEPPDHQ (or LAURDAN) dissolved in chloroform (1 mg/mL), was added to 100 µL of a lipid solution (10 mg/mL)to get a 100 : 1 lipid to dye ratio. The lipid-dye solution was dried under nitrogen ux and held in a vacuum chamber for 12 h to completely evaporate the solvent. To prepare vesicles, ultrapure water (600 µL) was added to hydrate the lipids. The solution was held above the melting temperature of the respective lipids ($T > T_m$) for 30 min and was vortexed every 10 min to yield unilamellar and multilamellar vesicles. The emission spectrum of the aqueous suspension was recorded with a spectrum analyzer (Wasatch-Photonics-VIS-NIR-spectrometer) while the temperature was controllably varied by a heat bath (Lauda Eco Silver).
The fluorescent dye was excited with high power LEDs with maximum wavelength at 380 nm for the excitation of Laurdan or at 470 nm for the excitation of Di-4-ANEPPDHQ, respectively. The LED was triggered to avoid bleaching of the fluorescent dye during the measurement. The integration time of the spectrum analyzer was between 300 ms and 2000 ms to collect enough light for detecting the entire emission spectrum. Before each measurement, the background signal of the pure water solution was measured and subtracted in the analysis.

3.2.3 Lipid Monolayer

A schematic view of the monolayer setup is presented in **Figure 3.2**. The film balance had a maximum area of 275 cm^2 and a minimum area of 75 cm^2. Barriers made of Teflon were used to control the area for quasi static compression/expansion with a speed of 10 cm^2/min. The lateral pressure of the lipid film was measured with a Wilhelmy-Plate.

To form a lipid monolayer, the lipid solution (1 mg/mL) with a final concentration of dye molecules (DI-4-ANEPPDHQ, LAURDAN) up to 4% per mole were carefully spread to an air/water interface on a Langmuir though (NIMA Technology Ltd. Conventry England). To measure the fluorescent emission the spectrum analyzer (Wasatch-Photonics-VIS-NIR-spectrometer) was used which was connected to a fluorescence microscope. Before detecting the emission spectrum, 5 minutes were waited to completely evaporate the solvent. The dye molecules formed domain structures, where some domains emitted a higher fluorescence signal than others. To suppress the diffusion of these domains, pieces of Teflon were built around the optical measuring spot. When the dye signal disappeared (the intensity became too low), a few microliter of the lipid-dye solution were spread again. Depending on the measurement, salts and buffer were added to the ultrapure water (MilliQ) sub-phase.

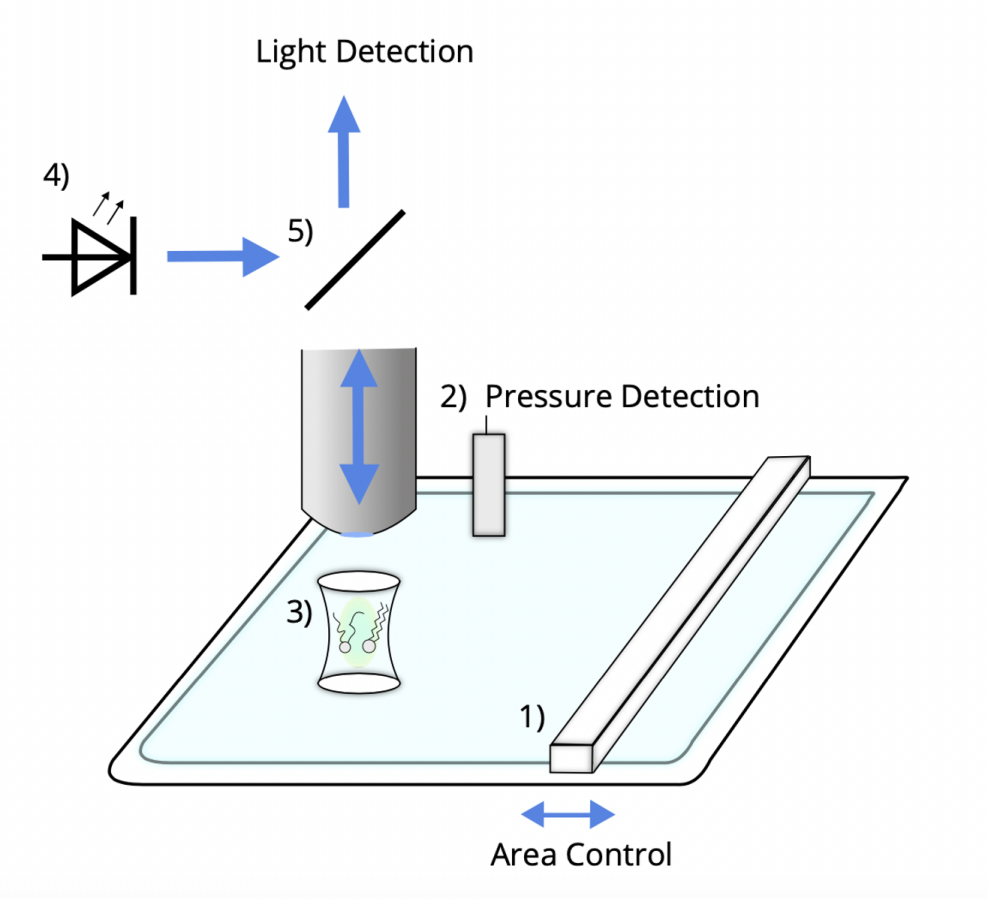

Figure 3.2: Langmuir film balance with optical measurement: The Teflon barrier (1) was used to control the area of the lipid monolayer. The speed of compression/-expansion for quasi static experiments was 10 cm^2/min. A pressure sensor with a Wilhelmy-plate (2) detected the lateral pressure of the surface. To record the emission spectrum, a fluorescence microscope was connected to the though ((3) Field of View (FOV)). A high-power LED (4) was used for exciting the fluorescent dye embedded into the lipid monolayer (Laurdan or Di-4-ANEPPDHQ). The excitation light was separated from the signal by a dichromate mirror (5). To detect the emission, a Spectrum analyzer for the entire emission spectrum or two photomultipliers with different band pass filter to detect the ratio of these wavelengths were used. The measurement was performed at room temperature (~ 20 °C).

3.2.4 Excitation of Acoustic Pulses in a Lipid Monolayer

Figure 3.3 presents a schematic picture of the setup to excite acoustic pulses. Acoustic pulses were excited with hexane or acetic acid gas. For inducing pulses, the gas was blown on the lipid monolayer. Therefore, nitrogen gas with a pressure of 0.6 bar was filled in a specific volume. After that, nitrogen was streamed into a bottle which was filled with hexane or acetic acid. Thereby part of the gas phase of liquid was streamed to the surface of the monolayer. At the point where the excitation medium hit the monolayer, the lipids were perturbated, and this perturbation propagated as a consequence of the conservation of momentum through the layer. In the case of hexane, the gas was incorporated into the lipid layer and a compression front propagated trough the lipids. When an acid was used, the released protons condensed the lipids at the point of excitation and an expansion front propagated trough the lipid layer.

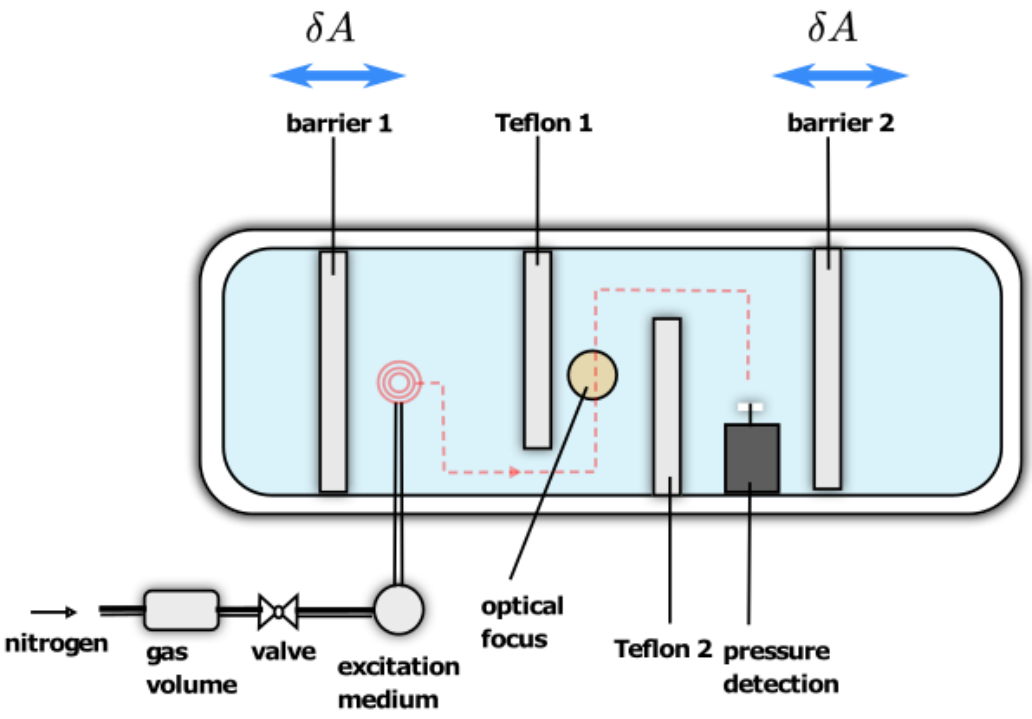

Figure 3.3: Sketch of the setup of acoustic pulse experiments. A specific volume of nitrogen N_2 is passed through the gas phase of the excitation medium and afterwards vaporized onto the lipids. Different excitation media were used to excite compression or expansion pulses, respectively. The acoustic pulse propagated through the monolayer and passed the optical measurement point and was detected by the pressure sensor.

A perturbation of the lipid monolayer was detected by two photomultipliers (rate

4 kHz) at 610 nm and 690 nm and by a pressure sensor. Consequently, the signal in pressure and of emission can be correlated. To guarantee that the pulses cross the optical measurement point the surface pressure is measured after the microscope. To get a stabilized signal of the dye molecules it is necessary to suppress the motion of the surface of the monolayer. Therefore, several barriers made of Teflon were put into the Langmuir balance (s. **Figure 3.3** Teflon 1,2).

3.3 Results and Discussion

3.3.1 Emission Properties of Di-4-ANEPPDHQ Embedded into Lipid Vesicles

In these experiments the correlation between the emission properties of fluorescent dyes embedded into lipid bilayer membranes and the transition point of the lipids are investigated. The lipid vesicles were made of DMPS, DLPS and DMPC. While DMPS and DLPS bear a negative charge at pH 7 at the headgroup, DMPC is electrically neutral. The lipids DMPS and DMPC are also prevalent in several cell types (Grünhagen et al. (1983)) and therefore relevant for biological systems.

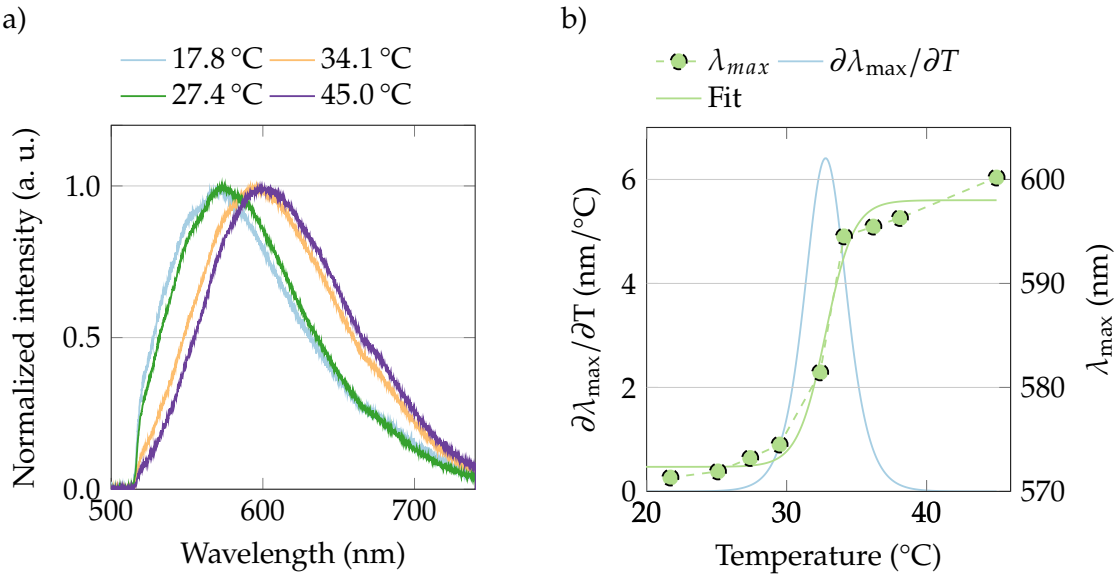

Figure 3.4: Emission properties of Di-4-ANEPPDHQ embedded into DMPS vesicles. (a) Temperature dependence of the emission spectrum of Di-4-ANEPPDHQ embedded into lipid vesicles made of DMPS around the main transition (T_m = 35.4 °C (Lewis and McElhaney (2000))). Mainly two spectra appear, one with the peak position around $\lambda_{\max} \approx 570$ nm and one at $\lambda_{\max} \approx 600$ nm. (b) Maximum of emission spectrum as a function of temperature. The derivative $\frac{\partial\lambda}{\partial T}$ (~ optical susceptibility) of a sigmoidal fit shows a maximum at T_m = 32.8 °C (figure taken from (Fabiunke et al. (2021))).

In **Figure 3.4 (a)** the emission spectra of lipid vesicles made of DMPS are shown at different temperatures around the melting point. It was found that the emission spectrum significantly changes in position when the state of the lipids was varied. Between 20 − 50 celsius the emission spectrum continuously shifted to longer wavelengths with increasing temperature. Below and above the transition point of DMPS

(T_m = 35.4 °C (Lewis and McElhaney (2000))) a small shift of about $\frac{\partial \lambda_{max}}{\partial T} \sim 0.5\,nm/°C$ occurred. In the regime between 32 °C and 35 °C the shift became nonlinear and increased up to around $\frac{\partial \lambda_{max}}{\partial T} \sim 6\,nm/°C$). Based on a sigmoidal fit, the maximum of the derivative $\frac{\partial \lambda_{max}}{\partial T}$ (optical susceptibility) was calculated and the transition point of the lipids were estimated to be 32.8 °C. These results are in good agreement with calorimetric measurements (Lewis and McElhaney (2000)).

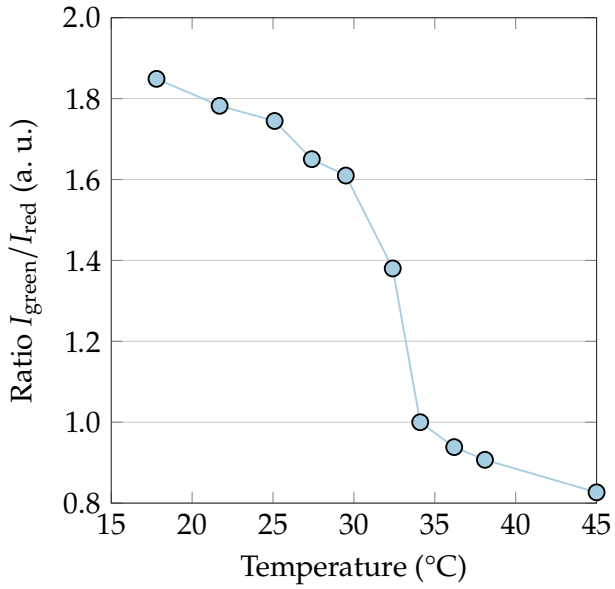

Figure 3.5: Ratio parameter of Di-4-ANEPPDHQ embedded into DMPS vesicles. The ratio $\frac{I_{green}}{I_{red}}$ for Di-4-ANEPPDHQ incorporated into DMPS vesicles plotted as a function of temperature. The intensities at (560 ± 10) nm and (610 ± 10) nm were extracted from spectra (c.f. Fig. a). The greatest change takes place at 33 °C, which is in very good agreement with literature values for the main transition T_m = 35.4 °C (Lewis and McElhaney (2000)) (figure taken from (Fabiunke et al. (2021))).

In the literature the shift of the emission spectrum is also often analyzed by the generalized polarization (GP: based on the polarization of light (Parasassi et al. (1991))). Therefore, the ratio parameter $\frac{I_{green}}{I_{red}}$ of two wavelengths at the green and at the red edge of the spectrum was calculated (s. **Figure 3.5**). The intensity of the green channel relatively increased to the intensity of the red channel. This led to an increase of the ratio parameter. The greatest changes occurred at 33 °C which corroborates that the shift is largest at the transition point of the lipid membrane. It can be concluded that the ratio parameter $\frac{I_{green}}{I_{red}}$ is indeed antiproportional to the maximum of the emission spectrum, when the right wavelengths at both flanks are chosen. However, without knowing the exact spectrum, the value seems to be meaningless.

These results were found to be conserved for lipids with a different length of the carbon chains but with the same headgroup (DLPS, **Figure 3.6a**). The emission spectrum was blue-shifted around the fluid-solid transition of the used lipids, respectively. Here, it can be concluded that the shift of the emission spectrum is strongly correlated to the main transition of the surrounding lipid matrix, whereas pure electrochromic interpretations (sensitivity to membrane potential) of the fluorescent dye Di-4-ANEPPDHQ are not sufficient. In theory, the transmembrane potential takes an important role for the change of the emission properties. The absence of a Nernst-potential in these experiments, because of the same chemical environment inside and outside of the lipid vesicles, clearly contradicts this explanation.
Furthermore, when the dye is incorporated into vesicles made of DMPC the spectrum shifted to red (lower energy) instead of blue during the disordered-ordered transition (DLPS, **Figure 3.6b**). This effect is abnormal as solvatochromic dyes are universally used to indicate a membrane ordering based on a blue shift (Dinic et al. (2011); Parasassi et al. (1998)). The fact that using vesicles made of DMPC where the optical susceptibility $\frac{\partial \lambda_{\max}}{\partial T}$ also showed a maximum at 24 °C, which is well correlated to the melting point (T_m = 23.8 °C (Seneviratne et al. (2003))), indicates that the systems are coupled but the mechanism is different.

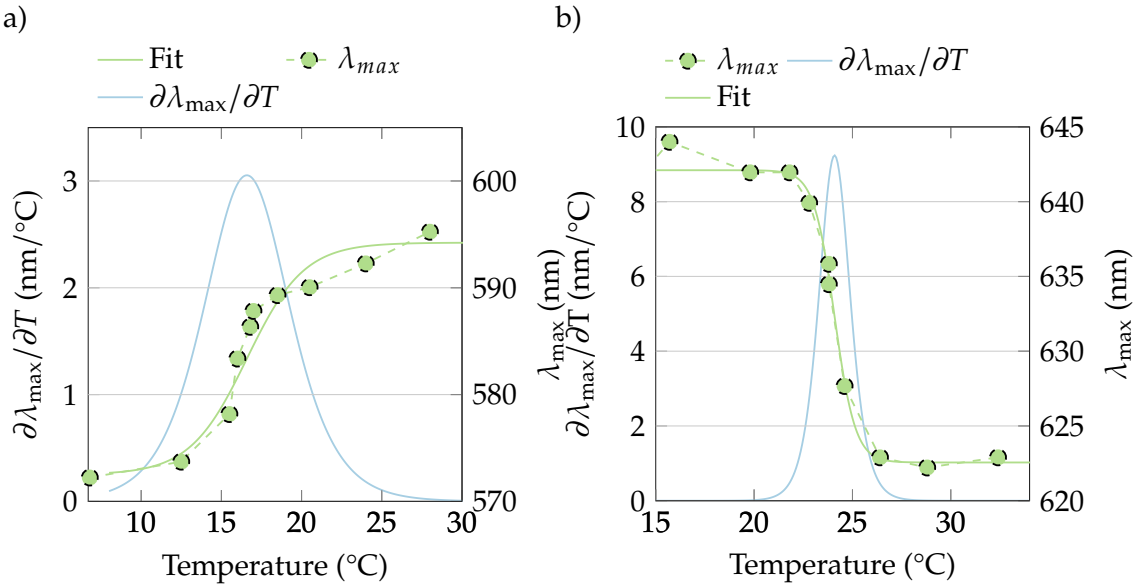

Figure 3.6: Peak emission of Di-4-ANEPPDHQ embedded into DLPS (a) and DMPC (b) vesicles as a function of temperature(a) Maximum of the emission spectrum of Di-4-ANEPPDHQ embedded into vesicles made of DLPS. The derivative was calculated from a sigmoidal fit. The transition point of the lipid membrane is estimated to be 16.6 °C. (b) Maximum of emission spectrum of Di-4-ANEPPDHQ embedded into vesicles made of DMPC as a function of temperature. The derivative $\frac{\partial\lambda}{\partial T}$ was calculated from a sigmoidal fit to the positions of the emission maxima. The transition point is estimated to be 24 °C (data were extracted from the emission spectrum such as in figure 3.4).

Experiments with the fluorescent dye LAURDAN also showed that the general mechanism seems to be similar for different solvatochromic dye molecules. Such as mentioned above, the emission spectrum shifted to shorter wavelength when the lipid system underwent a transition from disordered to ordered state. The largest shift in wavelength occurred at the transition point of the lipid-dye-system, respectively. This has already been reported in the literature and therefore LAURDAN is commonly used to detect the phase state of lipid-based systems (Parasassi et al. (1998); Parasassi et al. (1990); Parasassi et al. (1997)). The emission spectrum shifted up to 30 nm/°C, which is larger by a factor of 5 compared to Di-4-ANEPPDHQ. While the change of the emission properties of Di-4-ANEPPDHQ differed between DMPC and DMPS, the emission spectrum of LAURDAN shifted in all lipid systems to shorter wavelengths with an ordering of the membrane.

Amaro et al. (Amaro et al. (2017)) have demonstrated that the physical mechanism of the spectral response can be different depending on the specific solvatochromic dye. The authors suggested that the emission properties of the dye DI-4-ANEPPDHQ is

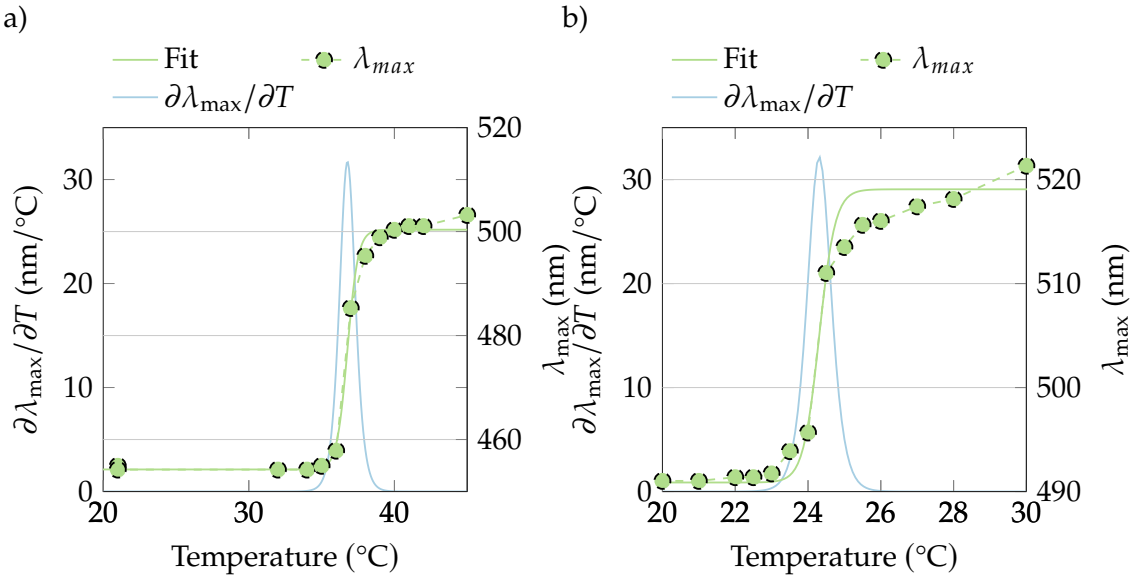

Figure 3.7: Peak of the emission spectrum of Laurdan embedded into lipid-based vesicle as a function of temperature. (a) displays the peak of the emission spectrum when the dye is incorporated into vesicles made of DMPS. The largest shift of the spectrum correlates very well to the transition point of DMPS (T_m = 35.4 °C (Lewis and McElhaney (2000))). Incorporated into vesicles made of DMPC (b) the largest shift took place at 24 °C which is also in agreement with the transition point of DMPC (Seneviratne et al. (2003)).

connected to the dielectric constant of the solvent, whereas the emission properties of LAURDAN follow hydrogen bonding effects.

A possible reason for the difference in sign of the shift between DMPC and DMPS measured with Di-4-ANEPPDHQ is the net charge of the headgroup. Thus, different magnitude and orientation of the dipole of the head group might play a role as the emission spectrum also shifted with the dielectric properties/dipole of different solvent molecules. Similar to these results, Vitha et al. (Vitha and Clarke (2007)) have also found a blue shift of the emission spectrum of DI-8-ANEPPS upon taking DMPC vesicles from gel to fluid. Therefore, depending on the observed system and the fluorescent molecules, the energy transfer can be different.

From a thermodynamic point of view, the energy distribution of the fluorescent dye and the thermodynamic fluctuations of the system are a more fundamental correlation. The energy fluctuation (width of the spectrum) of the dye molecule should be directly coupled to the fluctuation of the membrane, when the dye is part of the thermodynamic system. The coupling between dye system and membrane disappears if the coupling parameter $\frac{\partial\lambda}{\partial T}$ equals zero (s. section 2.4.1).

Since the fluctuations of the membrane system are in a maximum at the transition point, the fluctuation of the emission energy also needs to be maximal. This is equivalent to

the fluctuations in wavelengths of the emission spectrum $\Delta\lambda_{max}$ and therefore to the spectral width $\Delta\Gamma$. The evident existence of coupling between emission properties and the properties of the surrounding materials implies that large fluctuations in the solvation shell should show themselves in large fluctuations of the dye properties, independent of the exact molecular nature of coupling.
To observe the spectral width, the reciprocal curvature at the maximal intensity was used (s. Appendix A.2.1). The curvature γ is assumed to be proportional to the width and therefore to the energy fluctuations $\gamma \propto \Delta\Gamma \propto \Delta\lambda_{max}$. In **Figure 3.8** the reciprocal curvature is displayed as a function of temperature. It can clearly be seen that the width of the emission spectrum is at maximum during the transition of respective lipid-dye systems (DMPS, DLPS, Di-4-ANEPPDHQ, LAURDAN). These results show a very similar behavior compared to susceptibilities of a lipid system such as the heat capacity.

$$\langle \partial\lambda_{max}^2 \rangle \propto \alpha_1 \Delta\Gamma \propto \alpha_2 \Delta c_p \tag{3.1}$$

The width displays a distinctive maximum at the transition and indicates high fluctuations of the lipid-dye system. If a coupling parameter α_2 is known, the specific heat capacity of the local environment could theoretically be calculated (Shrivastava et al. (2018a)). These characteristic changes of optical parameters at phase transitions and of susceptibilities such as heat capacity or compressibility have already been demonstrated (Shrivastava et al. (2018a); Shrivastava and Schneider (2013); Steppich et al. (2010)).

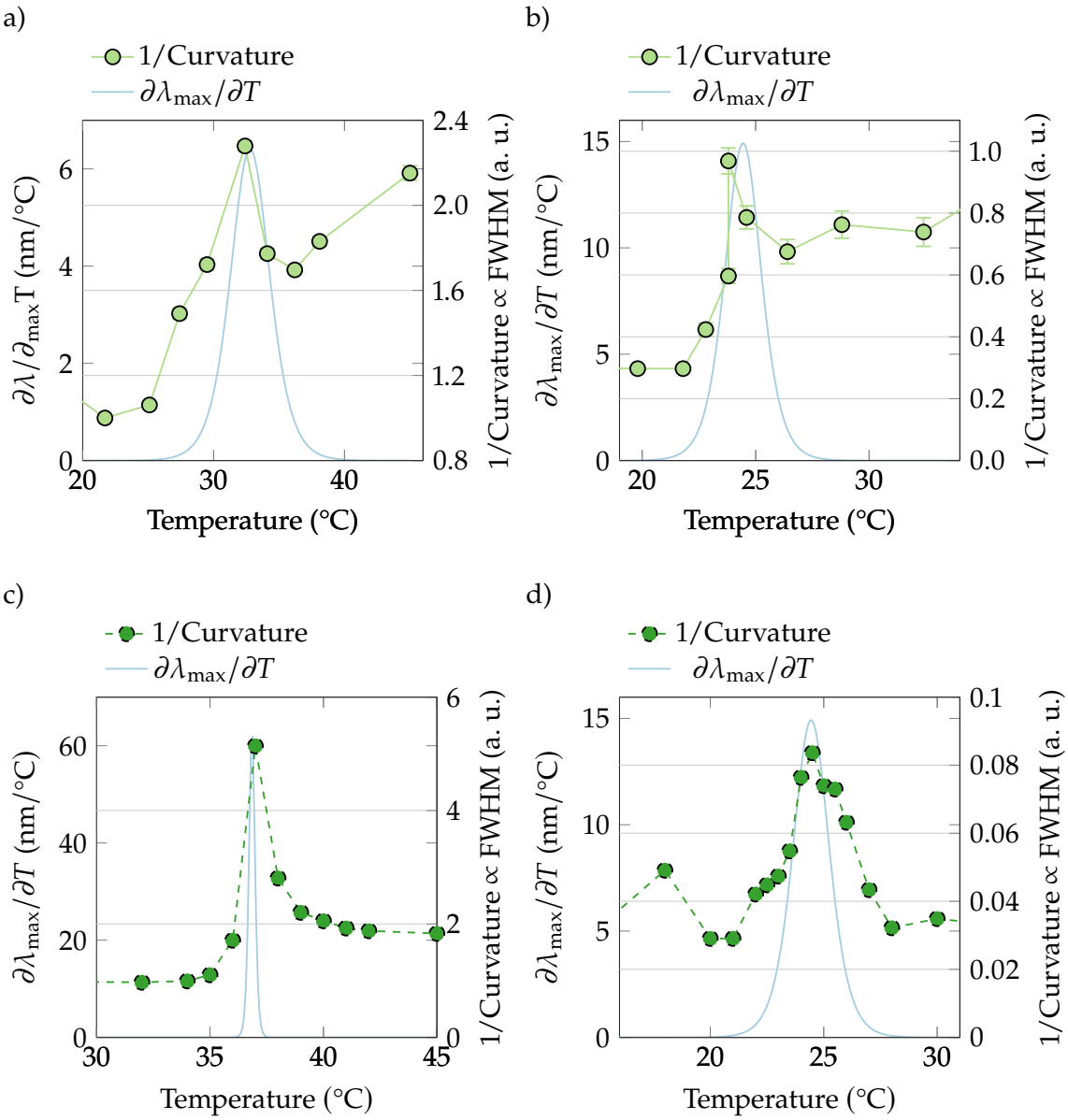

Figure 3.8: Spectral width of the emission spectra as a function of temperature. The reciprocal curvature (∝ FWHM) at the maximum of emission spectrum shows a distinct maximum at the transition of the vesicles, respectively ((a) DMPS: Di-4-ANEPPDHQ, b) DLPS: Di-4-ANEPPDHQ, c) DMPS: LAURDAN, d) DMPC: LAURDAN). a), b) and c) even displays a narrow spectrum at low temperature, a wider spectrum at the transition point and a wide spectrum at high temperatures. This is almost analogous compared to a typical compressibility of a lipid system.

3.3.2 Blue-shift of the Emission Spectrum in a Lipid-based Monolayer at the LE-LC-Transition

The fact that the fluorescent dye Di-4-ANEPPDHQ altered its emission properties at the transition point of lipid-vesicles in absence of any ion gradient makes the originally designed sensitivity to the electrical activity of cells less convincing. In the literature it has also been shown that the emission spectrum shifts with increasing concentration of cholesterol (Jin et al. (2005)). There are several approaches which can be used for the understanding of solvatochromic effects to the dye molecule. Especially changes of the dipole moments of the dye seem to be crucial in this picture.

Surface Potential

To test the electrical correlation of the dye signal, the surface charges, compressibility of a lipid monolayer and optical properties of the dye are investigated. The Langmuir film balance gives the opportunity to observe the compressibility, surface potential of the interface and the emission properties of the fluorescent dye, simultaneously. In the past different investigators studied the surface potential of a monolayer at the air-water interface. In the work of Fichtl (Fichtl et al. (2016)) the surface potential was measured as a function of the lateral pressure of a lipid-based monolayer (s. **Figure 3.9**). It showed that a step in the surface potential occurred at the transition point ($\pi \sim 20\,\mathrm{mN/m}$).

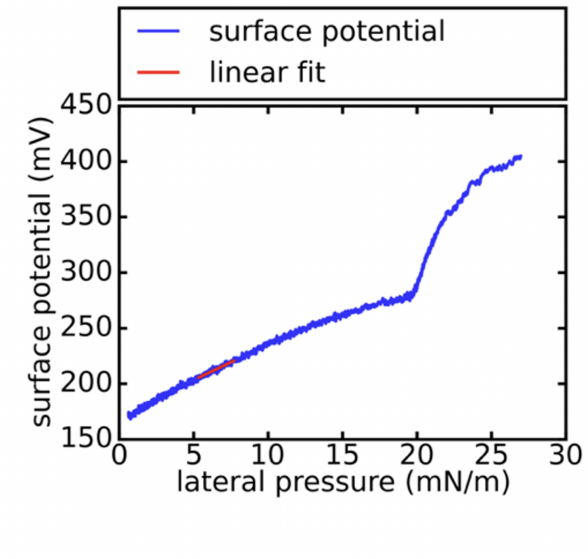

Figure 3.9: Isothermal measurement of surface potential as a function of the lateral pressure. The phase transition of the lipids from liquid-expanded to liquid-condensed phase is clearly visible ($\sim 20\,\mathrm{mN/m}$), conclusively demonstrating thermomechanic-electrical coupling (figure and caption taken from (Fichtl et al. (2016)).

The mathematical description of the surface potential Ψ is given by the vertical component of the dipole moment $\mu_\perp$, the dielectric constant ϵ and the area A:

$$\Psi_m = \frac{\mu_\perp}{\epsilon A} \tag{3.2}$$

However, the distribution of the dipoles of the single components according to the water and the lipids is not trivial. Furthermore, the dielectric constant of the monolayer should also change with the phase transition, and it is unknown for the different phases. Nevertheless, calculating the electric capacity of the monolayer with the expression of the derivative

$$C_T = \left(\frac{\partial q}{\partial \Psi}\right)_T = \left(\frac{\partial q}{\partial \pi}\right)_{T,A}\left(\frac{\partial \pi}{\partial \Psi}\right)_{T,A} = \left(\frac{\partial A}{\partial \Psi}\right)_{T,q}\left(\frac{\partial \pi}{\partial \Psi}\right)_{T,A} \tag{3.3}$$

with the charge q, the surface potential Ψ, the area A and the lateral pressure π shows that there is a maximum of the capacitance at the transition point of the lipids. This means that the fluctuations in charge q are large around the transition point. It shows that not only mechanical properties are coupled to the phase transition, but also electrical properties of the interface.

The lipid isotherms were recorded at room temperature ($\sim$ 20 °C) with a speed of 10 cm^2/min and the lateral pressure and the emission spectra of Di-4-ANEPPDHQ were measured simultaneously. The main transition of the lipid monolayer made of DMPS took place at about 14 m N/m and was indicated by a plateau region of the area-pressure curve (s. **Figure 3.10**). At the right-hand side of **Figure 3.10** the emission spectrum of Di-4-ANEPPDHQ embedded in the DMPS-monolayer is plotted at the two different phase states of the lipid layer (liquid-expanded (LE), liquid-condensed (LC)). Comparing the spectra at the different regions of the phase diagram of the interface (**Figure 3.10 a), b)**), it can be noted, that the position of the emission peak was slightly shifted to shorter wavelength with increasing lateral pressure. This is in line with the results from lipid vesicles. A more ordered phase of the lipid-based systems led to a shift to shorter wavelengths. Quenching effects of the fluorophore could be excluded because quenching should lead to a lowering of energy and therefore to a red shift of the emission spectrum. The emission peak on the left flank of the spectrum is a reflection artifact of the water surface and do not represent a property of the dye molecule. The intensity of this artifact correlates with the distance of the objective to the water surface also without dye molecules. The intensity increases when the distance is decreased.

The correlation between the position of the emission peak of the fluorescent dye and the lateral pressure of the isotherm becomes more apparent, when plotting the position of the maximum λ_{max} as a function of lateral pressure π (s. **Figure 3.11**).

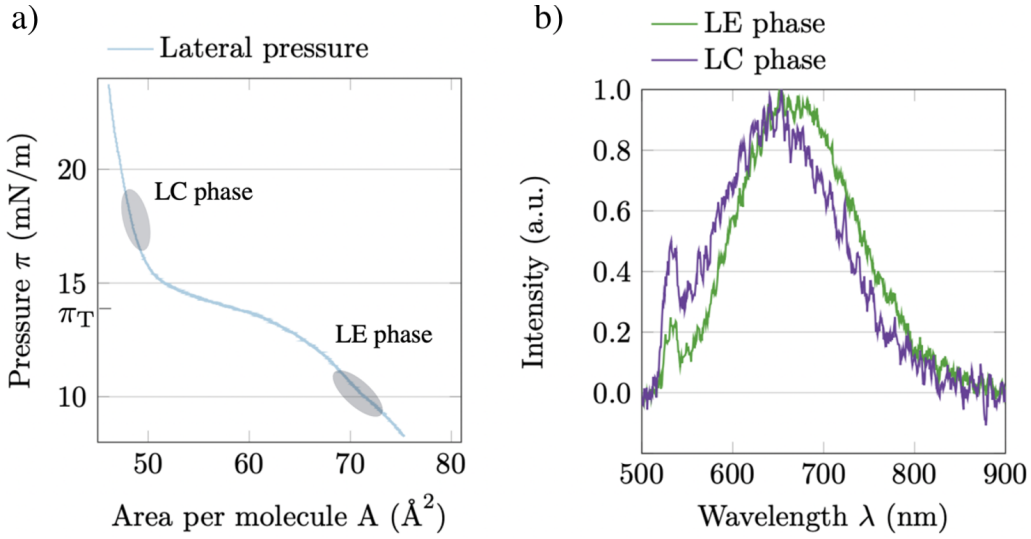

Figure 3.10: Emission spectrum of Di-4-ANEPPDQH at different phase regimes. (a) Lateral pressure π is plotted against the area per molecule A in cm^2. The plateau indicates the transition point of DMPS at around 14 m N/m. (b) The normalized emission spectrum of Di-4-ANEPPDHQ is plotted at LE-phase, and LC-phase of the monolayer. The peak in intensity at about 520 nm belongs to the resonance of the water to the excitation light of 488 nm (100 mM NaCl, 100 mM phosphate buffer, pH 7).

At around 14 m N/m a shift of the peak position from around 670 nm to about 650 nm appears, whereas the position of the maximum stays mainly constant at lower and higher lateral pressures π. This corresponds to the main transition regime of DMPS. The derivative of the area according to pressure (compressibility),

$$\kappa_T = \frac{1}{A}\frac{dA}{d\pi} \tag{3.4}$$

and the derivative of the emission wavelength according to pressure (optical susceptibility)

$$\eta_{o,T} = \frac{1}{\lambda_{\max}}\frac{d\lambda_{\max}}{d\pi} \tag{3.5}$$

clearly shows a correlation in their maximum positions (**Figure 3.11**). At the maximum of the compressibility the derivative of the sigmoidal fit becomes $\frac{\partial\lambda_{\max}}{\partial\pi} \sim 7\,\mathrm{nm/(mNm^{-1})}$. This almost similar behavior of these two observables, compressibility and the optical susceptibility, again shows the coupling between the mechanical properties of the membrane and the optical properties of the fluorescent dye. This has already been reported in (Shrivastava and Schneider (2013)) for the derivative in intensity with respect to lateral pressure of fluorescent dyes incorporated into lipid monolayers.

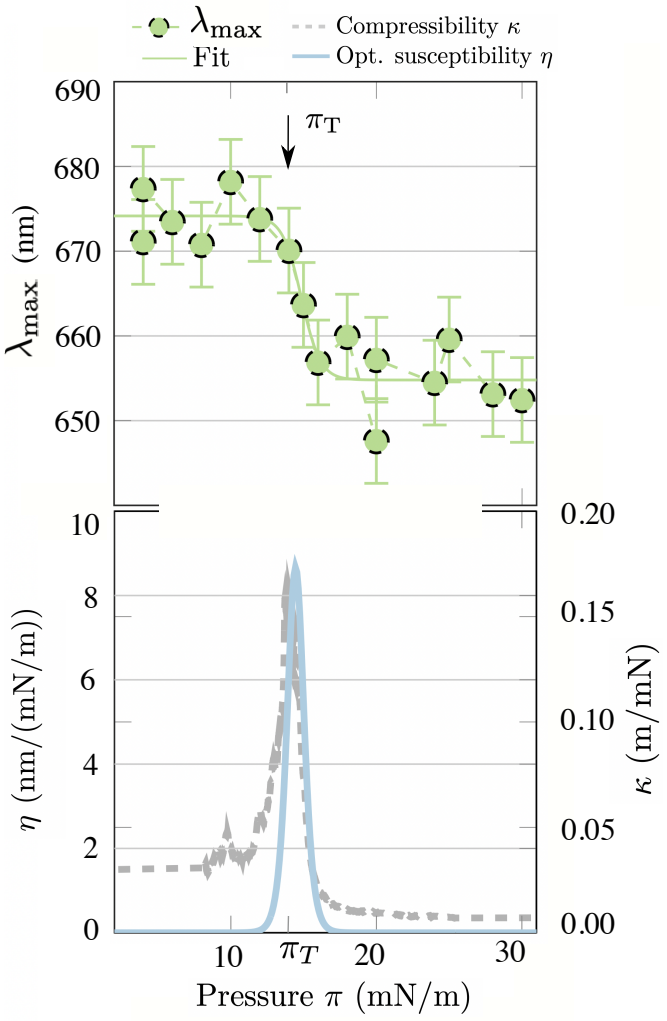

Figure 3.11: Optical coupling to the phase transition of the lipid monolayer made of DMPS: Optical coupling to the phase transition of the lipid monolayer made of DMPS: (upper) Peak of the emission spectrum as a function of lateral pressure π. A sigmoidal fit was used to calculate the derivative $\frac{\partial \lambda_{max}}{\partial \pi}$. (lower) The maximum of the derivative $\eta \propto \frac{\partial \lambda_{max}}{\partial \pi}$ is correlated to the maximum in compressibility κ_T of the lipid monolayer (100 mM NaCl, 100 mM phosphate buffer, pH 7).

Using the lipid DPPC with a different head group and therefore a different charge density of the surface also showed a shift of the emission spectrum at the maximum of the compressibility, where the LE-LC transition of the lipids took place. As mentioned above, the shift of emission wavelength is directly coupled to the physical state of the observed system and cannot be seen as a property of the dye molecules or of the lateral pressure. The correlation between the thermodynamic state of the membrane and the color of the embedded dye allows to connect the emission properties to other susceptibilities of interfaces.

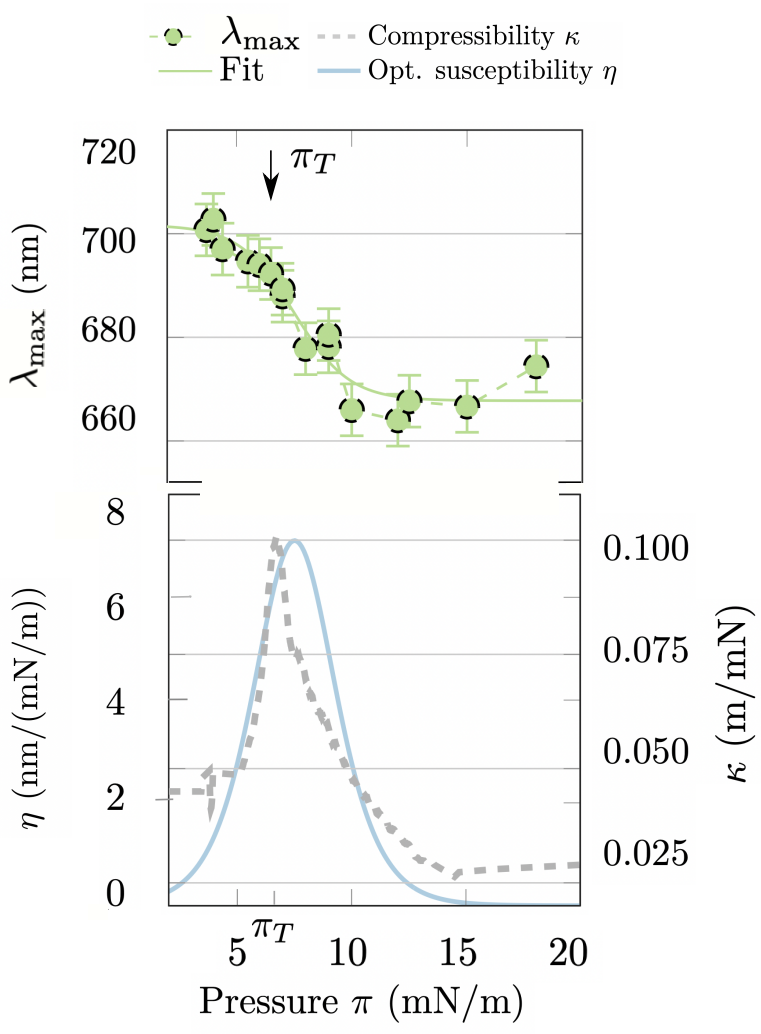

Figure 3.12: Optical coupling to the phase transition of the lipid monolayer made of DPPC: (upper) Peak of the emission spectrum as a function of lateral pressure. (lower) A sigmoidal fit was used to calculate the derivative $\eta \propto \frac{\partial \lambda_{max}}{\partial \pi}$ (100 mM NaCl, 100 mM phosphate buffer, pH 7).

During transition the internal energy of the dye molecules changes and causes a shift in wavelengths. The change of emission energy might be understood if dealing

with different solvent polarity and dipole moments. The difference in charge of the two types of phospholipids (DMPS, DPPC) did not affect the blue-shift of the emission spectrum during the disordered-ordered transition. However, the absolute wavelengths of the emission spectra were slightly changed (maximal emission in ordered phase: DMPS < 660 nm, DPPC > 660 nm). It can be concluded that the charge of the lipids is not the origin of the shifting spectrum.
Comparing the surface potential as a function of lateral pressure to the shift in wavelengths, a correlation between a step in the potential and a shift in wavelengths can be assumed. In control experiments, the emission spectrum changed in position with the dielectric constant or the dipole moments of the surrounding solvent molecules (s. **Figure 2.8**). A dependence of the optical properties on the dielectric properties seems to be plausible. As a conclusion, two main statements can be made: I) the emission properties do **not** change with the absolute surface potential **neither** correlate to the Nernst-potential of the lipid membrane. II) A change in dipole moments of the chemical environment causes a shift of the emission spectrum, which is in general closely related to the mechanical changes of the lipid monolayer at the phase transition. A fluid-solid transition induces a reorientation of the carbon chains or structural changes of the lipids (McConnell et al. (1984); Moehwald (1995); Overath et al. (1976); Stine (1994)). But nevertheless, it is important to say that the origin of the shift cannot be found in a purely electrical model as well as at the single molecule level as all variables are coupled to each other. It is obvious that a change of the structure of a lipid membrane have to influence the proton or ion densities and therefore the surface potential. These alterations has also to be correlated to the interaction energy of the lipid-dye-complex.

3.3.3 Blue-shift of the Emission Spectrum at the Freezing Point of DMSO

To investigate if the spectral responses depend on the local position of the dye molecules inside the membrane or on the macroscopic structural properties of phospholipids, the emission spectrum was measured in a membrane free bulk solution (solved in DMSO). When the dye molecules are solved in dimethyl sulfoxide (DMSO) at a concentration of 1 µM at 30 °C, the emission spectrum also changes at the freezing point of DMSO. **Figure 3.13** shows the peak emission wavelengths as a function of temperature. The spectrum shifts in a sigmoidal manner at about 17 °C from 655 nm nm to 645 nm. A fit was calculated to determine the greatest shift in wavelength. The maximum of the derivative $\frac{\partial \lambda}{\partial T}$ occurs at ~ 17 °C which is in good agreement with the melting point of DMSO (18.5 °C, Datasheet (2021)). It shows that the change of the emission spectrum is directly coupled to the thermodynamic state of the chemical

environment (solvation shell). It is also found that the width $\langle \partial\lambda^2 \rangle$ of the emission spectrum of Di-4-ANEPPDHQ is maximal at the freezing point of DMSO. It clearly demonstrates that the emission energy depends on the entropy potential (fluctuation, state) of the surrounding interface (solvation shell). Thereby, it does not matter which specific electric potential or molecular constituents were present. This means that a "specific response" (mechanical, electrical etc.) of a fluorescent dye molecule has to be treated with caution. Without considering the coupling between the emission properties and the susceptibilities (fluctuations) of the system, wrong dependencies could be concluded (electro-sensitivity).

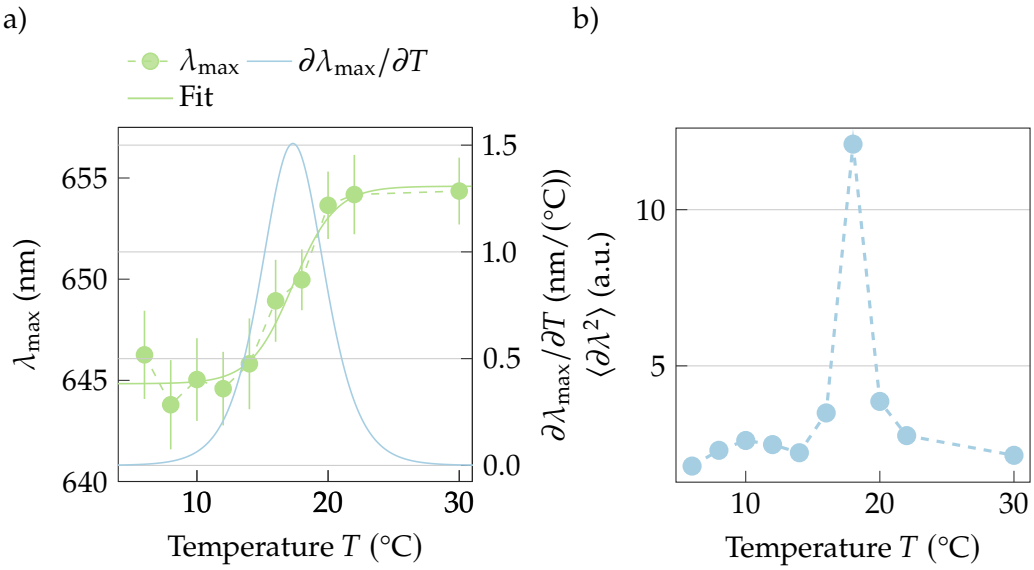

Figure 3.13: State-dependent fluorescence emission of Di-4-ANEPPHDQ in DMSO. (a) The maximal change of the emission maximum occurs at about 17 °C. This maximum is also in agreement with the melting point of DMSO (18.5 °C, Datasheet (2021)). (b) The width $\langle \partial\lambda^2 \rangle$ also shows a maximum at the melting point.

3.3.4 Blue-shift of the Emission Spectrum during Acoustic Pulses

Based on thermodynamics, the nerve pulse propagation can be described as an acoustic phenomenon (Heimburg and Jackson (2007); Kaufmann (1989a)). Observations of our group have shown that nonlinear acoustic pulses can be excited in a lipid monolayer. Such pulses share some main properties of action potentials, such as all-or-none behavior or excitation threshold. Therefore, it has been proposed that acoustic pulses may be a fundamental mechanism of communication of cells and between cells. Here it will be demonstrated how the fluorescent dyes react to adiabatic acoustic pulses, excited at the lipid interface. The influence of the transition points of the lipids will be of particular interest. The investigation of acoustic pulses seems to be an opportunity to connect static state experiments with dynamic pulse propagation and with biological functions.
In the past, fluorescence dyes have already been used to measure action potentials along nerve cells (Cohen et al. (1978); Foley and Muschol (2008); Loew et al. (1992)). However, as the emission properties of the fluorescent dyes changed due to the thermodynamic state of the interface, the question arises if the phase transition also plays a role for action potentials in living cells.

Ratio Parameter as Phase State Reporter

To investigate the dynamic behavior of the dye embedded into a lipid monolayer, Di-4-ANEPPDHQ is incorporated into a monolayer made of phospholipids and the emission of the dye was measured. Due to the short timescale of a density pulse, the entire spectrum of the fluorescent dye could not be observed. Instead, the ratio of the intensities at two different wavelengths (610 nm und 690 nm; ratio parameter $\frac{I_{610\,\mathrm{nm}}}{I_{690\,\mathrm{nm}}}$ or in more general $\frac{I_{\mathrm{green}}}{I_{\mathrm{red}}}$) was used. In these experiments the acoustic pulses were triggered by hexane gas and the pulses were additionally detected by a pressure sensor. This ensured that the pulse propagated through the layer. **Figure 3.14** shows the ratio parameter $\frac{I_{610\,\mathrm{nm}}}{I_{690\,\mathrm{nm}}}$ (intensities are shown in the appendix A.2.2) and the area A of the film balance as a function of lateral pressure. It can be recognized that the ratio parameter $\frac{I_{610\,\mathrm{nm}}}{I_{690\,\mathrm{nm}}}$ increased with increasing pressure. Nevertheless, the greatest change occurred at the plateau regime of the area-pressure-isotherm at around 17 mN/m. Accordingly, a maximal optical susceptibility (in general $\eta_{o,T} = \frac{\partial \lambda_{\mathrm{max}}}{\partial \pi} \propto \frac{1}{I_{\mathrm{green}}/I_{\mathrm{red}}} \frac{\partial I_{\mathrm{green}}/I_{\mathrm{red}}}{\partial \pi}$) within the transition regime of the lipid monolayer was measured (s. **Figure 3.14**). This maximum of the optical susceptibility η correlated with the maximum of the compressibility κ_T. It can be concluded that changes of the lateral pressure around the transition result in much smaller responses of the ratio parameter than in the transition regime. The optical susceptibility η increased by a factor of about 3 at the

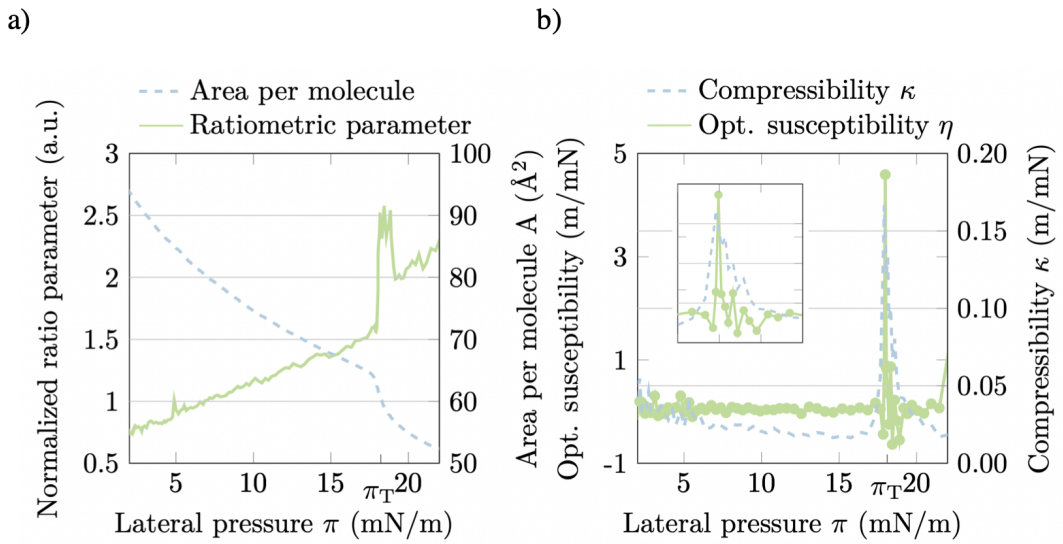

Figure 3.14: Optical Coupling of the ratio parameter to the area-pressure-isotherm: (a) Ratio parameter $\frac{I_{610\,nm}}{I_{690\,nm}}$ as a function of lateral pressure. The greatest change of the ratio parameter $\frac{I_{610\,nm}}{I_{690\,nm}}$ occurs around the plateau of the area-pressure isotherm. (b) Consequently, the maximum of the optical susceptibility correlates to the maximum in compressibility (100 mM NaCl, 100 mM phosphate buffer, pH 7).

transition point. These changes were in line with the blue-shift of the entire spectrum with a disordered-ordered transition of the lipids. A blue-shift corresponded to a higher ratio parameter and a red-shift corresponded to a lower ratio parameter. It is important to state, that the optical susceptibility η as well as the ratio parameter $\frac{I_{610\,nm}}{I_{690\,nm}}$ only represents a shift of the emission spectrum when the shape of the spectrum is constant. Changes of the shape obviously influence the single intensities and therefore the ratio parameter $\frac{I_{610\,nm}}{I_{690\,nm}}$.

Compression Pulses

To investigate the dependency of the state, pulses were excited in three fundamentally different regimes of the monolayer: transition (LE-LC), disordered (LE) and ordered (LC). **Figure 3.15c** shows the ratio parameter upon excitation of the lipid-based monolayer at the different regimes. After excitation with hexane gas, the ratio parameter showed a significant response to a pressure pulse at the disordered-ordered transition regime (**Figure 3.15**a LE-LC). The pressure amplitude did not change significantly at the different regions (**Figure 3.15b**), whereas the ratio parameter $\frac{I_{610\,nm}}{I_{690\,nm}}$ increased about 20 % at the transition regime LE-LC and less than 5 % around the

transition (regime LE, LC).
Perturbations of the ratio parameter $\frac{I_{610\,\mathrm{nm}}}{I_{690\,\mathrm{nm}}}$ took around 4 s which is in line with the duration of the change of the lateral pressure. Nevertheless, the exact duration time cannot be estimated because the reflection of the pulses at the Teflon barriers influenced and changed the measured shape of the pulses.
It can be concluded that state changes of the interfaces results in a blue shift as described above. The correlation between ratio parameter $\frac{I_{610\,\mathrm{nm}}}{I_{690\,\mathrm{nm}}}$ and pressure π strongly depends on the thermodynamic state of the interface. Since the excitation of such optical pulses only takes place in a specific part of the isotherm a threshold behavior can be assumed such as described for action potentials.

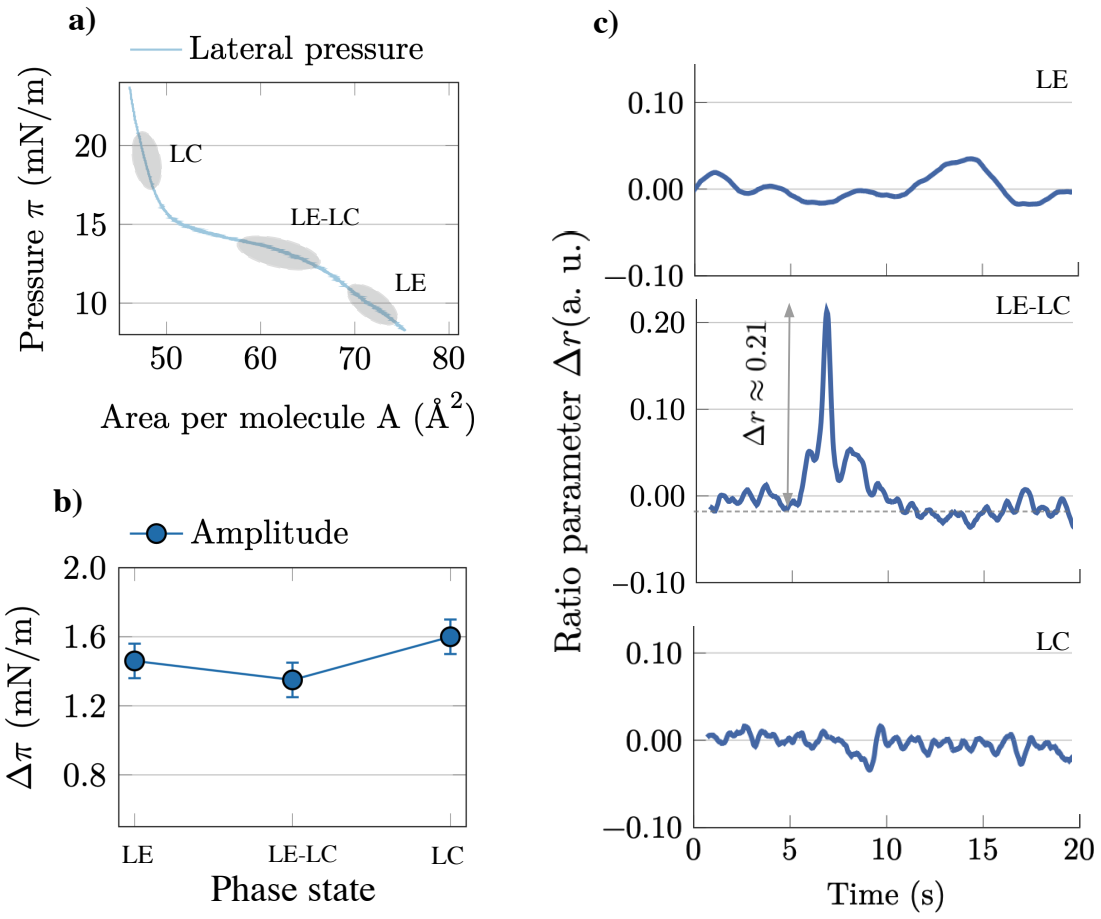

Figure 3.15: State dependence of the response of the ratio parameter during acoustic pulse propagation: (a) shows the $\pi - A$ isotherm and the different excitation regimes. (b) displays the amplitude in pressure of the excited acoustic pulses. The amplitude in pressure mainly stays constant around $\Delta\pi \sim 1.5\,\mathrm{m\,N/m}$, whereas the change of ratio parameter depends on the phase state regime. (c) Optical parameter when pulses are excited in different state regimes of a DMPS monolayer. A distinct pulse only occurs at the beginning of the transition regime of the monolayer. The optical parameter changes about 20 % (100 mM NaCl, 100 mM phosphate buffer, pH 7).

Expansion Pulses

Changing the compression pulse to an expansion pulse led to a different response regime and a different sign of the ratio parameter $\frac{I_{610\,nm}}{I_{690\,nm}}$ during acoustic pulses. **Figure 3.16** displays a typical time trace of the ratio parameter $\frac{I_{610\,nm}}{I_{690\,nm}}$ when an expansion pulse was excited. After excitation the ratio parameter decreased about 30 %. The second peak was a result of reflections at the Teflon pieces. Due to the fact, that the expansion pulse induced a decrease of the ratio parameter $\frac{I_{610\,nm}}{I_{690\,nm}}$ and the excitation regime was at the LC phase **Figure 3.15a**, there are less doubts of a transition during these acoustic pulses excited in vicinity of the transition. Nevertheless, the protons of the excitation medium also seemed to influence the state of the monolayer as the starting conditions were not reached. Also the relaxation of the lipids after the pulse propagation was longer compared to the compression pulses.

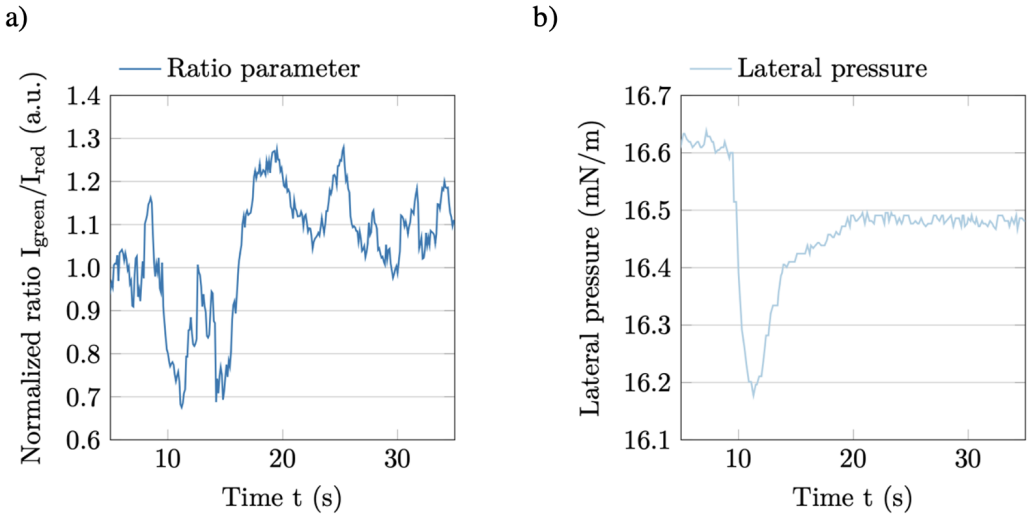

Figure 3.16: Expansions pulse through a lipid monolayer excited by acetic acid: The left figure (a) shows a typical time trace of the ratio parameter $\frac{I_{610\,nm}}{I_{690\,nm}}$ after triggering an expansion pulse at around 9 s. Analogous to the compression pulses, the ratio parameter $\frac{I_{610\,nm}}{I_{690\,nm}}$ decreases about 30 % within an assumed LC-LE transition. The right side of the figure (b) shows a typical time trace of the lateral pressure during pulse propagation (100 mM NaCl, 100 mM phosphate buffer, pH 7).

Electrophysiological Interpretation in Cells

Molecules of the styryl-dyes from the ANEPP-family are used as electrochromic fluorescent dyes which are usually described to be sensitive to the membrane potential. Therefore, the changes of the emission spectrum are attributed to the direct coupling to the transmembrane potential (Foley and Muschol (2008)). Since Di-4-ANEPPDHQ also shows significant changes in emission when the concentration of cholesterol is altered (Jin et al. (2006)), this mono-causality is questionable. Furthermore, as shown in previous chapters, the changes of the emission properties are indeed correlated to the phase transition of vesicles in pure water without ion gradients. Also, other studies have proven that the emission for instance of Di-8-ANEPP shows a much stronger response to changes of membrane dipole potential as compared to transmembrane potential (Gross et al. (1994)). All these studies are based on the assumption, that the changes are caused due to the membrane potential at a constant membrane state. However, a change in the transmembrane potential with no further consequences to the state of membrane seems to be unlikely. From a thermodynamic point of view, it is not plausible that a change of 100 mV across a nm thick bilayer do not influence other observables of the system. All parameters of the system are coupled and have to respond simultaneously. Various experiments, especially by Tasaki, have demonstrated that this also is indeed the case for biological systems. Mechanical, thermal, magnetical, chemical and optical components underwent significant changes during an AP (Ritchie and Keynes (1985); Tasaki (1999); Tasaki (2008); Tasaki et al. (1968); Wikswo et al. (1980)).

3.3.5 Conclusion

Changes in the emission properties of solvatochromic dye molecules are commonly described as sensitive to changes of the chemical environment. For example, this occurs in different chemical solutions such as water in comparison to ethanol or chloroform. Embedded into a membrane changes of the fluorescence are coupled to the thermodynamic state of the interface and are mostly independent of specific molecules. It was further proven that changes of the emission do **not** require a change of the transmembrane potential (Nernst-potential) as assumed in cell experiments. Thus, it is more probable, that the origin of different emission properties cannot be found at the single molecule level, but only by the investigation of the entire thermodynamic system and all its couplings.
The optical susceptibility, which showed a maximum at the transition regime of the membrane, could be measured. The direction of this shift of the emission spectrum was presumably coupled to the energy transfer between membrane, dye molecules and the chemical environment (water etc.). It depended on which variables were coupled to the entire entropy $S(E1, E2, ...)$ of the observed system. The fluorescent dye di-4-ANEPPDHQ showed further dependencies on the chemical environment and the head group of the lipids. Embedded in vesicles made of DMPC the emission spectrum shifted to longer wavelengths during transition while DMPS showed the typical shift to shorter wavelengths. This result is in conflict with the literature, where the position of the spectrum identifies the phase of lipid vesicles. Interestingly, this different direction of the shift did not occur in lipid-based monolayers.
These experiments also indicated that the energy fluctuations of the dye molecules are connected to the fluctuations of the membrane. The width Γ of the emission spectrum is maximal during the transition and is also proportional to all susceptibilities of the solvent-dye-system.

$$\langle \delta\lambda^2 \rangle \sim \Gamma \propto \langle \delta H^2 \rangle \sim c_p T \propto \langle \delta V^2 \rangle \sim \kappa_T V T \propto \langle \delta M^2 \rangle \sim V T \epsilon \tag{3.6}$$

This correlation is independent of the chemical environment such as pH and ion concentration of the surrounding aqueous solutions. As the dye is part of the interface, the emission energy became a variable of the entire entropy $S(\lambda, T, V, E...)$ and the energy distribution is directly coupled to the fluctuation of the interface. The emission process was determined by the physical state of the system.
Furthermore, when the dye was dissolved in DMSO, the emission spectrum also shifted to shorter wavelengths and the width was maximal when the melting point was crossed. This clearly demonstrated the fundamental mechanism of changes of the emission properties. Here, it cannot be clarified what the origin of the shifted emission spectrum is at a molecular level. It can only be concluded that it is strongly correlated

to the transition point of the surrounding chemical environment (lipids/DMSO).
These dyes (this should apply to all dyes that interact with the observed system) offer the possibility to get direct access to the physical state of a biological system by measuring the emission properties of incorporated fluorescent dyes. In living systems, the state dependence of other interfacial processes can be observed without major intervention in the cells.
Dynamic acoustic pulses at the lipid monolayer demonstrated that the shift in wavelengths strongly depends on the transition point of the observed system. When the layer was pushed into a transition regime, the ratio parameter changed up to ~ 20% according to the phase diagrams, whereas the ratio parameter did not change far away from the transition point. Therefore, the general interpretation of changes in emission spectra during action potentials in cell biology were questioned. Thermodynamically, the changes of a fluorescent dye molecule embedded into a lipid membrane were associated to a local propagating state change and not to a specific variable such as electrical or mechanical properties. Direct evidence of a phase transition during a biological process such as an action potential would lead to a new definition of cellular communication.

Phase State of living Matter

4 Phase State of Living Systems

4.1 Introduction

Phase transitions have not only been found in artificial systems, but also in biological matter (Hazel et al. (1998); Heimburg and Jackson (2005)). These transitions are very wide (about 10 °C) and are often considered to be irrelevant for biology. But in calorimetric measurements billions of cells are used to observe the heat capacity. Therefore, a wide transition does not reflect the behavior of a single cell.
However, if transitions can be shown to exist and to occur in the context of biological function (e. g. action potentials), they indeed have considerable relevance. Therefore, it is of main interest if the resting state is located in the vicinity of a transition and if an excitable living medium undergoes transient phase changes during the propagation of nerve pulses or action potentials. When the system is located in the vicinity of a transition point, external perturbations (mechanical, chemical etc.) can push the system into the transition regime. This transition can propagate through the medium as a consequence of the conservation of momentum and mass. If the transition is far away from the equilibrium state or even does not exist, this form of excitation is not possible.
The general textbook model of the excitation of cells is however often described as a purely electrical phenomenon. Measurements with fluorescent dyes, which are described as fluidity-sensitive, contradict the purely electrical (or specific ion-sensitive) approach (Georgescauld and Duclohier (1978); Tasaki et al. (1972)) and might indicate a transition during action potentials. Static experiments with a variation of variables such as temperature confirmed a change in fluidity of native membranes (Georgescauld and Duclohier (1979); Hazel et al. (1998); Sieber et al. (2014)). All these data clearly support the thermodynamic perspective on membrane properties, since membranes have to obey the laws of thermodynamics and conservation laws of energy and momentum. In order to understand the nature of the propagating pulse in an excitable cell, it will be crucial to follow membrane state changes. However, it is very desirable to extract direct evidence on the absence or presence of a transition during action potential propagation. This would also clarify whether collective state changes as proposed within a thermodynamic approach, or single molecule events as proposed by the dominate textbook model of Hodgkin and Huxley (Hodgkin and Huxley (1952a)), are the correct phenomenology of the nerve pulses.

In chapter 3 the thermodynamic state of a lipid-based interfaces related to the emission properties of incorporated fluorescent dyes (Di-4-ANEPPDHQ) was investigated. In order to characterize the thermodynamic state of a living system, the same fluorescent dye is embedded into the plasma membrane of the excitable plant cell *Chara australis*. Here, static changes of the state induced by temperature or extracellular pH as well as dynamic changes such as action potentials were observed.

4.2 *Characean* Plant Cells

The experiments were performed with single cells of the *Chara australis* algae. This species belongs to a group of freshwater algae - *charophyceae* - and grows in lakes with muddy grounds. The algae consist of two different types of cells. On the one hand there are the internodal cells, which form the stem of the plants. These cells are serval centimeters long and about 1 mm in diameter. On the other hand, branchlet cells exist, which branch out to the sides and usually are smaller. At the end of every cell, nodes are formed from which further cells grow. **Figure 4.1** shows the basic morphology, a microscopic image of the cell surface and a cross section of a cell.
The cell wall, which is made of polymers, forms the outer layer of the cell. The wall provides protection and can additionally filter the flux into the cell. Underneath the wall, the cell plasma membrane is formed, which is made of different lipids and proteins. The membrane separates the intracellular from the extracellular medium. In the cortex of the cell lies a dense array of chloroplasts, which are lined up such as single beads (s. **Figure 4.1**). They contain the fluorescent compound chlorophyll and are responsible for the process of photosynthesis. The cytoplasm and the vacuole are located at the innermost part. In such long cells, the cytoplasm forms a characteristic streaming (Shimmen (2007)), which functions as an important transport process. The stream runs helically once around the cell. The vacuole is a structure, separated by another membrane (tonoplast), inside the cell and is assumed to build a reservoir of materials.

Similar to neurons, the freshwater algae are able to develop action potentials when excited with a stimulus of a certain threshold. During an action potential the resting potential of about $-200\,\mathrm{mV}$ is depolarized by around $100\,\mathrm{mV}$. This transient change in voltage propagates through the cell after excitation. Although the action potential does not display hyperpolarization and differs in absolute velocities (**cm/s**) from those which occurs in animal cells (**m/s**, neurons), the action potentials are very similar to them. The shape mainly coincides, and it can only be generated by external stimuli with a certain excitation threshold (**all-or-none principle**).
Furthermore, the algae additionally show the existence of a cold and a heat block of

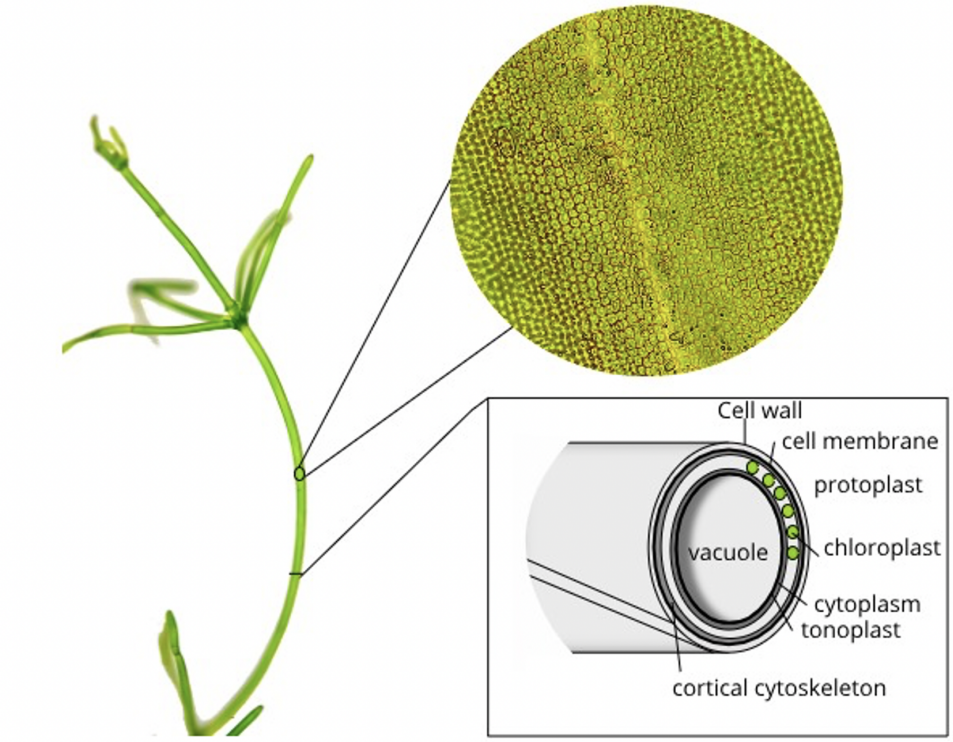

Figure 4.1: Structure of the freshwater plant cell *Chara australis* : On the left-hand side, the morphology of an algae *Chara australis* , consisting of the internodal and branchlet cells, is shown. The right-hand side shows an image of the cell surface of the algae by a magnification of 50x and a schematic cross section of the algae. The cell is made of serveral layers from outside to inside: Cell wall, cell membrane, cortical cytoskeleton, chloroplasts, cytoplasm, tonoplast and vacuole.

excitability. This means at low temperature (< 0 °C) and at high temperature (between 30 °C and 40 °C) the cell is not excitable. In the intermediate regime, the velocity increases with increasing temperature (Fillafer et al. (2021)). This behavior has been shown for several types of cells such as frog, cat or giant squid cells (Blatt (1974); Chapman (1967); Engelhardt (1951)). Similar blocks in excitation can be induced by pressure, protons (extracellular pH) or other ions (Fillafer et al. (2021)). All these strongly indicate that the physical foundation of the phenomenon has to be the same in all kinds of cells, even in human cells.

4.3 Materials and Methods

4.3.1 Cultivation of *Chara Australis*

The cells were planted in a layer of soil in a glass aquarium which was lled with deionized water. The plants were grown at a 12h:12h light:dark cycle at room temperature ($\sim$ 20 °C). Single internodal or single branchlet cells were cut and were stored in a solution containing 0.1 mM KCl, 0.1 mM NaCl and 0.1 mM Ca_2 prior to use.

4.3.2 Staining of Cells

Internodal cells were stained in a 10 µM solution of Di-4-ANEPPDHQ in artificial pond water (APW: 1 mM Ca_2, 1 mM KCl, 5 mM HEPES, pH set to 7.0 with NaOH) for 10 min. The staining solution contained < 1 % DMSO. After staining, the cells were washed with APW and mounted in a measurement chamber with vacuum grease. In some of the experiments the stained cells were plasmolyzed to separate the plasma membrane.

4.3.3 Detachment of Chloroplasts from the Cell Surface

The cortical cytoplasm of a *Chara* cell contains a dense stationary array of chloroplasts (Kamitsubo (1972)). The pigments located in these chloroplasts (mainly chlorophyll) convey the cell with an intense autofluorescence at wavelengths >625nm which partially overlaps with the emission spectrum of Di-4-ANEPPDHQ in the cell membrane. To create a window widely free of *chloroplasts*, the cells were irradiated by ultraviolet light ($\sim$ 380 nm) for 2 min (Kamitsubo (1972)). After serval hours the chloroplasts detached from the cell cortex and were removed from the region by the cytoplasmic streaming.

4.3.4 Plasmolysis of *Chara Australis*

In an intact cell of *Chara australis* the cell wall lies tight to the cell membrane with a turgor pressure of $\sim 6 \times 10^5\,\mathrm{N/m^2}$ (Barry (1970)). The turgor pressure can be reduced by a slow increase of the extracellular osmolarity (s. **Figure 4.2**). At a certain osmolarity the cell membrane separates from the cell wall. This was done by gradually replacing the extracellular APW-solution by an APW-solution with an increased sorbitol concentration. At an osmolarity of about 270 mOsm the membrane detaches. This procedure, also known as plasmolysis, reacts non-uniformly, so that

the membrane detaches at some points and is adhered at another. This results in an irregular waveform shape of the cell surface (s. **Figure 4.2** (right)). In some cases, the membrane is still connected to the membrane via some threats (*Hecht's threads*) even if the membrane is separated. With further plasmolysis the Plateau-Rayleigh instability occurs (Fillafer et al. (2018)).

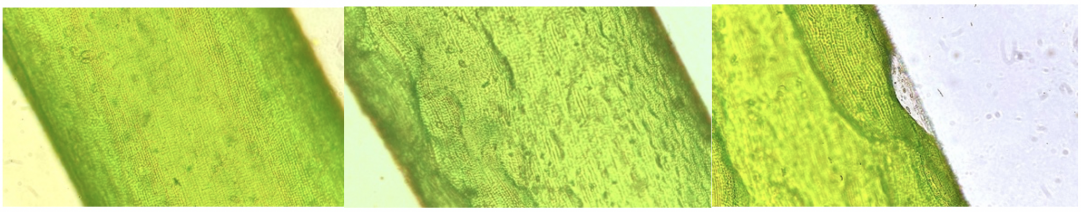

Figure 4.2: Plasmolysis of a *Chara australis*cell: Images of a *Chara australis* cell with different concentrations of sorbitol. From left to right the concentration of sorbitol increases until the cell plasmolyzes at about 270 mOsm.

4.3.5 Recording of Fluorescence Emission Changes

A Leica TCS SP5 confocal laser scanning system coupled to a Leica DMI 6000 Cs inverted microscope was used to image the plasma membrane of *Chara australis* cells labelled with di-4-ANEPPDHQ. To obtain a ratiometric parameter the fluorescence was recorded at two wavelength channels (green:(500 nm - 569 nm); red:(600 nm - 665 nm)). Combined with the plasmolysis of the cell, the location of the cell surface could be tracked during the pulse propagation of the cell. The ratio parameter was monitored continuously (3 Hz sample rate) to recognize the dynamic of the action potential. To differentiate the surface structure from the wall material, the averaged signal of a rectangular part of both structures were calculated. Therefore, the confocal images could be used to detect a mechanical shift of the surface by the observation of the intensity as a function of location.
To simultaneously detect the electrical and optical signatures of the action potential, an additional setup was constructed (s. **Figure 4.3**). The cell was placed in a plexiglass chamber, small extracellular compartments were electrically isolated against each other, and the transmembrane potential was recorded with Ag/AgCl-electrodes by the K^+-anesthesia technique (described in Luehring (2006)). To stimulate an action potential, an electrical stimulus was applied. The optical signal was recorded in one isolated compartment over the entire field of view (20x magnification). The fluorescent dye was excited with a high-power LED (Thorlabs, M470L4) with maximum wavelength at 470 nm. The emission signal was detected by a spectrum analyzer or two photomultiplier tubes equipped with green ((560 ± 10) nm) and red ((610 ± 10) nm) band pass filters. These photomultiplier signals were used to calculate the ratio parameter $\frac{I_{\text{green}}}{I_{\text{red}}}$.

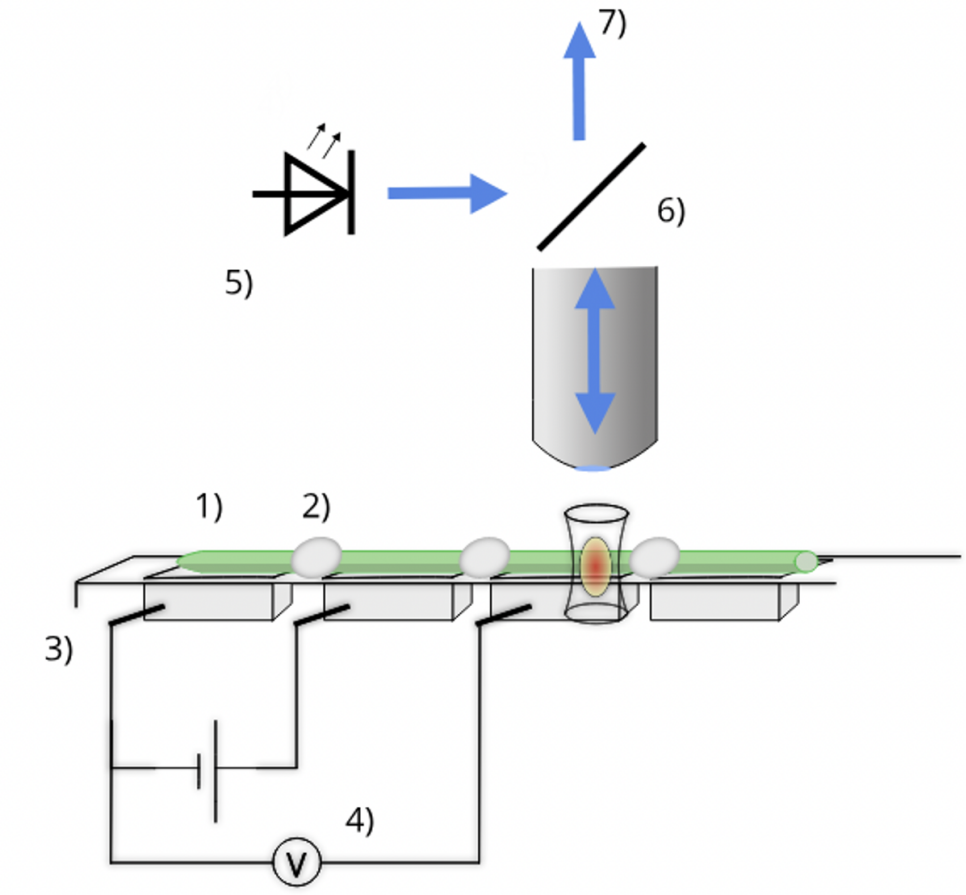

Figure 4.3: Schematic setup to record fluorescence emission changes of *Chara australis*: The alga (1) (green) was electrically isolated by vacuum grease (2) into an acrylic glass chamber with fixed Ag/AgCl-electrodes (3). The electrical stimulus was applied with a battery (4) and the potential was measured with the K^+anesthesia technique (Luehring (2006)). Simultaneously, the optical signal was recorded with a fluorescence microscope. The fluorescent dye was excited by a high-power LED (5). The excitation light was reflected by a dichromatic mirror (6) to the sample and emission was transmitted to the light detection (7, photomultiplier or spectrum analyzer).

4.3.6 Optical State Diagrams of *Chara Australis* Cell Membrane

A special microscope chamber (FCS2, Bioptechs) was coupled to an external heat bath (Lauda Eco Silver) in order to vary the environmental temperature of the cell. The optical signal was recorded as described above (5 kHz sample rate). To suppress the bleaching of the incorporated dye, an irradiation time of 200 ms every 5 min was used. This results in a net irradiation time of about 5 s for one temperature cycle from 20 °C to 2 °C and up to 40 °C.
In order to change the extracellular pH, the extracellular medium could be exchanged via two ports of the measurement chamber. To guarantee the change of the pH of the medium, the measuring chamber was flushed with thrice its internal volume.

4.4 Results and Discussion

4.4.1 Emission Properties of Di-4-ANEPPDHQ Incorporated into *Chara Australis*

To record the static and dynamic changes of the fluorescent dye, the background fluorescent emission has to be characterized. At the surface cortex of a *Chara australis* cells are several fluorescent components such as chlorophyll which overlap with the signal of the incorporated dye. Therefore, the secondary fluorescent background of the cells has to be separated from the primary emission of the fluorescent probe (di-4-ANEPPDQH).
Figure 4.4 displays the emission spectrum of the autofluorescence when excited at 470 nm. The highest intensities occurred at the red edge of the visible light spectrum at around 700 nm.

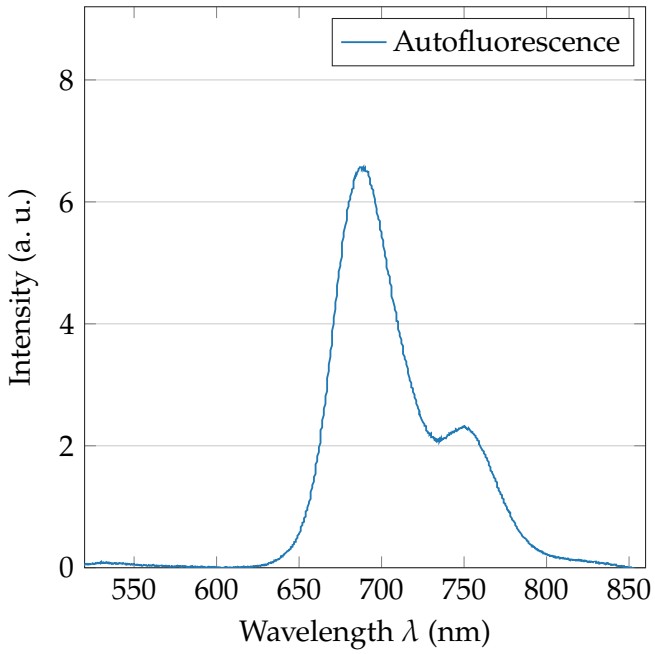

Figure 4.4: Autofluorescence of *Chara australis*: The graph shows the emission spectrum of the natural fluorescent structures of a chara australis cell when excited at 470 nm. The maximum of the spectrum is located at about 700 nm and correlates with the emission of chlorophyll (Pedrós et al. (2008)) which is incorporated into the chloroplasts (figure taken from Fabiunke et al. (2021)).

The main part of these autofluorescence signals correspond to the emission of chlorophyll (Pedrós et al. (2008)), but there are also other structures which contribute to the emission spectrum. Due to the great amount of chloroplast and therefore high intensity of the autofluorescence, the chloroplasts have to be removed from the cell

cortex as described in section 4.3.3. Only by removing the chloroplast, the signal of the embedded dye can significantly be detected. **Figure 4.5** displays the emission spectrum of the dye di-4-ANEPPDHQ incorporated into the *Chara australis* cell where most of the chloroplasts were removed. The intensity at the red edge of the spectrum is attributed to some chloroplasts which were still adhered or floating in the cytoplasm streaming. However, a significant emission peak between 550 nm to 625 nm occurred when the fluorescent dye di-4-ANEPPDHQ was incorporated. The difference curve of background and signal showed an almost similar spectrum compared to the spectrum of the dye incorporated into a lipid monolayer or lipid vesicle (s. **Figure 3.4**).

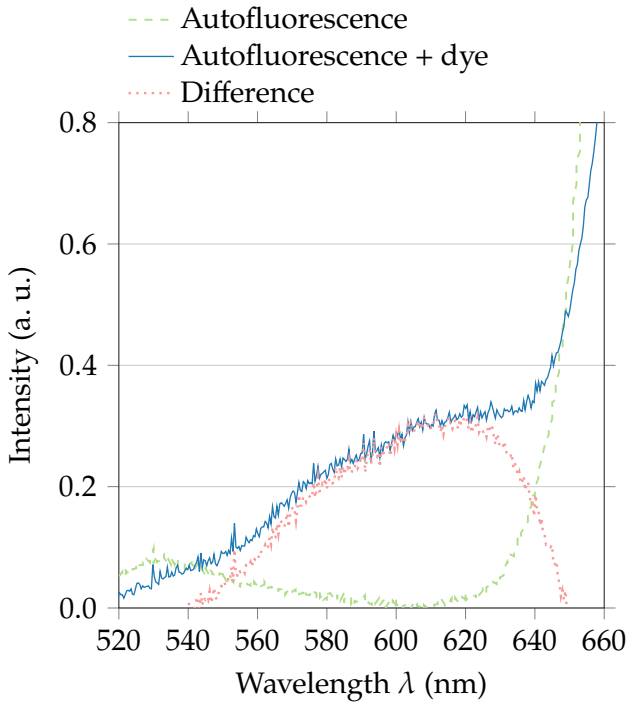

Figure 4.5: Emission properties of di-4-ANEPPDHQ incorporated into *Chara australis*: Autofluorescence of a *Chara australis* cell (green, dashed), total fluorescence emission from a cell stained with di-4-ANEPPDHQ (blue, solid), and emission after subtraction of the autofluorescence (red, dotted). The intense fluorescence at wavelengths > 625 nm is mainly due to chlorophyll (figure taken from Fabiunke et al. (2021)).

Based on the difference, the maximum of the emission spectrum appeared at approximately 610 nm and the full width at half maximum is about 80 nm. Small differences between the spectra of the cell-associated dye and the dye embedded into artificial lipid systems in position and width are attributed to the differences in the micro-chemical environment. Due to these slightly different spectra the state phase of the system

cannot unambiguously be determined by the maximum wavelength. Only relative changes of the spectrum can indicate changes in state.
Due to the high background fluorescent structures, small changes of the emission spectrum were analyzed by measuring the ratio parameter $\frac{I_{\text{green}}}{I_{\text{red}}}$ (green: (560 ± 10) nm and red: (610 ± 10) nm) as a indicator of a transition.

4.4.2 Sub-Cellular Localization of Fluorescence Emission Changes

In standard wide-field microscopy the optical resolution (micrometer) is not sufficient to conclude which structures are dyed with the fluorescent probe. For this reason, the emission signal represents the sum of all cell-associated fluorophores. To understand state changes, it is of main interest which structure causes the changes in emission. For the localization of the dye molecules, the cell was plasmolyzed. By plasmolysis the cell surface was separated from the cell wall. Additionally, the cell was investigated with a confocal microscope system.
Figure 4.6 shows that the fluorescent dye was interestingly incorporated into the cell surface (membrane and other cortical organelles) as well as into the cell wall. Epiphytes and residual membrane materials which were still attached after plasmolysis explains the localization of the dye molecules at the cell wall. Nevertheless, the resolution limit of the confocal microscope forbids an exact identification of the dye location at the cell surface. The affinity of the dye to incorporate into lipophile substances (Jin et al. (2006)) makes it reasonable to assume that the dye is primarily located in the plasma membrane at the cell surface.

Also, the extraction of a vesicle from cell membrane material supports the assumption that the fluorescent dye was incorporated into substances of the cell membrane. For this purpose, the cell was plasmolyzed and the cell wall was cut with a syringe cannula connected to a micromanipulator (described earlier in (Muchowski (2017))). By changing the solution to lower sorbitol concentrations again (deplasmolyze), the membrane moved to the wall and a vesicle was extruded out of the cut cell wall. **Figure 4.7** shows a vesicle made of membrane material under wide field (left) and fluorescent emission (right). The fact that the vesicle showed fluorescent emission, substantiated the incorporation of the dye into the cell surface.

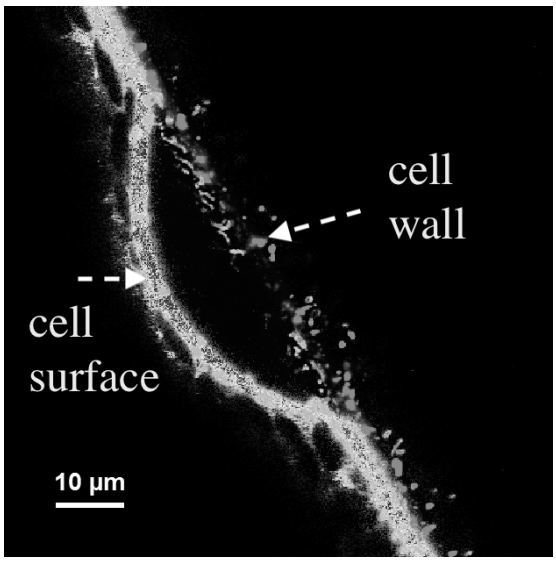

Figure 4.6: Fluorescent emission of di-4-ANEPPDHQ incorporated into a plasmolyzed *Chara australis* cell: The confocal image shows that the dye is incorporated into the cell surface as well as into the cell wall. In the confocal image, a plasmolyzed cell without any visible connections to the cell wall is displayed.

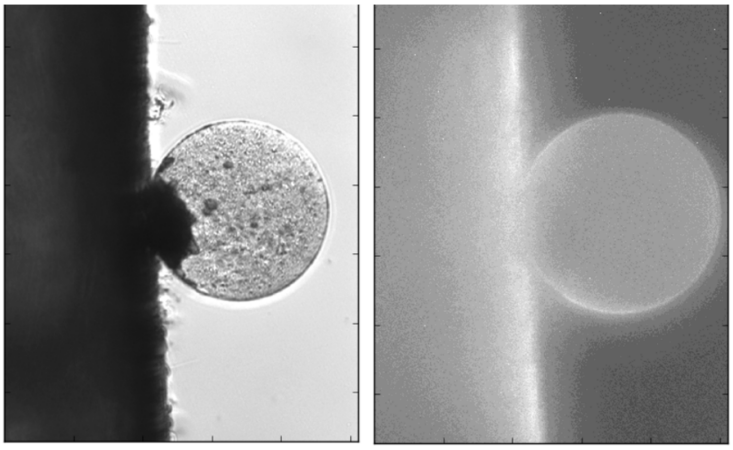

Figure 4.7: Extruded membrane vesicle out of a *Chara australis* cell: On the left-hand side, a wide field image of the vesicle is shown. On the right-hand side, the fluorescence of the same image is shown. The dye is embedded into the extruded vesicle (measured by S. Fiolka (Bachelor thesis)).

4.4.3 Phase Diagrams of Living Cells

The static state diagrams of living cells offer the opportunity to stress several predictions of cell processes, excitability and nerve pulse propagation. Therefore, the phase transition point of an intact biological system is of central interest. In most studies (calorimetry etc.) extraction of membrane molecules of many cells are necessary to capture membrane properties such as heat capacity (Beljanski et al. (1997)). However, fluorescent dyes which are sensitive to the transition point, provide a way of detecting state changes of a single cell in vivo. The dye molecules can be used in concentrations of micromolar and thereby with presumably minor effects to the resting state and excitability of the observed living system. To understand the role of phase transitions in biology, it is absolutely necessary to measure phase diagrams of living cellular tissue. Furthermore, drawing a connection between different variables and clear predictions of excitability, chemical reactions, propagation velocity and adaption will be feasible.

Bleaching of the Dye Molecules Affects the Ratio Parameter

For the investigation of the influence of irradiation to the cell and the optical signal, the ratiometric parameter $\frac{I_{\text{green}}}{I_{\text{red}}}$ and the membrane potential of a dyed cell was simultaneously measured over time. The ratio parameter $\frac{I_{\text{green}}}{I_{\text{red}}}$ as a function of time is shown in **Figure 4.8**. Whereas the membrane potential did not change (data not shown), the ratio parameter $\frac{I_{\text{green}}}{I_{\text{red}}}$ increases about 9 % upon high constant irradiation. After 60 s irradiation, the increase showed a slight saturation behavior, indicated by a decreasing slope. The changes of the ratio parameter were a result of an asymmetric bleaching of the two emission channels. The red channel also detected part of the signal of the autofluorescence, whereas the green signal did not. Thereby a difference in bleaching was emerged, which led to an increase of the ratio parameter. These changes were probably not related to a change in state of the cell. A reduction of irradiation time or intensity decreased this effect significantly.
In all further experiments the excitation light was used at low intensities, and it was triggered to decrease the effective irradiation time to maximal 20 s.

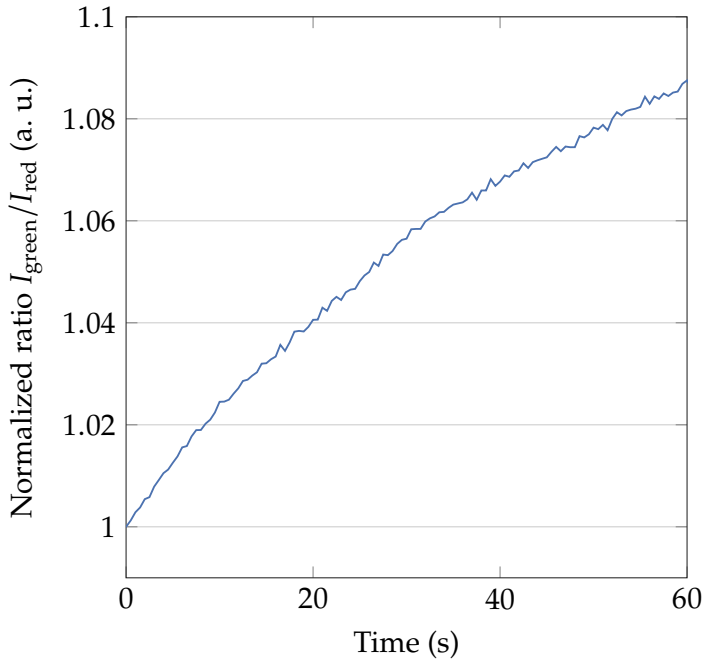

Figure 4.8: Bleaching of the fluorescent dye di-4-ANEPPDHQ: Changes of the ratiometric parameter $\frac{I_{green}}{I_{red}}$ of a dyed *Chara australis* cell as a function of time for continuously high irradiation when all parameters are kept constant (temperature, no stimulation). Note: Typical net irradiation time in the experiments was about 20 s. (The plot represents 4 measurements with 2 different cells; Fabiunke et al. (2021)).

Emission Properties as a Function of Temperature

An obvious thermodynamic variable of a system is certainly the temperature. It is well known that the temperature has also a significant influence of living organisms such as denaturation of proteins which shifts the system into a non-viable regime. In the thermodynamic theory, the properties of membrane tissues also have to change with temperature. If the excitable medium becomes softer the propagation velocity of action potentials should be clearly affected as predicted for an acoustic pulse at an interface $v \propto \sqrt{(1/\kappa\rho)}$ (Fillafer and Schneider (2013b)). To a certain extent, the temperature can also influence the excitability of a system. It is well known that cooling has an anesthetic effect to biological functions and leads to a slowing down of the velocities of action potentials (Blatt (1974)). In contrast, an increasing temperature leads to an increased propagation velocity of nerve pulses in several kind of cells (Fillafer and Schneider (2013a)). For temperatures above 40 °C cells typically are not excitable which is normally attributed to denaturation of cell components. The evidence of a disordered-ordered transition in the living algae leads to a physical phenomenology of excitation regimes and should lead to a shift of the emission spectrum of the

incorporated dye molecules.

To measure the optical state diagrams of the excitable cellular membrane directly, the ratio parameter $\frac{I_{\text{green}}}{I_{\text{red}}}$ was measured as a function of temperature. As mentioned above the ratio parameter $\frac{I_{\text{green}}}{I_{\text{red}}}$ constantly increased with continuing irradiation. To suppress this effect, the LED was triggered. A typical temperature cycle was measured from 20 °C to 2 °C and up to 40 °C. The lower limit in temperature is determined by the freezing point of the extracellular aqueous solution. At temperatures between 35 °C and 40 °C the algae are irreversibly damaged, which is also known as heat-block.

Figure 4.9 displays that the ratio parameter $\frac{I_{\text{green}}}{I_{\text{red}}}$ increased approximately linearly by 22 % upon cooling from 20 °C to 2 °C. Between 20 °C and 40 °C the ratio mainly stayed constant. The increase of the ratio by cooling was completely reversible whereas a heating cycle was not. The uncertainties of the data points represent the fluctuations between different measurements of several cells ($n = 6$). These results indicate a blue shift or broadening of the emission spectrum upon cooling, starting at the resting state (growth conditions about 20 °C).

Cooling of *characean* cells results also in a depolarization of the membrane potential.

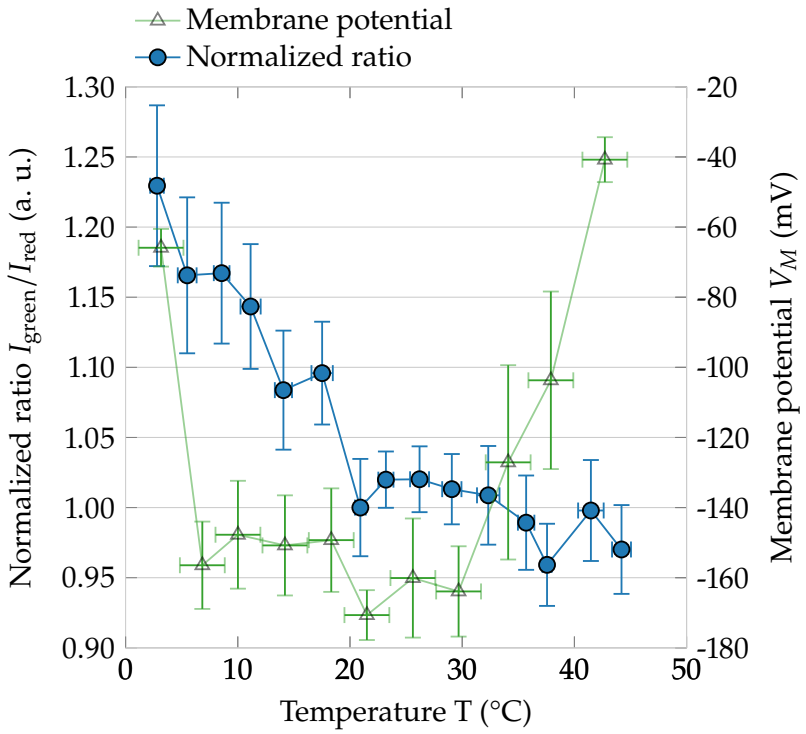

Figure 4.9: Ratio-potential-temperature phase diagram of *Chara australis*: Ratio parameter $\frac{I_{\text{green}}}{I_{\text{red}}}$ of di-4-ANEPPDHQ incorporated into a *chara australis* cell as a function of temperature. The ratio increased with decreasing temperature. Between 20 °C and 40 °C the ratio parameter mainly stayed constant (average of 5 different cells). The membrane potential (average of 3 different cells) also decreased between 20 °C and 5 °C. Additionally, the membrane potential depolarized at about 35 °C. This is in line with the heat block of the *Chara australis*.

Figure 4.9 demonstrates that going from 20 °C to 0 °C the resting potential in *Chara* cells mainly stayed constant and only increased near 0 °C in a nonlinear behavior up to $\sim -60\,\mathrm{mV}$. Also, other authors have shown that the potential slightly rises upon cooling (Beilby and Coster (1976)). These results are in line with an electrochromic interpretation of the dye signal, where a blue shift of the spectrum is expected by depolarization. For temperature between 30 °C and 40 °C the ratio parameter mainly stayed constant. This does not seem to be apparent in the electrophysical data and in the data of Beilby and Coster (Beilby and Coster (1976))). In temperature ranges between 30 °C and 40 °C the potential depolarized irreversibly. In an electrochromic interpretation of the emission properties, the depolarization has also to be reflected in the ratio parameter. In this case the causal coupling between membrane potential and emission spectrum no longer exists. Therefore, it can be concluded that the origin of the increasing ratio upon cooling is **not** the depolarization of the membrane potential. The transient changes of the slope of the ratio parameter upon cooling could be differently interpreted as a manifestation of a state transition (c. chapter 3). Those state changes have previously been reported by others (Beljanski et al. (1997)). The analysis of a plasma membrane-enriched fraction by differential scanning calorimetry indicated two reversible heat capacity maxima in characteristic temperature regimes (15 °C - 20 °C and 30 °C - 35 °C). The transition at the lower temperature regime (15 °C - 20 °C) correlates very well with the found changes of the slope of the ratio upon cooling.

Furthermore, by comparing the optical results and measurements of the velocity of action potentials as a function of temperature (Fillafer et al. (2021)), two facts can be summarized. First the slowing down of the velocity upon cooling correlates very well with the increase of the ratio parameter. Secondly, the heat-block of excitability of the system and second transition, observed by Beljanski et al. (Beljanski et al. (1997)), does not seem to influence the optical ratio parameter.

In the thermodynamic picture, a phase transition of the membrane and the resulting non-linearity are directly related to the excitability of the cell (Cold- and Heat-block). This means that a shift into a transition or away from the transition results in a non-excitability of the system. Furthermore, the state of the membrane also controls the velocity of pulse propagation. For the specific case here, an increasing ratio parameter could indicate a transition of the lipid membrane. This is accompanied by a maximum in compressibility and therefore the pulse propagation velocity should decrease. However, also other variables such as viscosity and the coupling to the environment are suggested to strongly influence the velocity of the action potentials (Griesbauer et al. (2010); Kappler et al. (2017)). Compared to artificial membranes, the optical data indicates a relatively broad transition regime between 20 °C and 0 °C. This is not contradictory, as a more complex system with several components (proteins, different lipids) could produce a broader transition regime than a mono-component

system. Also, other studies of phase transitions in living systems showed a relatively broad transition regime of about 10 °C - 20 °C (Heimburg and Jackson (2005)).

4.4.4 Emission Properties as a Function of Extracellular pH

The external pH was also chosen to record a thermodynamic phase diagram, because it has a well-defined thermodynamic meaning. Protons are known to induce a thermodynamic state change in lipid-based membranes (Blume and Eibl (1979)). With a charged membrane, the increase of the proton concentration leads to alteration of the charge density at the surface which mainly depends on the pK(s) of the membranes. Eukaryotic cells are typical negatively charged (Mehrishi and Bauer (2002)) and, therefore, an acidification should lead to an increase of proton adsorption and discharging the surface which should also lead to a more ordered state of the interface. **Figure 4.10** displays the ratio parameter as a function of the external pH value. It clearly shows a significant increase of the ratio upon acidification, whereas alkalization did not change the ratio parameter significantly. Qualitatively, the changes in the ratio parameter $\frac{I_{\text{green}}}{I_{\text{red}}}$ with acidification (increase about 20 %) and the changes with cooling the temperature (increase about 20 %) were indeed similar. These results validated previous studies of changes of the conduction velocity of *charophyceae* and other cell types. Furthermore, acidification leads such as cooling to a conduction block of the cells. This is in line with a phase transition of the membrane which determined the excitability.
Taken together, the increased ratio upon acidification and cooling indicates a blue shift of the emission spectrum. It is of particular interest if there are thermodynamic transitions of the plasma membrane in vicinity of the resting state of the living system. Both, studies of the fluorescence as a function of temperature and pH indicates a transition of the membrane. The similarity between the two parameters also supports the thermodynamic point of view of living matter.

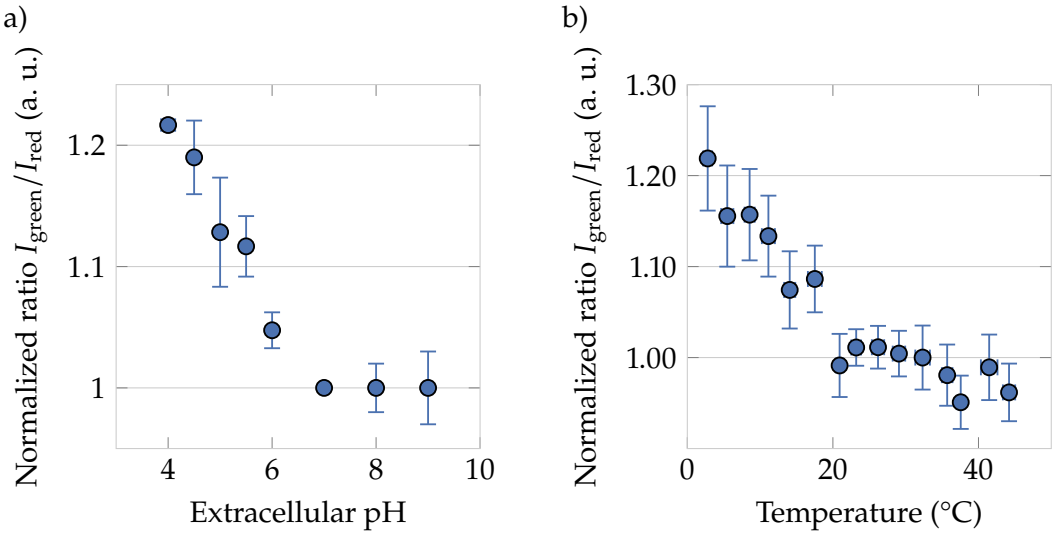

Figure 4.10: Ratio parameter phase diagrams: (a) Ratiometric parameter $\frac{I_{green}}{I_{red}}$ as a function of the extracellular pH-value. The ratio was normalized to the reference point at room temperature (~ 20 °C) and a pH of 7. (b) Ratiometric parameter $\frac{I_{green}}{I_{red}}$ of Di-4-ANEPPDHQ in a *Chara australis* cell as a function of temperature. The ratio increases with decreasing temperature (figure taken from Fabiunke et al. (2021)).

Combined Changes of Extracellular pH-Value and Temperature

Other studies have shown that the changes of the propagation velocity caused by the acidification could be compensated by heating. The analysis of Fillafer et al. (Fillafer et al. (2021)) showed that 1 pH unit corresponds to about 4 °C. This means that lowering the temperature by 4 °C is equivalent to decreasing the pH by one unit in the appropriated pH regime. It is obvious that this has limitations by the pK value of the lipid membrane of the living system. But it is well known that protonation of molecules occurs in a specific range. Only within this range around the pK value an influence on the main transition point of a lipid membrane can be observed (Fichtl et al. (2016)).

According to studies with lipid-based systems the transition point of a membrane shifts depending on the pK(s) to higher or lower temperature. **Figure 4.11** displays the ratio parameter $\frac{I_{green}}{I_{red}}$ as a function of temperature with an extracellular pH value of 4.7. It shows that the ratio parameter $\frac{I_{green}}{I_{red}}$ continuously increases upon cooling as well between 40 °C and 2 °C. However, below 10 °C a saturation seems to occur.

The optical susceptibility parameter $(\partial\lambda_{max}/\partial T)$ is maximal in the transition regime and only slightly alters around the transition. Consequently, a change of the slope of the ratio between 22 °C and 15 °C indicates a state change of the cell membrane. This clearly supports the assumption that cells are located in the vicinity of a phase

transition and this main transition can be shifted by external influences.
In summary, different environmental conditions (such as pH7, pH 4.7 etc.) can directly influence the main phase transition point of the cells. Fluctuations of the transition point (T_m) between different cells are possible evolutionary processes. When external conditions change, only organisms whose transition is close to the "new" state are able to adapt and survive. The distribution of the transition points in cells can occur, for example, due to different compositions of the living system.

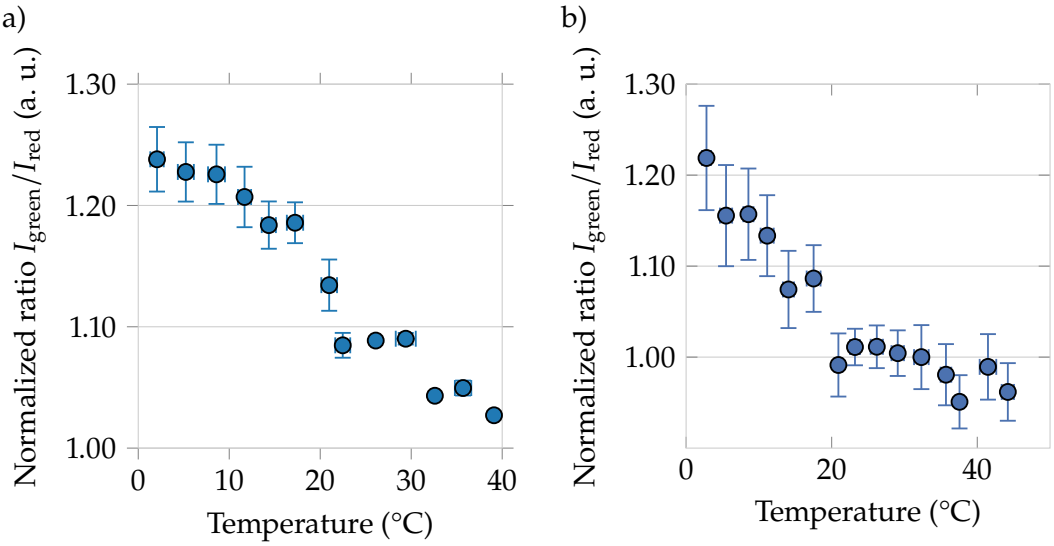

Figure 4.11: Ratio parameter phase diagrams at different pH values: (a) shows the ratio parameter as a function of temperature at an extracellular pH of 4.7. When the temperature was decreased from 22 °C to 15 °C the ratio increased in a nonlinear way. Below 15 °C and above 25 °C comparative small changes occur (average of 4 different cells). (b) displays the ratio parameter as a function of temperature at an extracellular pH of 7 (s. Figure 4.10).

4.4.5 Action potential in *Chara Australis*

The state diagrams of cells offer the opportunity to stress predictions of the thermodynamic view of living matter. However, it is crucial to investigate equilibrium **and** non-equilibrium events in cells. It has been previously proposed that acoustic sound waves are the physical foundation of nerve pulses. In particular, the nonlinearity of a membrane (thermodynamic system) is necessary in order to support nonlinear sound waves in cell biology. This nonlinearity is also proposed as foundation of the specific properties of action potentials (all-or-none-behavior, threshold etc.). Therefore, it is of main interest whether the membrane or the medium of propagation undergoes a transient state change during the propagation of an action potential. Here the emission properties of the state sensitive dye di-4-ANEPPDHQ embedded into the *Chara australis* plant cell are investigated during an action potential. The existence of a state change during the propagation of action potentials in livings cells has not been shown yet. With the knowledge of the previous chapter, a perturbation which changes the phase state (blue-shift) should propagate through the cell.

Figure 4.12 shows the overlay of the electrical signal and the optical signal (ratio parameter $\frac{I_{\text{green}}}{I_{\text{red}}}$) as a function of time. The upper time trace (a) displays a clear response of the membrane potential and also of the ratiometric parameter $\frac{I_{\text{green}}}{I_{\text{red}}}$ after triggering an action potential. The membrane potential decreases typically about 100 mV during the action potential and the ratio parameter increases up to 4 %. The two curves show a simultaneous increase of the signal. Furthermore, the maxima occur at the same time at about 18 s. Only the duration differs slightly. Since the optical signal is much more localized than the electrical signal, an offset seems to be reasonable. In general, it can be concluded, that there is a correlation between the membrane potential and the emission properties of the fluorescent dye during the action potential, which confirms the assumption that both are consequences of the same physical origin.

To ascertain that the fluorescent dye responds to the action potential and not the several cellular autofluorescence, the fluorescence of an undyed cell is measured during an action potential (s. **Figure 4.12**b). In this case, the fluorescence shows no significant response to the electrical impulse. Therefore, it can be concluded that the changes in the signal originated unambiguously from the embedded fluorescent dye.

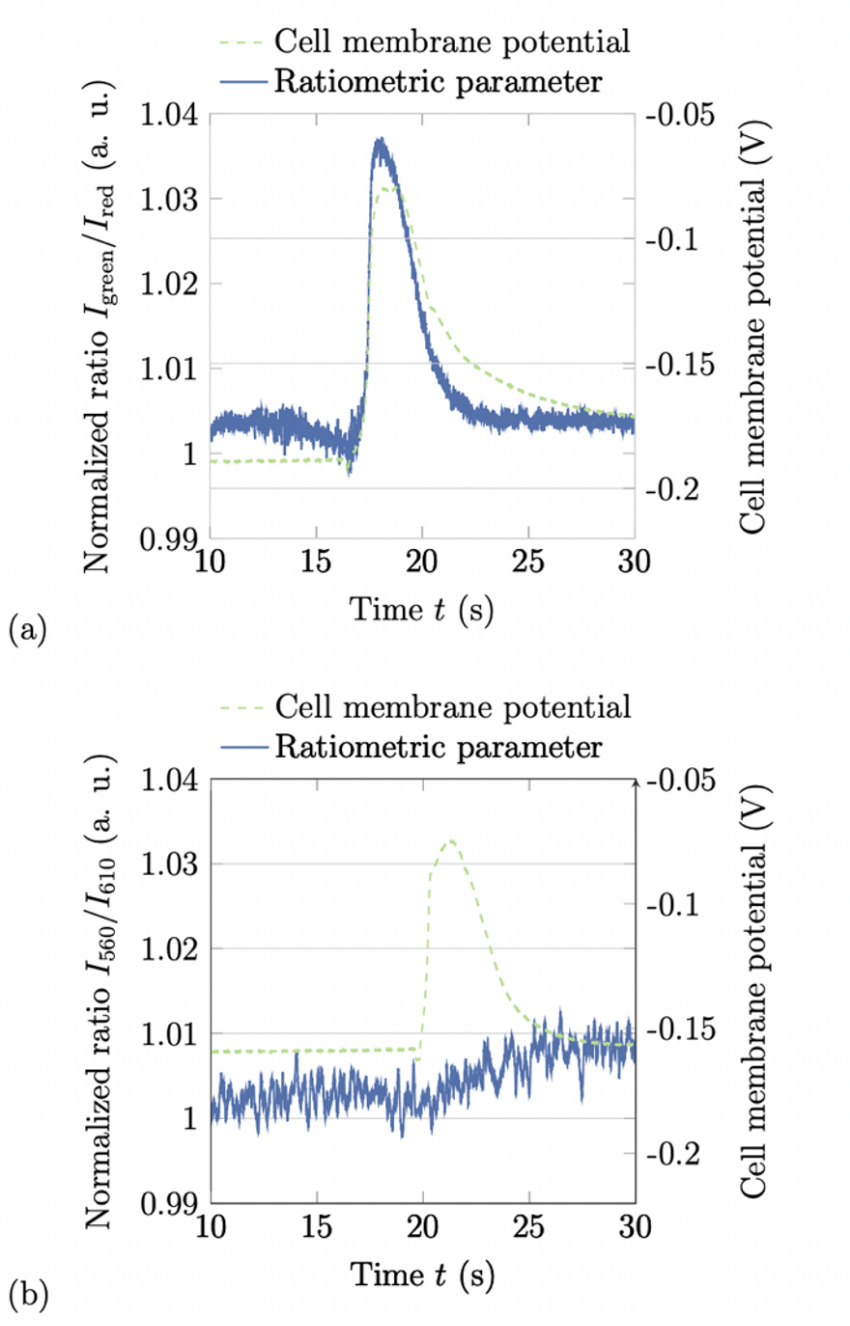

Figure 4.12: Fluorescent emission of di-4-ANEPPDHQ incorporated into a plasmolyzed chara *Chara australis* cell (a) Time course of the ratio parameter $\frac{I_{green}}{I_{red}}$ and the membrane potential when an action potential was stimulated in a cell stained with di-4-ANEPPDHQ. (b) Response of the ratio parameter and the membrane potential during an action potential in an undyed cell (figure taken from Fabiunke et al. (2021)).

Localization of the Signal Signature

As mentioned before, the material of the cell wall also contains a substantial amount of di-4-ANEPPDHQ. Therefore, it is of interest in which structure the changes during action potentials take place. For this purpose, the fluorescent signal was confocally recorded of the cell surface as well as of the cell wall during an action potential (s. **Figure 4.13**). After triggering an action potential, the ratio parameter $\frac{I_{\text{green}}}{I_{\text{red}}}$ at the cell surface increased by 10 - 20 % of the baseline, whereas the ratio did not change at the wall structures. The higher amplitude of the pulse compared to the experiments of the previous section mainly depended on the different emission channels of the confocal microscope. The superposition of the signal from the wall (no changes) and surface (changes) also played a role for the measured response. The duration time of about 5 s of the optical pulse and the shape was consistent with duration and shape of the electrophysical action potentials (s. **Figure 4.13**). At this point, it can be concluded that the action potential propagates through the cell surface structure as predicted in several theories of the nerve pulse propagation. It is consistent with the conjecture that the excitable medium of a cell is indeed the cell membrane (Baker et al. (1961); Kaufmann (1989a); Tasaki et al. (1962); Terakawa (1985)).

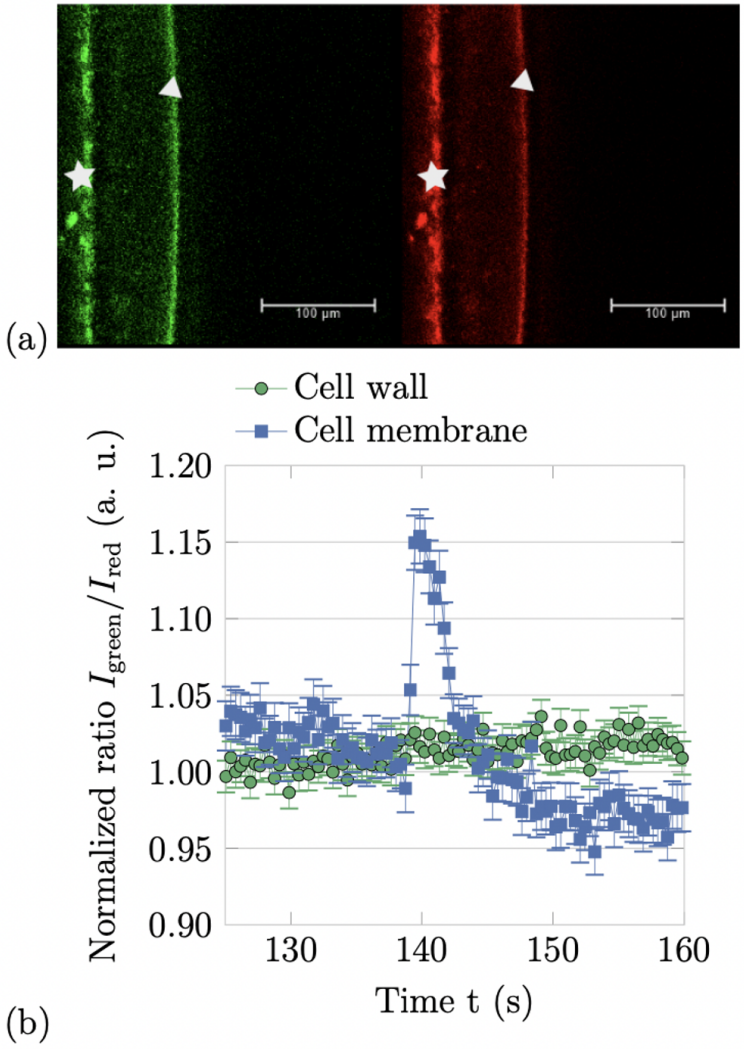

Figure 4.13: Fluorescent emission of Di-4-ANEPPDHQ incorporated into a plasmolyzed chara *Chara australis* cell (a) Confocal microscopy image of a plasmolyzed *Chara australis* cell in the green 500 nm – 569 nm (left) and red (600 nm – 665 nm (right). The surface of the cell membrane is marked with a triangle and the wall with a star. (b) Dynamic changes of the ratio $\frac{I_{green}}{I_{red}}$ during an action potential. Mean value and standard deviation of the ratio $\frac{I_{green}}{I_{red}}$ calculated at the surface and wall of a plasmolyzed cell. The time trace shows a typical optical response to an action potential. The average ratio at the membrane (squares) increases, whereas the signal at the wall (circles) does not (8 experiments, 4 cells) (figure taken from Fabiunke et al. (2021)).

4.4.6 Changes of the Emission Spectrum during Action Potential

Due to the fact that the ratio parameter changed for various reasons (asymmetric broadening, shift of the emission spectrum) it requires more precise investigations to understand the alteration of the emission spectrum during the action potential. The analysis of the single emission channels shows that the intensity of the green channel increases, whereas the intensity of the red channel decreases (**Figure 4.14**). The opposite direction of the change leads to the assumption that the emission spectrum shifts to shorter wavelength during an action potential. The difference of the intensity changes, 10 % at the green and 3 % at the red channel, can be explained by the position of the wavelength bands within the spectrum. The wavelength 610 nm is located in the vicinity of the maximum of the spectrum and 560 nm is located on the left side of the spectrum. At the flank a shift is expected to cause greater relative changes than at the maximum. A blue-shifted emission spectrum is consistent with other studies of emission changes during nerve pulse propagation (Cohen et al. (1978); Obaid et al. (2004)).

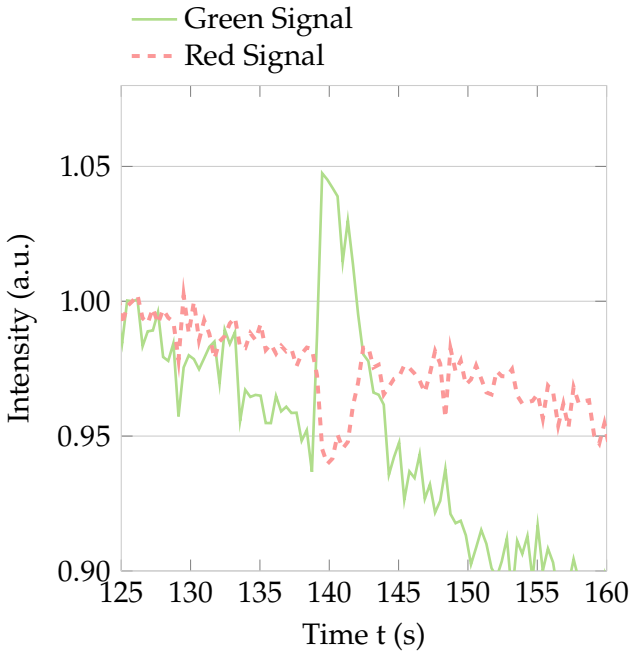

Figure 4.14: Individual signals of the green (560 nm**) and red (**610 nm**) channels after triggering an action potential:** The intensity of the green channel increases whereas the intensity of the red channel decreases. This indicates a transient blue shift of the emission spectrum (figure taken from Fabiunke et al. (2021).

In order to further understand the changes of the emission properties the entire emission spectrum was investigated during an action potential. Due to the high emission of chlorophyll it is not possible to record the solitary emission spectrum of

di-4-ANEPPDHQ. After detaching the chloroplasts, a substantial intensity overlaid the recorded emission spectrum of the dye molecules. To eliminate the autofluorescence a short pass filter (650 nm) was equipped to the spectrum analyzer. An integration time of 100 ms was needed to record the spectrum of di-4-ANEPPDHQ. Furthermore, the distinction of cell surface and cell wall was not feasible in practice. The permanent superimposition of the autofluorescence, signal from the cell wall as well as the signal form the membrane made it impossible to observe an unambiguous change of the spectrum during an action potential. Also, the relatively broad spectrum (100 nm) overlays a possible shift of the maximum. **Figure 4.15a** displays the emission spectrum

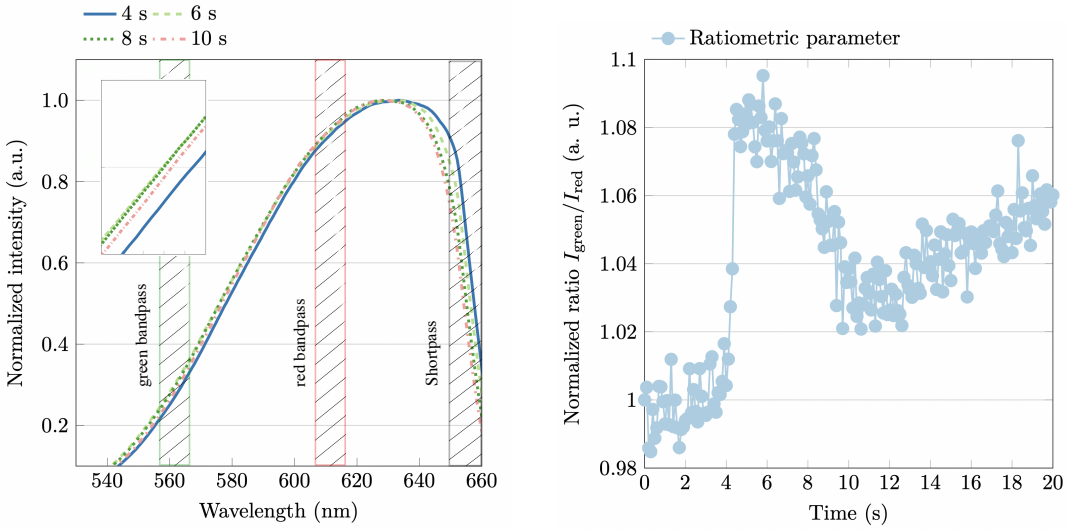

Figure 4.15: Entire emission spectrum of di-4-ANEPPDHQ during an action potential: (a) Emission spectra at different points in time recorded with a 650 nm shortpass filter mounted to the spectrum analyzer to cut the emission of chlorophyll. The action potential was triggered at about 4 s. To see the time course, the wavelength range from 570 nm - 580 nm is plotted in the inset. (b) shows the ratio parameter calculated from the extracted intensities at (560 ± 10) nm (green edge) and (610 ± 10) nm (red edge). The ratio parameter increases during the action potential analogous to the measurements before.

at different times when an action potential was triggered (at ~ 4 s). It can be seen that the maximum and the right side of the spectrum shifted to shorter wavelengths over time. This effect is mainly attributed to the bleaching process of the chlorophyll and is not related to any state changes of the cell. The intensity of the left flank of the spectrum slightly increased when an action potential was triggered. After the pulse the intensity decreased again (s. inset 570 nm - 580 nm). The increase of intensity at the green edge indicated a shift to blue wavelengths or a broadening of the emission spectrum. The red channel only shows a slightly changing slope of bleaching.
The ratio parameter $\frac{I_{green}}{I_{red}}$ (**Figure 4.15b**) extracted from the entire spectrum is in line with the results of the previous experiments (section 4.4.5). After triggering an action

potential, the ratio increased by about 8-9 %. The changes of the ratio parameter over time were caused by the bleaching effects of the chlorophyll. The intensity of the emission of chlorophyll decreased at 610 nm, whereas at 560 nm no changes appeared. This caused an asymmetric bleaching of the two signal channels and therefore an increase in the ratio parameter. This constant bleaching seems unrelated to a change of the emission spectrum of the dye molecules or the state of the membrane.

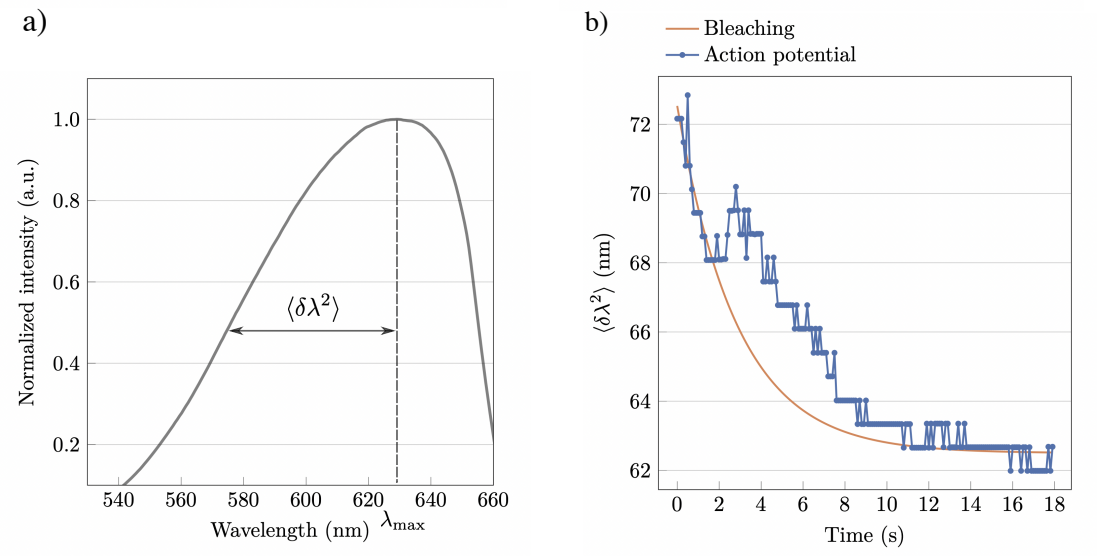

Figure 4.16: Estimation of the width of the emission spectrum of di-4-ANEPPDQH during an action potential: (a) The distance between the peak position and the left flank at half maximum in wavelengths is used to estimate the half width of the emission spectrum. (b) shows the distance between the peak position and the flank over time without triggering an action potential (bleaching) and with triggering an action potential.

To extract possible changes of the shape of the emission spectrum (width, $\langle \delta\lambda^2 \rangle$), the position of the emission peak in wavelength and the left flank was observed over time. The distance between the left flank and the peak position was used to estimate the half width of the spectrum (s. **Figure 4.16a**). An exponential decrease of this parameter over time without triggering an action potential, supports the assumption that the bleaching of chlorophyll affects the measured spectrum. Due to the bleaching of the red wavelengths the measured width decreased. When an action potential was triggered an additional shift of the left flank led to an increase of the estimated width (s. **Figure 4.16b**). After correcting the decrease of the bleaching, a broadening of about (4 ± 1) nm becomes apparent during the propagation of the action potential (s. **Figure 4.17**). It should be mentioned here that the superposition of the chlorophyll fluorescence and the short pass filter pretends to detect the real shape of the spectrum. The calculation of the estimated width was not distinguishable from a shift of the spectrum and vice versa. This means that the changes observed here can

only seen as an indicator for a broadening of the spectrum. Nevertheless, a change of the distribution of the emission wavelengths clearly indicated a phase transition of the local environment during the propagation of an action potential in *Chara australis*.

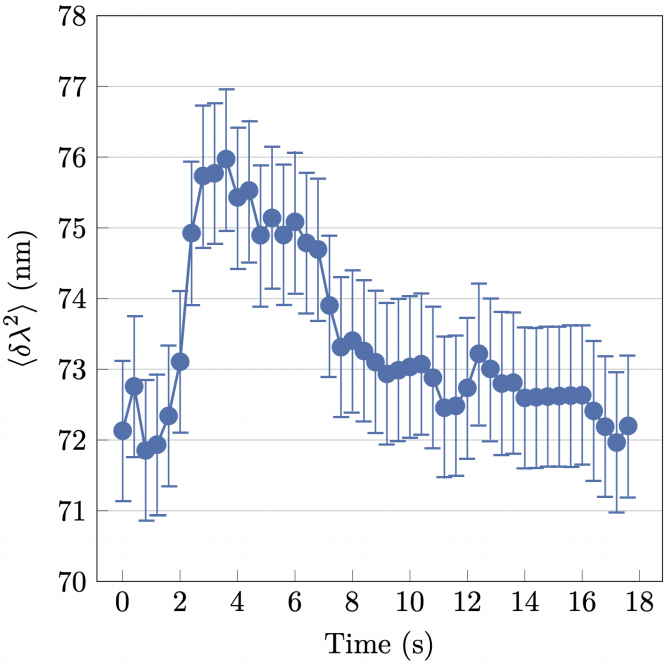

Figure 4.17: Calculated half width of the emission spectrum as a function of time when triggering an action potential.: The half width of the spectrum $\langle \delta\lambda^2 \rangle$ increased about (4 ± 1) nm during an action potential. The error bars represent the uncertainty of the spectrum analyzer.

Taken together, the results allow to conclude that the emission spectrum responded during an action potential similar to the single emission channels, but the superposition of the signal (cell surface, cell wall) and the asymmetric bleaching hindered the unambiguously detection of the shift of the position in wavelength or the width at half maximum. Therefore, measuring the ratio parameter $\frac{I_{\text{green}}}{I_{\text{red}}}$ seems to be the preferred method to detect small changes of the emission properties of labeled cells with high background fluorescence.

4.4.7 Mechanical Displacement of the Cell Surface during an Action Potential

The results of the previous sections demonstrate a general correlation between membrane potential and the emission of the fluorescent dye. In a thermodynamic point of view the change of the phase state during pulse propagation of a system does not only influence the emission spectrum of incorporated fluorescent dyes, but also influences all other physical properties of the system. Therefore, a propagating state change as proposed by Kaufmann (Kaufmann (1989a)) has to be accompanied by changes of the local pH and the permeability etc. Also, mechanical aspects, which can be extracted from the confocal measurements, should respond to a transition pulse. Because the cell surface (membrane) has been separated from the wall during plasmolysis, changes of the position of the cell surface can be observed. Previous studies have shown that several cell types undergo a swelling during an action potential (Tasaki (2008)).

To follow the dynamics of the cell surface during an action potential, the position of the fluorescent signal at the cell surface was tracked over time. For this purpose, the signal was correlated to the corresponding pixel of the confocal image. The starting point was set to zero and all changes were displayed in micrometers calculated by the pixel size. The positive y axis corresponds to the inside and the negative y axis to the outside of the cell (s. Appendix A.2.3).

In **Figure 4.18** the relative position of the membrane in micrometers is visualized as a function of time. It can be identifies that the membrane position is shifted about $(4.5 \pm 0.8)\,\mu m$ after triggering an action potential. This means a step of the cell surface to the center of the cell. Due to the complex distortion of the surface of the cell by the plasmolysis neither a swelling nor shrinking of the entire volume can be identified (Fillafer et al. (2018)).

To correlate the shift in position to the optical pulse and thereby to the electrical component a sigmoidal fit was calculated. The derivative of the fit, which showed the maximal shift in position, is plotted together with the ratio parameter (inset **Figure 4.18**). It shows a clear correlation between the maximal shift in position and the maximal amplitude of the ratio parameter $\frac{I_{\text{green}}}{I_{\text{red}}}$.

To further understand the pulse propagation and all the aspects connected the correlation in time is of main interest. Whereas the optical data shows that the electrical pulse is clearly correlated to the change in emission the mechanical response did not show any relaxation processes of the shift in position at the timescale of the experiments ($\sim 10\,s$). However, it has already been shown that the mechanical relaxation time is much longer in *Chara* cells (3 min (Fillafer et al. (2018))). While we can conclude that mechanical changes are triggered by the action potential, they appear to be further influenced by other cellular components (cytoskeleton etc.) than

just the membrane.
Nevertheless, this results again demonstrated the coupling of different components of the system (mechanical, optical, electrical etc.) during the propagation of an action potential as proposed by a thermodynamic theory (Andersen et al. (2009); Kaufmann (1989a); Kaufmann (1989b)). Taken together the mechanical and the electrical changes during an action potential are clearly correlated to the optical and therefore seem to have the same physical origin.

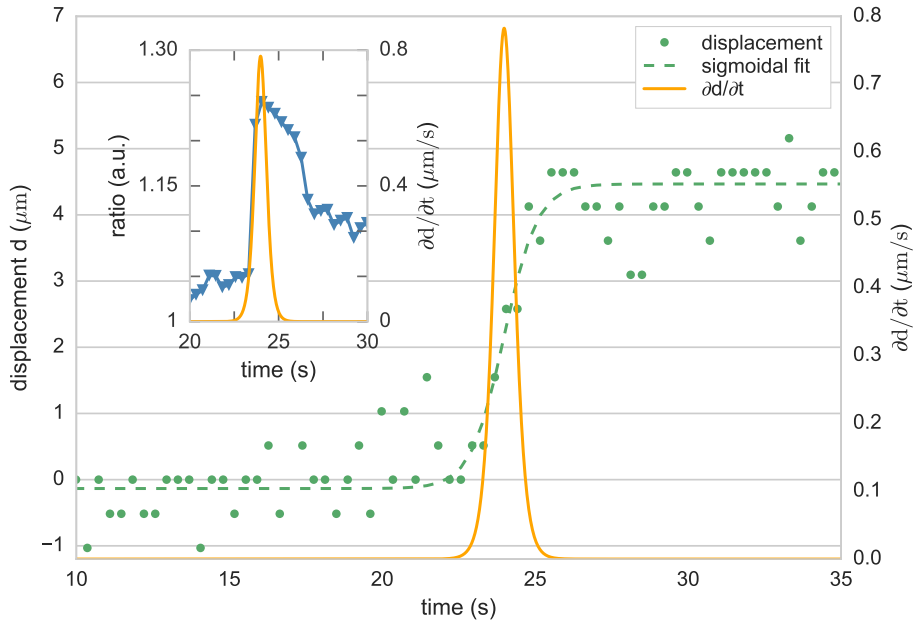

Figure 4.18: Mechanical response of the cell surface during an action potential: The position of the cell surface is set to zero and tracked over time. After triggering an action potential, the cell surface shrinks (4.5 ± 0.8) µm to the middle of the cell. The derivative of a sigmoidal fit was used to identify the position of the step. The inset shows the correlation between the optical and the mechanical response during an action potential. The maximum of the optical pulse coincides with the maximum of the mechanical derivative.

Based on the theory by K. Kaufmann (Kaufmann (1989a)), it can be said, that an alteration of the phase state of the membrane and therefore changes in forces and fluctuations of all observables take place. The theory predicts changes in mechanical susceptibilities (compressibility) as well as changes in lateral pressure which are related to the surface tension. All these inevitably lead to a mechanical response of the cell surface to an action potential. With the assumption that a phase transition propagates through the membrane, the compressibility is even in a maximum and thus the system is very soft. Without a change in the osmotic pressure a twitch of the surface seems to be reasonable.
It is mentioned here, that the displacement of the cell surface can also occur based on

osmotic volume changes. An alteration of the transmembrane pressure could arise when the chemical potential of the extra- or intracellular medium (osmolarity) is changed. The difference of the chemical potential will be equilibrated by transfer of water. It has been discovered that a Cl^- and K^+ efflux took place during the excitation of *Chara* cells. Furthermore, Ca^{2+} is suggested to be involved in the membrane excitation of *Characeae*. Thereby, there is no clear discrimination between the influx of Ca^{2+} or the release of Ca^{2+} from internal stores.

Nevertheless, a change of the concentration of Ca^{2+} has been observed of about several µM (Kikuyama and Tazawa (1983); Plieth et al. (1998); Williamson and Ashley (1982)). The work of Oda and colleagues (Oda (1976)) has shown that a Cl^- efflux of (1777 ± 126) and a K^+ efflux of (1812 ± 123) picomoles/cm^2 per impulse takes place. If the ion transfer is equilibrated by the transfer of water, the cell surface has to uniformly shrink. But in experiments, inward as well as outward deflections were observed.

Nevertheless, these experiments demonstrate the strength of the thermodynamic model. The mechanical aspect is not only a logical consequence of the transition, but is also connected to **all** other observables (electrical, optical etc. s. **Figure 4.19**). A propagating phase transition has to be accompanied by fluctuation of all thermodynamic observables. To clarify the physical foundation of the communication between cells, it seems to be crucial to take all these phenomena into account.

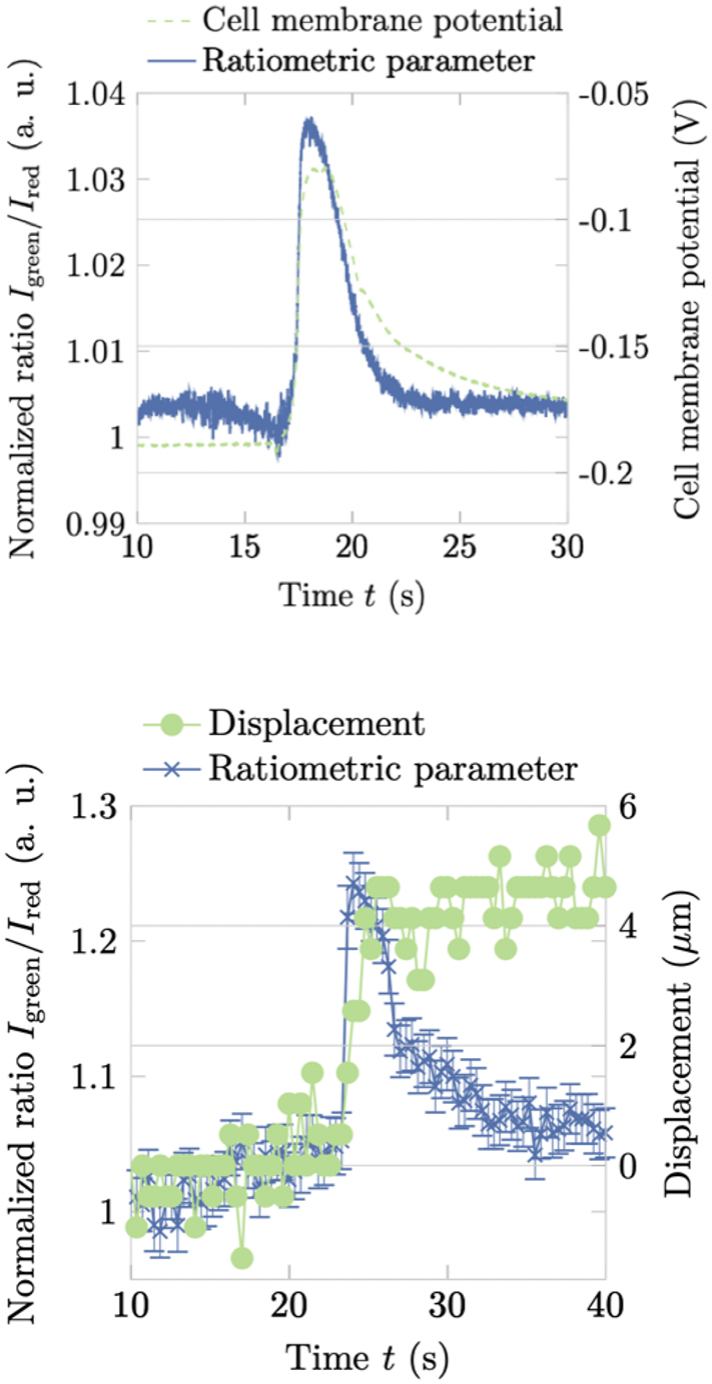

Figure 4.19: Correlation between the electrical, optical and mechanical aspect of the action potential of *Chara australis cells*: The upper time trace shows the coupling between electrical and optical components. The trace at the bottom displays the coupling between the optical and the mechanical shift of the membrane.

4.4.8 Changes of Cell Membrane State during an Action Potential

Thermodynamic interpretation based on results with lipid based artificial systems

The experiments with artificial lipid systems (vesicles and monolayer s. chapter 3) demonstrated that the emission properties (spectral width, wavelengths) of solvatochromic dyes such as di-4-ANEPPDHQ and LAURDAN significantly change during the transition of the thermodynamic state of the membrane. Therefore, the contradictory changes of the emission channels (green and red) during the action potential indicates an alteration of the membrane state during the propagation of action potentials. In the common use of solvatochromic dyes, the transient blue shift indicates a change from fluid to gel-like phase (or liquid-expanded to liquid-condensed phase). However, based on the phenomenology of di-4-ANEPPDHQ in artificial bilayers, two different suggestions are possible. In the case of vesicles made of charged lipids (DMPS), the transition from fluid to gel-like phase was accompanied by a blue shift of the emission spectrum. Based on this model, the blue shift leads to the suggestion that during an action potential the system becomes more ordered. This is in agreement with the thermodynamic theory of nerve pulse propagation. But on the other hand, if the data from vesicles made of DMPC are used the opposite seems to be true. A blue shift here corresponds to a transition from the gel-like to the fluid state of the membrane. Consequently, it seems obvious that the interpretation of the changes of the emission properties of those dyes has some limitations. The artificial membrane systems showed that the chemical microenvironment - charged lipids or uncharged lipids - crucially influences the reaction of the lipid-dye system. In biology it is well agreed that the membrane resting state is in a fluid state and the lipids of the membrane are charged, so DMPS seems to be the proper model system for the analysis of living systems. Furthermore, the emission spectrum is slightly different for the living system and for the two lipid systems (**Figure 3.4 ,3.6**), respectively. Therefore, the state-dependent shift of the emission spectrum cannot be transferred directly.
From the analysis of the entire emission spectrum a broadening of the spectrum was also identified as a possible reason for the increase of the ratio parameter. Such a broadening occurred in artificial membranes during the phase transition of the surrounding lipid matrix. A wide emission spectrum and therefore a wide distribution of microscopic states of the fluorophore is correlated with high fluctuations of the environment (transition). In general, it can be concluded that the emission properties indeed changed during the action potential (shift or broadening) which is a clear indicator for a phase transition.

Another indicator for a transition during the action potential is clearly the mechanical shift of the membrane during the propagation. A transition of the membrane has to affect, all variables of the observed system. In this case a mechanical response of the membrane to the pulse propagation seems to be necessary. This behavior during nerve pulse propagation has also been shown by others (Tasaki (1999); Tasaki (1999)). Due to the complex distortion of the membrane of *Chara* cells, an unambiguous direction of the mechanical pulse occurred. Furthermore, also osmotic changes of the chemical environment could result in a change of the position. However, the combination of the optical data and the mechanical data supports the assumption of a state transition pulse during nerve pulse propagation.

These results and the results of section 3.3.4 (acoustic pulses in lipid monolay-

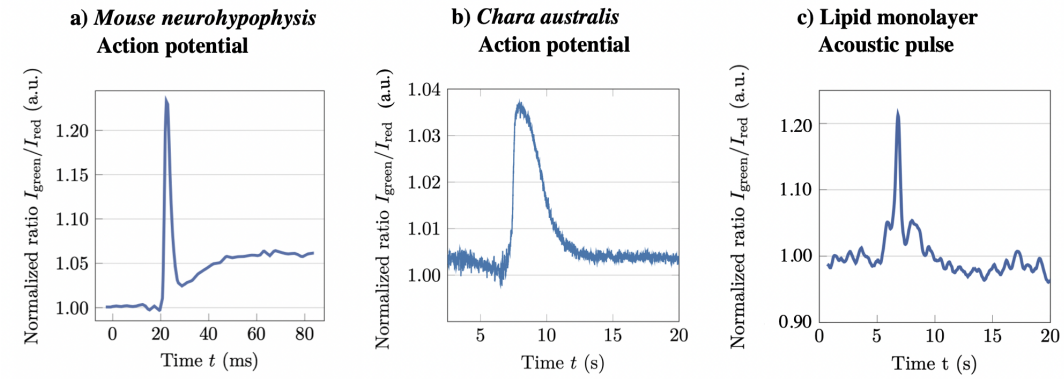

Figure 4.20: Similarity between action potentials in living cells and acoustic pulses in a lipid monolayer: a) taken from the manuscript (Foley and Muschol (2008)). The ratio parameter increased during the action potential about 20 %. The same quantitative results have been found in measurements of action potentials in *Chara australis* cells (Fabiunke et al. (2021)). Furthermore, when a transition is induced by a pressure pulse in a lipid monolayer experiment, the ratio parameter also increased by about 20 %. The same phenomenology in all three system gives an alternative interpretation of the physical foundation of action potentials.

ers) indicated, that whenever a significant change of the ratio parameter (shift or broadening of the spectrum) occured, a state change of the involved interfaces is the foremost suspected origin. Other dyes which are closely related to di-4-ANEPPDHQ have been used to study the pulse propagation of cells. A triggered action potential in *neurohypophyses* also shows an increase of the ratio parameter $\frac{I_{green}}{I_{red}}$ analogously (Foley and Muschol (2008)). This response was identical with the response during the propagation of an acoustic pulse at the lipid-monolayer in the main transition regime. Therefore, a change of the emission spectrum is suggested, which indicates an ordering of the membrane interface during the excitation in all of the three systems (*neurohypophysis, Chara australis* and lipid monolayer **Figure 4.20**).

It can be concluded, that neither Nernst potentials nor specific protein channels gener-

ate the optical signature and are the fundamental basis of nerve pulse propagation. In a thermodynamic picture, the pulses in lipid monolayer and in excitable cells have the same physical origin (transitions), which also includes among others changes of mechanical, electrical, thermal, chemical nature.

4.4.9 Conclusion

Here the emission properties of the fluorescent dye di-4ANEPPDHQ incorporated into the plasma membrane of *Chara australis* as a function of variables with defined thermodynamic meaning have been investigated. It was shown that the ratio parameter increases upon cooling as well as upon acidification of the extracellular medium. These results are in line with the increase of the ratio parameter in artificial lipid-based systems (DMPS charged lipid) during a disordered-ordered transition. In general, it is well accepted that living cells have a charged membrane and therefore DMPS membranes seem to be a proper reference system. Moreover, the phase diagrams are similar and only differ in the absolute temperature.
Based on the thermodynamic phase diagrams of the freshwater algae the following conclusions can be made. Qualitatively, the increase of the ratio indicated a blue shift of the emission spectrum and therefore an ordering of the membrane structure. Compared to changes of the membrane potential as a function of temperature, it is clearly demonstrated that the emission of the dye molecules is not simply coupled to the transmembrane potential. Whereas the potential depolarized between 30 °C and 40 °C the ratio does not change. The electrochromic generally used for describing this dye family is not sufficient.
It was also demonstrated that significant changes of the emission spectrum took place during the propagation of an action potential. Qualitative similar changes during an action potential and upon cooling indicate an ordering of the excitable medium. This is also conserved when compared to the optical state diagrams of the artificial lipid systems. Furthermore, these data support the idea that an action potential is a manifestation of a propagating ordering transition.
In summary, these results corroborate that the foundation of the action potentials is to be found in fundamental physical laws. All these are in line with the assumptions of Sutherland (Sutherland (1908, 1905)), Wilke (Wilke and Atzler (1912)), Doerner (Doerner (1971)) or K. Kaufmann (Kaufmann (1989a)).

Conclusion and Outlook

5 Conclusion and Outlook

It is well known that fluorescent dye molecules change their emission properties, when the chemical environment is altered. This phenomenon is often correlated to a change in specific variables such as polarity. So called electrochromic dye molecules are used to detect the potential changes during nerve pulse propagation.
However, in this thesis it was demonstrated that the specific emission properties of dyes are strongly coupled to the thermodynamic phase of the surrounding lipid membrane. On the one hand, when a transition is crossed, the emission spectrum shifts in wavelengths and on the other hand the emission spectrum is the widest during the phase transition. At this point high fluctuations of the observed system lead to a wide distribution of quantum mechanical states of the dye molecules. These results demonstrate that the thermodynamic state of the surrounding environment is directly correlated to the quantum mechanical state of the fluorescent dye.
Changes in emission are not specifically coupled to lipid systems. For instance, the spectrum changes as well when an unspecific solvent (here: DMSO) undergoes a phase transition (freezing). This correlation between changes in emission (wavelengths shifts and broadening of the entire emission spectrum) and the transition regime of completely different systems (DMSO + dye and lipid membrane + dye) confirms the assumption that the complex of all surrounding molecules determines the emission properties of the fluorophores. Nonlinearities in the state diagram result in nonlinear changes of the interaction between dye and solvent which are not purely electrical but are inseparably integrated in all parameters (mechanical, optical, electrical, chemical etc.) of the observed interface (solvation shell).
Accordingly, the correlation to single variables (transmembrane potential) of an intricate biological system without knowing the phase state is not possible. In a simple artificial membrane (defined state) the emission spectrum shifts when a transition is crossed in quasi-static and in dynamic experiments. Based on the similarity between nonlinear acoustic pulses and action potentials in *Chara australis* cells we believe that the phenomenology of the change of the fluorescent spectrum is related to the thermodynamics of the system. The spectrum changes during action potentials in *Chara australis* as well as during acoustic pulses in lipid monolayer. Compared to the literature, similar changes are found during action potentials in mouse *neurohypophysis* (Foley and Muschol (2008)). In artificial systems the changes only occur at the transition regime of the chemical environment. Therefore, a state change during the propagation of action potentials in living system is the foremost probable origin. This clearly supports the idea of a propagating phase transition during nerve pulse propagation.

The textbook theory of nerve pulse propagation is based on the activity of specific enzymes and the transfer of mainly three ions (Cl^-, Na^+ and K^+) which determine the resting potential of a cell. Based on this, the transient variation of the membrane potential during the nerve pulse is used to explain a change of the emission of the incorporated fluorescent dye molecule (increase of the ratio parameter). At a lipid monolayer neither an ion gradient/transfer nor a transmembrane potential exists, but nevertheless the ratio parameter increases during a nonlinear acoustic pulse. Consequently, the ion transport can be excluded as the origin of the dye signature in monolayer as well as in cell membranes. A transition also induces an electro-mechanical alteration of the surrounding lipid system and therefore changes of the dipole moments seem to be necessary. It is important to note that this is an inseparable process and is not a sufficient criteria for proving the electrical sensitivity of the fluorescent dye.

The state of all observables can be described by an interfacial entropy potential $S(n_1, n_2, ...)$. As shown in other works, high fluctuations are also coupled to the enzyme activity (Fichtl et al. (2018); Nuschele (2010)) as well as membrane conductivity (Wunderlich et al. (2009)) and as shown here to the optical susceptibility. With access to state diagrams of living organisms, exact predictions about the transition point - high fluctuations - can be made.

Additionally, any perturbation of the system which leads to a transition, will generate nonlinear propagating pulses. These again influence all observables. Thereby, pulses could regulate biological function which are controlled by the phase state of the interfaces in equilibrium. From a physical perspective the system (cell membrane) has to be characterized (state diagram) from experimentally accessible variables. The molecular structure is completely irrelevant in this approach. Thus, it is possible to describe action potentials in very different biological systems (algae, neurons) without knowledge of the specific molecular composition.

The goal of this thesis was to show that fluorescent dye molecules incorporated into the system of interest offer the opportunity to investigate state diagrams of living organisms and provide experimental evidence that nerve pulses are accompanied by a phase transition. In contrast to other methods (calorimetry), the impacts on the cells by the method itself are negligible. Still, it has to be noted that all added molecules (e. g. dyes) might influence the thermodynamic state of the living organism. Nevertheless, changes of the emission properties of dye molecules are coupled to the state of the interface and are a variable of the entropy potential. With that, changes of other observables can be estimated. Furthermore, nonlinear pulses such as action potentials can directly be observed and connected to the state of the cell. All-or-none behavior as well as excitability in general can be explained by studying the state diagrams. The wide variety of action potential existing (plants, unicellular organisms, animals) requires a physical foundation independent of the exact molecular constituents.

Furthermore, the fluorescence might offer the opportunity to map the phase state not only of plant cells or neurons, but of entire organs such as the brain. It is of particular interest to characterize these phase states and whether they are in the vicinity of a transition.

Appendix

Appendix A

A.1 Ratio Parameter as a Function of pH

Figures A.1 and A.2 show typical measurements of changing the extracellular pH. When the pH is changed the ratio parameter increases correlating to the pH.

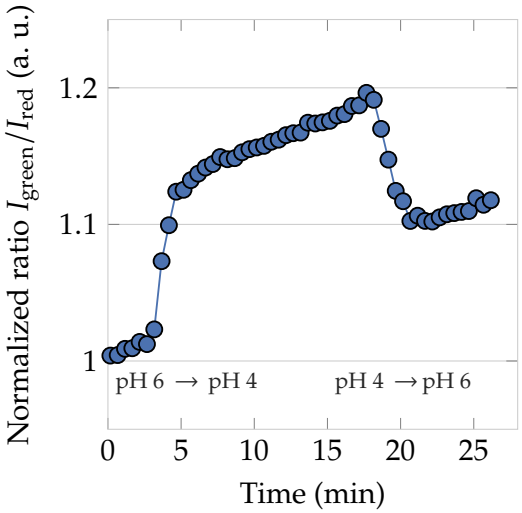

Figure A.1: Reversibility of the ratiometric parameter I_{green}/I_{red} when the pH value of the extracellular medium of a Chara australis cell was changed from pH 6 to pH 4 and back.The LED was triggered every 30 s for 2 s to reduce the irradiation time. The change of the ratio over time is taken into account by a compensation calculation (figure taken from Fabiunke et al. (2021)).

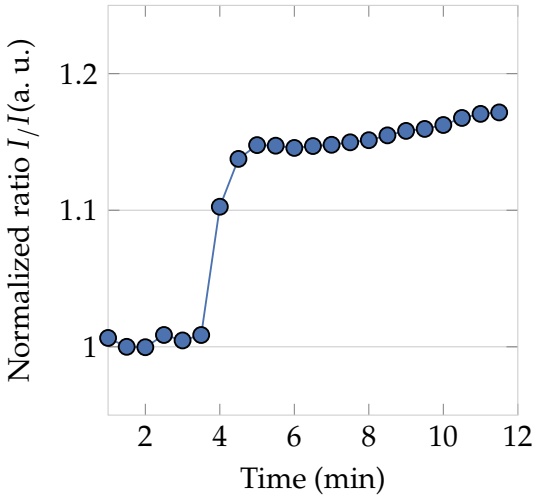

Figure A.2: Typical changes of the ratiometric parameter $I_{\text{green}}/I_{\text{red}}$ when the pH value of the extracellular medium of a Chara australis cell was changed from 7 to 4.5 (at about 3 min). The LED was triggered every 30 s for 2 s to reduce the irradiation time.(figure taken from Fabiunke et al. (2021)).

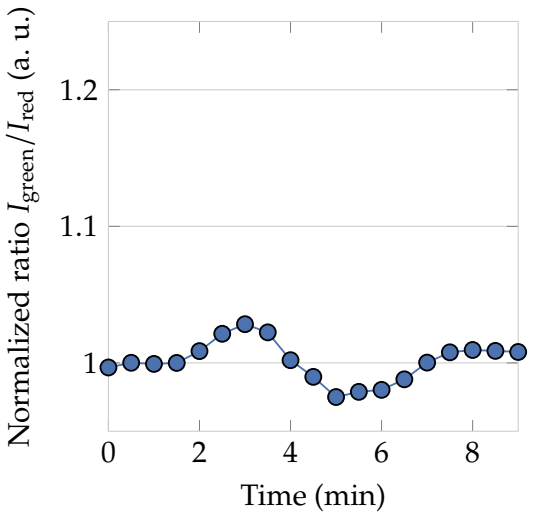

Figure A.3: Typical change of the ratiometric parameter $I_{\text{green}}/I_{\text{red}}$ when the pH value oft he extracellular medium of a Chara australis cell was changed from 7 to 10 (at about 2 min). The LED was triggered every 30 s for 2 s to reduce the irradiation time. Note: Alkalization leads to a biphasic behavior. This change between 2 and 7 min is represented in the uncertainties for pH 8 and 9 Fig 4.10 (figure taken from Fabiunke et al. (2021)).

A.2 Details of Methods

A.2.1 Curvature of the Emission Spectrum

To get the width of the emission spectrum, a polymon was calculated of the upper 10 % (intensities $> 0.9 \cdot I_{\max}$ of the spectrum. The second derivative (curvature c) of the fit at the position of the maximum is anti-proportional to the radius of curvature.

$$I(\lambda) = a\lambda^4 + b\lambda^3 + c\lambda^2 + d\lambda + e, \tag{A.1}$$

$$c(\lambda) = 12a\lambda^2 + 6b\lambda + 2c \tag{A.2}$$

$$r \propto |\frac{1}{c(\lambda)}| \tag{A.3}$$

It is further assumed that the radius of curvature at the maximum position is proportional to the width Γ of the emission spectrum $r \propto \Gamma$.

A.2.2 Lipid Monolayer: Intensities

The dye molecules did not incorporate into the lipid monolayer homogeneously. Therefore, there were regimes where dye molecules were located and other regimes where no signal could be detected. To minimize the streaming of the surface Teflon pieces were used. Nevertheless, the signal of the monolayer wasn't stable for more than 30 min.
Due to the already mentioned inhomogeneous dye distribution, it was not possible to measure a complete isotherm cycle. After a slow compression of the lipid monolayer, the signal was not completely reversible with expansion. Analogously, starting with an expansion of the monolayer, the compression was not detectable anymore.
Figure A.4 shows that during a lateral pressure pulse both intensities decrease. The non linear decrease of the intensities (also during the isotherm s. A.5) leads to an increase of the ratio parameter.

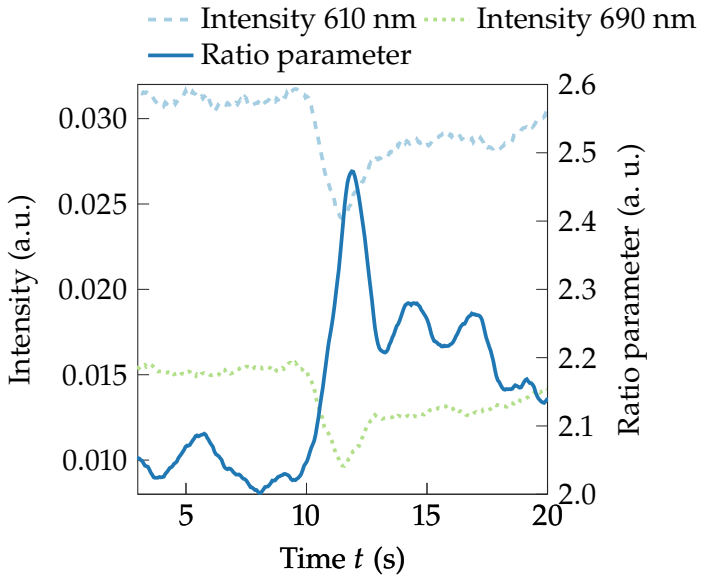

Figure A.4: Individual signals of the green ((610 ± 10) nm) and red ((690 ± 10) nm) channels after triggering an acoustic pulse. The ratio parameter $I_{\text{green}}/I_{\text{red}}$ increases during the acoustic pulse. This indicates a transient blue shift of the emission spectrum.

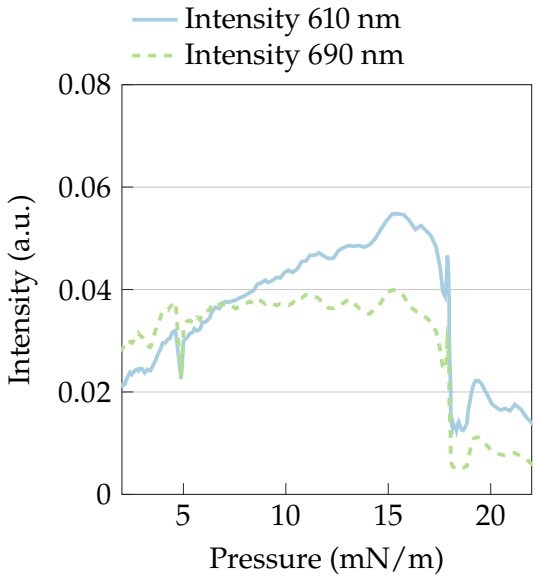

Figure A.5: Single intensity channels ((610 ± 10) nm and (690 ± 10) nm) during a quasi-static isotherm. At low pressures both intensity channels slowly increase, whereby the intensity at (610 ± 10) nm increased more relative to (690 ± 10) nm. At a lateral pressure of about 18 mN/m both intensities decrease. This decrease of the intensities indicated the transition of the lipids

A.2.3 Displacement

To determined the position of the cell surface, a squared part around the surface of the confocal pictures was used (s. Figure A.6). With a cross section of the intensities the maximum (surface position) could be estimated. After triggering an action potential these position shifted in position. From the shift in pixel, the displacement could be measured.

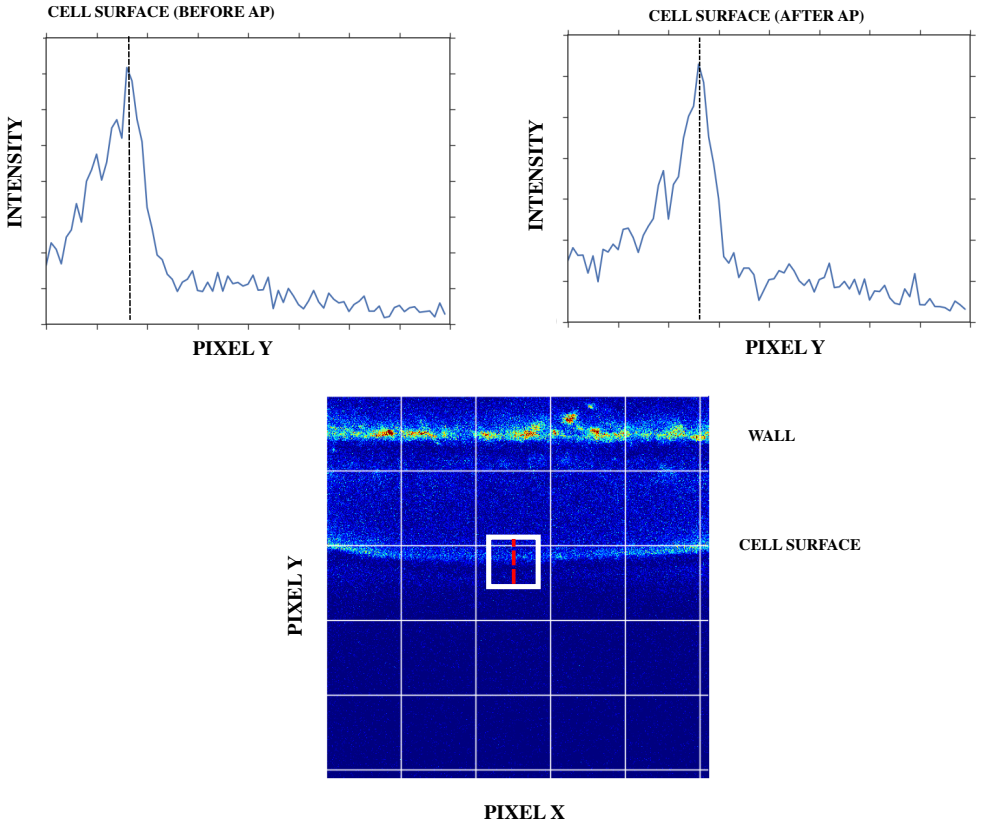

Figure A.6: Calculation of the displacement of cell surface. The lower picture shows the confocal image of a plasmolyzed cell, whereby the upper structure belongs to the cell wall and the structure blow to the cell surface. The rectangle marks the part which is used to calculate the position of the cell surface. A cross section (dotted line) of the intensities clearly shows a maximum at the cell surface (upper pictures). It can be seen that the position of the maximum in intensity changes after triggering an action potential.

A.2.4 Staining Procedure of *Chara Australis*

Young cells from the upper end of the cell are best suited for staining chara australis cells. In older cells, the cell wall is often overgrown with epiphytes into which dye

molecules are also deposited and superimpose the actual signal.
For staining, from 1-10 micrormolar dye solution can be used. The DMSO content, which dissolves the dye in the aqueous solution, must not exceed 2 %, otherwise the cell will plasmolyze or burst. The cell was covered with the dye solution and stored in the dark for at least 5 min. After that, the solution can be exchanged with the APW solution. Washing the cell with the APW solution additionally improves the signal to noise ratio. After the staining procedure the cells could be used for maximal 2 h.

Bibliography

Aidley, D. (1998). *The Physiology of Excitable Cells*. Cambridge University Press.

Amaro, M., Reina, F., Hof, M., Eggeling, C., and Sezgin, E. (2017). Laurdan and di-4-aneppdhq probe different properties of the membrane. *Journal of Physics D: Applied Physics*, 50:aa5dbc.

Andersen, S., Jackson, A. D., and Heimburg, T. (2009). Towards a thermodynamic theory of nerve pulse propagation. *Progress in Neurobiology*, 88:104–113.

Antonov, V. F., Anosov, A. A., Norik, V. P., Korepanova, E. A., and Smirnova, E. Y. (2003). Electrical capacitance of lipid bilayer membranes of hydrogenated egg lecithin at the temperature phase transition. *European Biophysics Journal*, 32:55–59.

Baker, P. F., Hodgkin, A. L., and Shaw, T. I. (1961). Replacement of the protoplasm of a giant nerve fibre with artificial solutions. *Nature*, 190:885–887.

Barry, P. H. (1970). Volume flows and pressure changes during an action potential in cells of chara australis. *J. Membrane Biol.*, 3:335–371.

Beilby, M. J. (2007). Action potential in charophytes. *International Review of Cytology*, 257:43–82.

Beilby, M. J. and Coster, H. G. L. (1976). The action potential in chara corallina: Effect of temperature. *Plant Physiology*, 3:275–89.

Beljanski, M. V., Andjus, P. R., Hadi-Pavlovi, A., Sreji, R. A., and Vueli, D. (1997). Differential scanning calorimetry of the plasma membrane-enriched fraction in chara. *Plant Science*, 125:171–176.

Bernstein, J. (1902). Untersuchungen zur Thermodynamik der bioelektrischen Ströme. erster Theil. *Pflügers Arch.*, 92:521–562.

Blatt, F. J. (1974). Temperature dependence of the action potential in nitella flexilis. *BBA - Biomembranes*, 339:382–389.

Blume, A. and Eibl, H. (1979). The influence of charge on bilayer membranes calorimetric investigations of phosphatidic acid bilayers. *Biochimica et Biophysica Acta*, 558:13–21.

Brewer, J., de la Serna, J. B., Wagner, K., and Bagatolli, L. A. (2010). Multiphoton excitation fluorescence microscopy in planar membrane systems. *Biochimica et Biophysica Acta - Biomembranes*, 1798:1301–1308.

Chapman, R. A. (1967). Dependence on temperature of the conduction velocity of the action potential of the squid giant axon. *Nature*, 213:1143–4.

Cohen, L. B., Salzberg, B. M., and Grinvald, A. (1978). Optical methods for monitoring neuron activity. *Ann. Rev. Neurosci.*, 1:171–82.

Cole, K. S. and Curtis, H. J. (1938). Electrical impedance of nerve during activity. *Nature*, 142:209–210.

Datasheet (2021). Voluntary safety information following the safety data sheet format according to regulation (ec) no. 1907/2006 (reach); dimethyl sulfoxide (DMSO). *Carl Roth*. HN47, Rev. 4.

Dempster, J. A., Van Os, C. H., and Van Hoek, A. N. (1992). The quest for water channels. *NIPS*, 7:172–176.

Dinic, J., Biverståhl, H., Mäler, L., and Parmryd, I. (2011). Laurdan and di-4-aneppdhq do not respond to membrane-inserted peptides and are good probes for lipid packing. *Biochimica et Biophysica Acta - Biomembranes*, 1808:298–306.

Doerner, K. F. (1971). Nerve impulse propagation affected by sol-gel changes in axoplasm. *Journal of Theoretical Biology*, 32:159–164.

Donnan, F. G. (1924). The theory of membrane equilibria.

Edwards, F. A., Konnerth, A., Sakmann, B., and Takahashi, T. (1989). A thin slice preparation for patch clamp recordings from neurones of mammalian cenral nervous system. *European Journal of Physiology*, 414:600–612.

Einstein, A. (1903). Eine Theorie der Grundlagen der Thermodynamik. *Annalen Der Physik*, 316:170–187.

Einstein, A. (1910). Theory of opalescence of homogeneous fluids and fluid mixtures in the neighbourhood of the critical state. *Annalen der Physik*, 338:1275–1298.

Engelhardt, A. (1951). Die Temperaturabhängigkeit der Erregungsleitungsgeschwindigkeit im Kalt- und Warmblüternerven. *Zeitschrift für vergleichende Physiologie*, 33:125–128.

Fabiunke, S., Fillafer, C., Paeger, A., and Schneider, M. F. (2021). Optical studies of membrane state during action potential propagation. *Progress in Biophysics and Molecular Biology*, 162:69–78.

Fichtl (2015). Integration der Biochemie in die Physik der Grenzfläche. PhD thesis, Universität Augsburg.

Fichtl, B., Shrivastava, S., and Schneider, M. (2016). Protons at the speed of sound: Predicting specific biological signaling from physics. *Scientific Reports*, 6:22874.

Fichtl, B., Silman, I., and Schneider, M. F. (2018). On the physical basis of biological signaling by interface pulses. *Langmuir*, 34:4914–4919.

Fillafer, C., Mussel, M., Muchowski, J., and Schneider, M. F. (2018). Cell surface deformation during an action potential. *Biophysical Journal*, 114:410–418.

Fillafer, C., Paeger, A., and Schneider, M. F. (2017). Collision of two action potentials in a single excitable cell. *Biochimica et Biophysica Acta - General Subjects*, 1861:3282–3286.

Fillafer, C., Paeger, A., and Schneider, M. F. (2021). The living state: How cellular excitability is controlled by the thermodynamic state of the membrane. *Progress in Biophysics and Molecular Biology*, 162:57–68. On the Physics of Excitable Media. Waves in Soft and Living Matter, their Transmission at the Synapse and their Cooperation in the Brain.

Fillafer, C. and Schneider, M. F. (2013a). On the temperature behavior of pulse propagation and relaxation in worms, nerves and gels. *PLoS ONE*, 8:1–6.

Fillafer, C. and Schneider, M. F. (2013b). Temperature and excitable cells. testable predictions from a thermodynamic perspective. *Communicative Integrative Biology*, e26730:1–5.

Foley, J. and Muschol, M. (2008). Action spectra of electrochromic voltage-sensitive dyes in an intact excitable tissue. *Journal of Biomedical Optics*, 13:064015.

Follmann, R., Rosa, E., and Stein, W. (2015). Dynamics of signal propagation and collision in axons. *Physical Review E - Statistical, Nonlinear, and Soft Matter Physics*, 92.

Galvani, L. A. (1791). Kräfte der Electricität bei der Muskelbewegung. *Comm. Bonon. Sc. et Art. Inst. et Acad. T. 7.*

Georgescauld, D. and Duclohier, H. (1978). Transient fluorescence signals fro pyrene labeled pike nerves during action potential possible impications for membrane fluidity changes. *Academic Press, Inc.*, 85:1186–1191.

Georgescauld, D. and Duclohier, H. (1979). Temperature dependence of the fluorescence of pyrene labeled crab nerve membranes. *Molecular Cellular Biochemistry*, 27:147–153.

Gorter, B. E. and Grendel, F. (1925). On bimolecular layers of lipoids on the chromocytes of the blood. *Journal of experimental medicine*, 41:439–43.

Griesbauer, J., Bössinger, S., Wixforth, A., and Schneider, M. F. (2012). Propagation of 2d pressure pulses in lipid monolayers and its possible implications for biology. *Physical Review Letters*, 108.

Griesbauer, J., Wixforth, A., and Schneider, M. F. (2010). Wave propagation in lipid monolayers. *Biophysj*, 97:2710–2716.

Gross, E., Bedlack, R. S., and Loew, L. M. (1994). Dual-wavelength ratiometric fluorescence measurement of the membrane dipole potential. *Biophysical Journal*, 67:208–216.

Grünhagen, H., Eibl, H., Krebs, G., and Reiter, P. (1983). Phospholipid and fatty acid composition of tetrodotoxin receptor-rich membrane fragments from electrophorus electricus. *BBA*, 732:675–682.

Hazel, J. R., McKinley, S. J., and Gerrits, M. F. (1998). Thermal acclimation of phase behavior in plasma membrane lipids of rainbow trout hepatocytes. *The American journal of physiology*, 275:R861–9.

Heimburg, T. and Jackson, A. D. (2005). On soliton propagation in biomembranes and nerves. *Proceedings of the National Academy of Sciences of the United States of America*, 102:9790–9795.

Heimburg, T. and Jackson, A. D. (2007). On the action potential as a propagating density pulse and the role of anesthetics. *Biophysical Reviews and Letters*.

Hodgkin, A. and Huxley, A. F. (1952a). A quantitative description of membrane current and its application to conduction and excitation in nerve by. *J. Physiol.*, 117:500–544.

Hodgkin, A. L. and Huxley, A. F. (1952b). Currents carried by sodium and potassium ions through the membrane of the giant axon of loligo. *Journal of physiology*, 116:449–472.

Jin, L., Millard, A. C., Wuskell, J. P., Clark, H. A., and Loew, L. M. (2005). Cholesterol-enriched lipid domains can be visualized by di-4-aneppdhq with linear and nonlinear optics. *Biophysical Journal*, 89:L04–L06.

Jin, L., Millard, A. C., Wuskell, J. P., Dong, X., Wu, D., Clark, H. A., and Loew, L. M. (2006). Characterization and application of a new optical probe for membrane lipid domains. *Biophysical Journal*, 90:2563–2575.

Kamitsubo, E. (1972). A window technique for detailed observation of characean cytoplasmic streaming. *Experimental Cell Research*, 74(2):613–616.

Kappler, J., Shrivastava, S., Schneider, M. F., and Netz, R. R. (2017). Nonlinear fractional waves at elastic interfaces. *Physical Review Fluids*, 2:1–18.

Kaufmann, K. (1989a). Action potential.

Kaufmann, K. (1989b). Lipid membrane: on the role of the phospholipid bilayer membrane in free energy coupling.

Kikuyama, M. and Tazawa, M. (1983). Transient increase of intracellular Ca^{2+} during excitation of tonoplast-free chara cells. *Protoplasma*, 117:62–67.

Klein, M. J., Kox, A. J., Renn, J., and Schulmann, R. (1993). *The collected paper of Albert Einstein,The Swiss Years: Wirtings 1909-1911, Doc 19 Notes from a lecture on fluctuations*, volume 3. Press Princton.

Lewis, R. N. and McElhaney, R. N. (2000). Calorimetric and spectroscopic studies of the thermotropic phase behavior of lipid bilayer model membranes composed of a homologous series of linear saturated phosphatidylserines. *Biophysical journal*, 79:2043–2055.

Leys, S. P. (2015). Elements of a 'nervous system' in sponges. *Journal of Experimental Biology*, 218:581–591.

Loew, L. M., Cohen, L. B., Dix, J., Fluhler, E. N., Montana, V., Salama, G., and Jian-young, W. (1992). A naphthyl analog of the aminostyryl pyridinium class of potentiometric membrane dyes shows consistent sensitivity in a variety of tissue, cell, and model membrane preparations. *The Journal of Membrane Biology*, 130:1–10.

Luehring, H. (2006). Algen unter Strom: Das Experiment. *Biologie in unserer Zeit*, 36:313–321.

McConnell, H. M., Tamm, L. K., and Weis, R. M. (1984). Periodic structures in lipid monolayer phase transitions (two-dimensional systems/lateral diffusion/fluorescence microscopy/membranes).

Mehrishi, J. N. and Bauer, J. (2002). Electrophoresis of cells and the biological relevance of surface charge. *Electrophoresis*, 23:1984–1994.

Moehwald, H. (1995). *Phospholipid Monolayers*. Elsevier Science B.V., 1 edition.

Muchowski, J. (2017). Thermodynamical characterization of an excitable plant cell membrane. Master thesis, TU Dortmund.

Mussel, M. and Schneider, M. F. (2019). It sounds like an action potential: Unification of electrical, chemical and mechanical aspects of acoustic pulses in lipids. *Journal of the Royal Society Interface*, 16.

Neher, E. and Sakmann, B. (1976). Single-channel currents recorded from membrane of denervated frog muscle fibres. *Nature*, 260:799–802.

Neher, E., Sakmann, B., and Steinbach, J. H. (1978). The extracellular patch clamp: A method for resolving currents through individual open channels in biological membranes. *Pfluegers Arch. European Journal of Physiology*, 375:219–228.

Nuschele, S. (2010). The role of interfaces in enzyme activity and cell adaptation. PhD thesis, Augsburg.

Obaid, A. L., Loew, L. M., Wuskell, J. P., and Salzberg, B. M. (2004). Novel naphthylstyryl-pyridinium potentiometric dyes offer advantages for neural network analysis. *Journal of Neuroscience Methods*, 134:179–190.

Oda, K. (1976). Simultaneous recording of potassium and chloride effluxes during an action potential in chara corallina. *Plant and Cell Physiology*, 17:1085–1088.

Ostwald, W. (1890). Elektrische Eigenschaften halbdurchlässiger Scheidewände.

Overath, P., Thilo, L., and Hermann, T. (1976). Lipid phase transitions and membrane function. *TIBS*, pages 186–189.

Parasassi, T., Gratton, E., Yu, W., Wilson, P., and Levi, M. (1997). Two-photon fluorescence microscopy of laurdan generalized polarization domains in model and natural membranes. *Biophysical Journal*, 72:2413–2429.

Parasassi, T., Krasnowska, E. K., Bagatolli, L., and Gratton, E. (1998). Laurdan and prodan as polarity-sensitive fluorescent membrane probes. *Journal of Fluorescence*, 8:365–373.

Parasassi, T., Stasio, G. D., d'Ubaldo, A., and Gratton, E. (1990). Phase fluctuation in phospholipid membranes revealed by laurdan fluorescence. *Biophysical Journal*, 57:1179–1186.

Parasassi, T., Stasio, G. D., Ravagnan, G., Rusch, R. M., and Gratton, E. (1991). Quantitation of lipid phases in phospholipid vesicles by the generalized polarization of laurdan fluorescence. *Biophysical Journal*, 60:179–189.

Pedrós, R., Moya, I., Goulas, Y., and Jacquemoud, S. (2008). Chlorophyll fluorescence emission spectrum inside a leaf. *Photochemical and Photobiological Sciences*, 7:498–502.

Plieth, C., Sattelmacher, B., Hansen, U. P., and Thiel, G. (1998). The action potential in chara: Ca^{2+} release from internal stores visualized by Mn^{2+}-induced quenching of fura-dextran. *Plant Journal*, 13:167–175.

Ritchie, J. M. and Keynes, R. D. (1985). The production and absorption of heat associated with electrical activity in nerve and electric organ. *Quarterly Reviews of Biophysics*, 18:451–476.

Sachs, F. and Qin, F. (1993). Gated, ion-selective channels observed with patch pipettes in the absence of membranes: Novel properties of a gigaseal. *Biophysical Journal*, 65:1101–1107.

Seneviratne, V., Frech, R., and Furneaux, J. E. (2003). Phases and phase transitions of P(EO)6LiSbF6. *Electrochimica Acta*, 48:2221–2226.

Sezgin, E., Sadowski, T., and Simons, K. (2014). Measuring lipid packing of model and cellular membranes with environment sensitive probes. *Langmuir*, 30:8160–8166.

Shimmen, T. (2007). The sliding theory of cytoplasmic streaming: Fifty years of progress. *Journal of Plant Research*, 120:31–43.

Shrivastava, S., Cleveland, R. O., and Schneider, M. F. (2018a). On measuring the acoustic state changes in lipid membranes using fluorescent probes. *Soft Matter*, 14:9702–9712.

Shrivastava, S., Kang, K. H., and Schneider, M. F. (2015). Solitary shock waves and adiabatic phase transition in lipid interfaces and nerves. *Physical Review E - Statistical, Nonlinear, and Soft Matter Physics*, 91:1–7.

Shrivastava, S., Kang, K. H., and Schneider, M. F. (2018b). Collision and annihilation of nonlinear sound waves and action potentials in interfaces. *Journal of the Royal Society Interface*, 15.

Shrivastava, S. and Schneider, M. F. (2013). Opto-mechanical coupling in interfaces under static and propagative conditions and its biological implications. *PLoS ONE*, 8.

Shrivastava, S. and Schneider, M. F. (2014). Evidence for two-dimensional solitary sound waves in a lipid controlled interface and its implications for biological signalling. *Journal of the Royal Society Interface*, 11.

Sieber, M., Hanke, W., and Kohn, F. P. M. (2014). Modification of membrane fluidity by gravity. *Open Journal of Biophysics*, 04:105–111.

Singer, S. J. and Nicolson, G. L. (1972). The fluid mosaic model of the structure of cell membranes. *Science*, 175:720–731.

Steppich, D., Griesbauer, J., Frommelt, T., Appelt, W., Wixforth, A., and Schneider, M. F. (2010). Thermomechanic-electrical coupling in phospholipid monolayers near the critical point. *Physical Review E*, 81:1–5.

Stine, K. J. (1994). Investigations of monolayers by fluorescence microscopy. *Microscopy research and technique*, 27:439–450.

Sutherland, W. (1905). The propagation of the nerve impulse. *American Journal of Physiology*, 14:112119.

Sutherland, W. (1908). The nature of the conduction of nerve impulse. *American Journal of Physiology-Legacy Content*, 23:115–130.

Takashima, S. (1979). Admittance change of squid axon during action potentials. change in capacitive component due to sodium currents. *Biophysical Journal*, 26:133–142.

Tasaki, I. (1949). Collision of two nerve impulses in the nerve fibre. *Biochemica et Biophysica ACTA*, 3.

Tasaki, I. (1999). Rapid structural changes in nerve fibers and cells associated with their excitation processes. *The Japanese journal of physiology*, 49:125–138.

Tasaki, I. (2008). On the reversible abrupt structural changes in nerve fibers underlying their excitation. *Phase Transition in Cell Biology*, pages 1–21.

Tasaki, I., Singer, I., and Takenaka, T. (1965). Effects of internal and external ionic environment on excitability of squid giant axon a macromolecular approach. *The Journal of General Physiology*, 48.

Tasaki, I., Watanabe, A., and Hallett, M. (1972). Fluorescence of squid axon membrane labelled with hydrophobic probes. *J. Membrane Biol.*, 8:109–132.

Tasaki, I., Watanabe, A., Sandlin, R., and Carnay, L. (1968). Changes in fluorescence, turbidity, and birefringence associated with nerve excitation. *Proceedings of the National Academy of Sciences*, 61:883–888.

Tasaki, I., Watanabe, A., and Takenaka, T. (1962). Resting and action potential of intracellularly perfused squid giant axon. *PNAS*, 48:1177–1184.

Terakawa, S. (1985). Potential-dependent variations of the intracellular pressure in the intracellularly perfused squid giant axon. *Journal of physiology*, 369:229–248.

Vitha, M. F. and Clarke, R. J. (2007). Comparison of excitation and emission ratiometric fluorescence methods for quantifying the membrane dipole potential. *Biochimica et Biophysica Acta - Biomembranes*, 1768:107–114.

Volta, A. and Banks, J. (1800). I. on the electricity excited by the mere contact of conducting substances of different kinds. *The Philosophical Magazine*, 7:289–311.

Wikswo, J. P., Barach, J. P., and Freeman, J. A. (1980). Magnetic field of a nerve impulse: First measurements. *Science*, 208:53–55.

Wilke, E. and Atzler, E. (1912). Experimentelle Beiträge zum Problem der Reizleitung im Nerven.

Williamson, R. E. and Ashley, C. C. (1982). Free Ca^{2+} and cytoplasmic streaming in the alga chara. *Nature*, 296:647–651.

Wunderlich, B., Leirer, C., Idzko, A., Keyser, U. F., Wixforth, A., Myles, V. M., and Heimburg, T. (2009). Phase-state dependent current fluctuations in pure lipid membranes. *Biophysj*, 96:4592–4597.

Acknowledgment

In science, as in all other fields, successful work is only possible through the support of others. Therefore, I would like to thank all those who have supported and helped me in my research.
First of all, I would like to thank Prof. Dr. Matthias F. Schneider for making my work at his chair possible and for introducing me to the exciting topic of this new perspective to physics in biological systems. I am also thankful to him for giving me so much freedom in my research.
Furthermore, I would like to thank Prof. Dr. Luis Bagatolli for being the second adviser of my thesis and for his help with the experiments with fluorescent dyes in lipid monolayer. Especially, I would also like to thank Dr. Christian Fillafer, who was always available to answer any questions and to have fruitful discussions about experimental setups or results of the research.
It was an honor to meet Dr. Konrad Kaufmann and to listen to his lectures, plays and music. Without him we might not even know how many open questions and controversies still exist in the field of physics or biology.
It was also a successful cooperation with Prof. Dr. Ilse Foissner and Dr. Aniela Sommer from Salzburg. From the work with the confocal microscope one important part of the work was developed.
Special thanks also go to Anne and Gregor for their help in developing ideas, experiments, for critical reviewing my thesis and for the great atmosphere at work. I would like to thank Daniel, Matan, Kevin and all members of the group, working was always a lot of fun. Many thanks to Lisa for supporting all of us.
I am grateful to my whole family for their continuous support and for their help. Finally, I would like to thank my girlfriend Carina for all her support, for always being understanding, for all the helpful discussions and for making me happy everyday.